DOI:10.14753/SE.2017.2041

Examination of the neuronal network regulating satiety using refeeding as a satiety model

Ph.D. Thesis

Györgyi Zséli

Semmelweis University
János Szentágothai Ph.D. School of Neuroscience

Institute of Experimental Medicine
of the Hungarian Academy of Sciences

Supervisor: Csaba Fekete MD, DSc

Official reviewers: Zita Puskár PhD
Balázs Gaszner MD, PhD

Head of the Final Examination Committee: Miklós Tóth MD, DSc

Members of the Final Examination Committee: Katalin Halasy PhD, DSc
Zsuzsanna Várnainé Tóth PhD

Budapest
2017

DOI:10.14753/SE.2017.2041

1. TABLE OF CONTENTS

DOI:10.14753/SE.2017.2041

DOI:10.14753/SE.2017.2041

DOI:10.14753/SE.2017.2041

2. LIST OF ABBREVIATIONS

3V	- 3rd ventricle
AAV	- adeno-associated virus
ABC	- avidin-biotin complex
aco	- anterior commissure
ACo	- anterior cortical amygdaloid nucleus
AgRP	- agouti-related protein
AH	- anterior hypothalamic area
AIA	- agranular insular area
α-MSH	- alpha-melanocyte-stimulating hormone
AP	- area postrema
AQ	- aqueduct (Sylvius)
ARC	- arcuate nucleus
ARCdmp	- arcuate hypothalamic nucleus, dorsomedial posterior part
BBB	- blood-brain barrier
BST	- bed nucleus of the stria terminalis
BSTL	- bed nucleus of the stria terminalis, lateral division
BSTLD	- bed nucleus of the stria terminalis, lateral division, dorsal part
BSTM	- bed nucleus of the stria terminalis, medial division
BSTMA	- bed nucleus of the stria terminalis, medial division, anterior part
BW	- body weight
C	- central canal
CART	- cocaine-and amphetamine-regulated transcript
CCK	- cholecystokinin
CEA	- central nucleus of amygdala
CEAc	- central nucleus of amygdala, capsular part
CEAl	- central nucleus of amygdala, lateral part
CEAlc	- central nucleus of amygdala, laterocapsular part
CEAm	- central nucleus of amygdala, medial part
CGRP	- calcitonin gene-related peptide
CNO	- clozapine-N-oxide
CNS	- central nervous system

cp - cerebral peduncle, basal part
CREB - cAMP response element-binding protein
CRH - corticotropin-releasing hormone
cst - commissural stria terminalis
CTB - cholera toxin β subunit
DAB - diaminobenzidine
DBH - dopamine-β-hydroxylase
DMN - hypothalamic dorsomedial nucleus
DREADD - Designer Receptor Exclusively Activated by Designer Drugs
DTAF - dichlorotriazinylamino fluorescein
ec - external capsule
ECu - external cuneate nucleus
FITC - fluorescein isothiocyanate
fr - fasciculus retroflexus
fx - fornix
$GABA_A$ receptor - gamma-aminobutyric acid A-type receptor
GH - growth hormone
GHSR - growth hormone secretagogue receptor
GLP-1 - glucagon-like peptide 1
HuC/HuD - human neuronal protein
Hyp - hypothalamus
ic - internal capsule
IgG - immunoglobulin g
INSR - insulin receptor
IP - interpeduncular nucleus
IR - immunoreactive
ir - immunoreactivity
IRt - intermediate reticular nucleus
KO - knockout
LEPR - leptin receptor
LH - lateral hypothalamic area
LPO - lateral preoptic area

LSV	- lateral septal nucleus ventral part
MC3R, MC4R	- melanocortin 3 and 4 receptors
MD	- mediodorsal thalamic nucleus
MeAD	- medial amygdaloid nucleus anterodorsal part
ml	- medial lemniscus
mlf	- medial longitudinal fasciculus
MO	- medial orbital cortex
mtV	- mesencephalic trigeminal tract
Ni-DAB	- diaminobenzidine with nickel ammonium sulfate
NPY	- neuropeptide Y
NTS	- nucleus tractus solitarii
NTSl	- nucleus of the solitary tract, lateral part
NTSm	- nucleus of the solitary tract, medial part
opt	- optic tract
ox	- optic chiasm
PAG	- periaqueductal gray
PAGvl	- ventrolateral periaqueductal gray
PB	- phosphate buffer
PBl	- parabrachial nucleus, lateral part
PBlc	- lateral parabrachial nucleus, central part
PBld	- lateral parabrachial nucleus, dorsal part
PBle	- lateral parabrachial nucleus, external part
PBlv	- lateral parabrachial nucleus, ventral part
PBm	- parabrachial nucleus, medial part
PBme	- medial parabrachial nucleus external part
PBmm	- medial parabrachial nucleus medial part
PBN	- parabrachial nucleus
PBS	- phosphate buffered saline
Pe	- periventricular hypothalamic nucleus
PeF	- perifornical nucleus
PFA	- paraformaldehyde
PHAL	- Phaseolus vulgaris-leucoagglutinin

Pir	- piriform cortex
pm	- principal mammillary tract
Pn	- pontine nuclei
POMC	- pro-opiomelanocortin
Prl	- prelimbic cortex
PSTN	- parasubthalamic nucleus
PVA	- paraventricular thalamic nucleus anterior part
PVN	- hypothalamic paraventricular nucleus
PVNl	- lateral parvocellular subdivision of the PVN
PVNmp	- paraventricular hypothalamic nucleus, medial parvicellular part
PVNpo	- paraventricular hypothalamic nucleus, posterior part
PVNv	- ventral parvocellular subdivision of the PVN
PVT	- paraventricular thalamic nucleus
py	- pyramidal tract
PYY	- peptide YY
Re	- reuniens thalamic nucleus
Rh	- rhomboid thalamic nucleus
RRF	- retrorubral field
S1ULp	- primary somatosensory cortex, upper lip region
scp	- superior cerebellar peduncle (brachium conjunctivum)
siRNA	- small interfering ribonucleic acid
SO	- supraoptic nucleus
sol	- solitarii tract
sp5	- spinal trigeminal tract
SSs	- supplementary somatosensory area
STN	- subthalamic nucleus
TSA	- tyramide signal amplification
Tu	- olfactory tubercle
VL	- lateral ventricle
VPM	- ventral posteriomedial nucleus of the thalamus
xscp	- superior cerebellar peduncle decussation
Y1R	- neuropeptide Y1 receptor

DOI:10.14753/SE.2017.2041

ZI - zona incerta

DOI:10.14753/SE.2017.2041

3. INTRODUCTION

The balance between the energy intake and energy expenditure is very tightly controlled by the central nervous system (CNS) (Schwartz et al., 2000) as indicated by the relatively stable body weight of most adults despite the very high variability of the daily food intake and locomotor activity (Morton et al., 2006). For this precise regulatory process, the communication of the brain and the peripheral organs is inevitable. The brain has to sense the amount and the composition of the consumed food, the actual condition of the adipose depots and the needs of other peripheral organs. This peripheral organ-brain communication is primarily mediated via two main routes: circulating factors can reach the brain via the bloodstream, while effects of other inputs are mediated by visceral sensory nerves: the sensory fibers of the vagus nerve and the sympathetic nerves (Morton et al., 2006) **(Figure 1**).

The circulating blood carries both peripheral hormones and metabolites like fatty acids, amino acids and glucose. All of these substances mediate important energy homeostasis-related signals toward the brain. The white adipose tissue derived leptin informs the brain about the amount of energy stored in the white adipose tissue, insulin that is secreted in the Langerhans islets of the pancreas carries information about the blood glucose level, but also about the size of adipose tissue, while ghrelin released from the mucosa of the stomach serves as a hunger signal (Morton et al., 2006). Other gastrointestinal hormones like cholecystokinin (CCK) and peptide YY (PYY) mediates information about the food consumption (**Figure 1**) (Schwartz et al., 2000). The circulating metabolites can also act directly on the neurons of the CNS. For example, glucose sensing plays important role in the regulation of food intake as indicated by the obesity phenotype of the animals after gold-thioglucose induced ablation of the hypothalamic neurons (Debons et al., 1977) and the hyperphagia induced by the inhibition of glucose sensing (Debons et al., 1977).

The primary central target of these circulating signals is the hypothalamic arcuate nucleus (ARC) (Schwartz et al., 2000). Neonatal ablation of the ARC results in leptin resistance and an obesity syndrome (Dawson et al., 1997). Neurons of the ARC integrate the blood-derived information with neuronal signals and transmit this message toward the so called second-order neuronal groups.

DOI:10.14753/SE.2017.2041

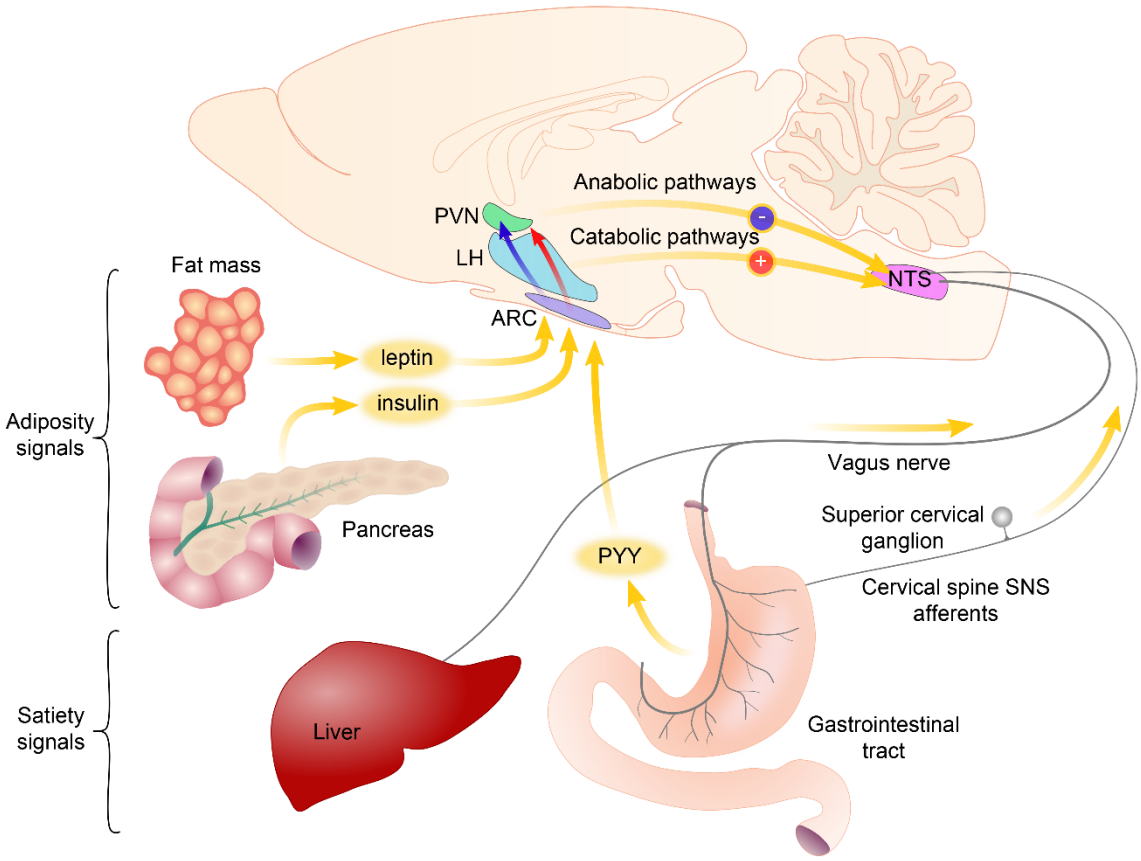

Figure 1 Schematic illustration of pathways transmitting energy homeostasis-related signals from the peripheral organs to the central nervous system. The circulating blood contains satiety-related hormones like PYY released from the gastrointestinal tract and adiposity hormones like leptin and insulin. The primary central target of these hormones is the arcuate nucleus (ARC). Neurons of the ARC sense and integrate these signals and transmit toward second order neuronal groups like the hypothalamic paraventricular nucleus (PVN) and the lateral hypothalamus (LH). The vagus nerve and the sympathetic nerves carry information about the amount and the quality of the consumed food sensed by mechano- and chemosensitive receptors and by detecting locally released hormones. Axons of these nerves terminate on the neurons of the nucleus tractus solitarii (NTS). Descending pathways from the hypothalamus influence the sensitivity of the NTS neurons to vagus derived inputs. Modified from Schwartz et al. *Nature* 2000.

The energy homeostasis-related signals that are conveyed by the peripheral nerves can reach the brain via the nucleus tractus solitarii (NTS). The vagus nerve mediates most of these inputs. The sensory fibers of the vagus nerve innervate the visceral organs and sense mechanical and chemical stimuli and also have receptors for some of the gastrointestinal hormones like CCK (Li, 2007; Phillips and Powley, 2000). Therefore, the vagus nerve can convey information about the consumed food to the NTS. Currently, far less information is available about the role of the sympathetic sensory fibers, but the information carried by these fibers is also relayed by the NTS (Loewy, 1990). After signal integration, the NTS relays this information toward the forebrain. The parabrachial nucleus (PBN) is a major relay nucleus in this pathway in rodents (Loewy, 1990). It

receives energy homeostasis-related inputs from the NTS and sends widespread inputs to the forebrain. Recent studies from Dr. Palmiter's group (Carter et al., 2015; Carter et al., 2013; Wu et al., 2012; Wu and Palmiter, 2011) uncovered a key role of the PBN in the regulation of food intake. The PBN is also a key node, where the ascending and descending energy homeostasis-related circuits interact (Wu and Palmiter, 2011). A major anorexigenic output of the PBN projects to the central nucleus of the amygdala (CEA) (Carter et al., 2013), where the energy homeostasis-related signals are integrated with stress and emotion-related information.

3.1. Energy homeostasis-related circulating factors

During the early years of the research on the regulation of the energy homeostasis, three main hypothesis were raised about the regulation of food intake: the glucostatic, satiety and adiposity hypotheses (Woods, 2013). According to the glucostatic hypothesis, the changes of glucose levels in the circulation initiates and terminates the food intake (Mayer and Thomas, 1967). This hypothesis was supported by the hypoglycemia induced vigorous food intake and the hyperphagia provoked by administration of 2-deoxyglucose, a substance known to cause cellular hypoglycemia (Woods, 2013). The glucostatic hypothesis was, however, challenged by the fact that the circulating glucose level is higher at the initiation of most meals than the level what would induce food intake (Woods, 2013) suggesting that, though alteration of glucose levels certainly regulate feeding, glucose is not the primary factor in the regulation of food intake.

The satiety hypothesis is based on the experiments by Davis et al. (Davis et al., 1967) demonstrating that blood derived from sated rats can decrease food intake. Since in their experiment, blood from fasted rats did not increase the food intake, they hypothesized that food intake is initiated by the decrease of circulating satiation factors rather than increase of hunger factors (Davis et al., 1967). The first identified hormone that met the criteria of a satiation hormone was cholecystokinin (CCK). This hormone is secreted by the I cells of duodenum and jejunum in response to food intake (Stengel and Tache, 2011). In humans, CCK level peaks in the blood 15 min after the onset of eating (Stengel and Tache, 2011). Among nutrients, proteins and fats are the most potent stimulators of CCK release (Stengel and Tache, 2011). Administration of CCK markedly inhibits the size of the consumed meal (Gibbs et al., 1973). CCK, however, has no effect

on the cumulative food intake (Stengel and Tache, 2011). Thus, during eating, nutrients stimulate the release of CCK and this hormone terminate the meal, but the animals compensate with increase of the number of meals.

Subsequently, it was recognized that the regulation of food intake also depends on the size of adipose tissue suggesting that so called adiposity signals that inform the brain about the lipid stores should also be involved in the feeding regulation (Woods, 2013). The first recognized adiposity factor was insulin. It is rapidly secreted from the β cells of the pancreatic Langerhans islands in response to the increase of blood glucose levels after carbohydrate intake (Begg and Woods, 2012), but the circulating insulin level is also proportional to the size of adipose tissue (Woods, 2013). The first identified function of insulin was its role in the regulation of blood glucose level (Begg and Woods, 2012). Insulin facilitates the uptake of glucose by the peripheral organs including the muscle and liver where glucose is stored as glycogen. Insulin also inhibits the glucose production in the liver (Begg and Woods, 2012). Insulin, however, has far more widespread effect on the metabolism. For example, it also increases the cellular intake of amino acids and the storage of lipids in the adipose tissue (Begg and Woods, 2012).

Insulin also has been shown to regulate food intake (**Figure 1**). Peripheral insulin injection increases food intake due to its hypoglycemic effect, but administration of insulin into the brain inhibits food intake and causes weight loss (Woods et al., 1979).

Since the fluctuations of insulin level in the cerebrospinal fluid only slowly follows the changes observed in the circulation, the central insulin level is mainly influenced by the adiposity and not by the quick changes of glucose level (Woods et al., 1979). Thus when the size of adipose tissues is increased, the elevated central insulin level inhibits food intake.

The white adipose tissue derived hormone, leptin, is also an adiposity signal (**Figure 1**). It was discovered as the hormone that is missing from the highly obese ob/ob mouse (Halaas et al., 1995). Similarly to rodents, the mutation of leptin gene also causes early onset obesity in humans (Farooqi et al., 1998). The blood level of leptin and its synthesis in the white adipose tissue are increased in obese animals and are decreased by fasting (Frederich et al., 1995). Administration of leptin to non-obese animals results in marked inhibition of food intake and decrease of body weight (Halaas et al., 1995). Leptin influences almost all aspects of energy homeostasis. In addition to the regulation of food

intake, leptin also stimulates the energy expenditure, increases lipolysis and also regulates the development of neuronal pathways regulating energy homeostasis (Morton et al., 2006). In addition to the size of adipose tissue, the leptin level is also regulated by other hormones including insulin, glucocorticoids and neuronal signals ensuring that leptin could regulate the energy homeostasis according to the needs of the organism (Morton et al., 2006).

During the years of energy homeostasis research, the glucostatic, satiety and adiposity hypotheses of the food intake regulation replaced each other, but the current view is that satiation and adiposity signals and metabolites like glucose continuously interact with each other to defend body weight, maintain stable circulating glucose levels and provide appropriate amount of energy for all organs.

Similarly to the above mentioned circulating factors, most of the peripheral energy homeostasis-related signals have anorexic effect supporting the hypothesis of Davis (Davis et al., 1967) saying that meal is initiated by the decreased level of satiation factors in the blood and not by increase of hunger factors. However, in 1999, Kojima and his fellow workers identified a new peptide hormone, ghrelin, from the stomach that turned out later to have very potent orexigenic effect (Kojima et al., 1999; Nakazato et al., 2001). Ghrelin was discovered as the endogenous ligand of the growth hormone secretagogue receptor (GHSR) (Kojima et al., 1999). In accordance, ghrelin stimulates the release of growth hormone (GH) from the pituitary (Kojima et al., 1999). In addition to the pituitary, GHSR, however, has a widespread distribution in the hypothalamus indicating that the regulation of GH secretion in the pituitary is not the only function of this hormone (Nakazato et al., 2001). Indeed, it was found that intracerebroventricular administration of ghrelin caused a marked increase of food intake in rats (Nakazato et al., 2001). Ghrelin is synthesized by the oxyntic glands in the fundus of stomach (Date et al., 2000). The plasma ghrelin level has both short term, circadian, regulation and it also has long term regulation that is influenced by the amount of stored energy (Iwakura et al., 2015). The ghrelin level peaks just before the time of expected meal and declines after food consumption (Iwakura et al., 2015). Therefore, ghrelin is considered as a hunger hormone, however, the meal pattern of ghrelin knock out mice is normal suggesting that ghrelin is not absolutely necessary for the initiation of food intake (Iwakura et al., 2015). The circulating ghrelin level is negatively correlated with the body mass index. Thus ghrelin

level is lower in obesity and higher in lean individuals (Iwakura et al., 2015). The weight loss induced increase of ghrelin levels may be an important factor that makes difficult the maintenance of the decreased body weight (Iwakura et al., 2015).

3.2. The hypothalamic arcuate nucleus as the primary sensor of the circulating energy homeostasis-related signals

The ARC is located at the base of the hypothalamus, on both sides of the third ventricle behind the optic chiasm. This nucleus is closely associated to the blood-brain barrier (BBB) free median eminence and it has been shown that even within the ARC, some of the blood vessels lack BBB markers (Norsted et al., 2008) suggesting that circulating factors can relatively easily access the neurons of the ARC. Indeed, neurons in the ARC express leptin, ghrelin and insulin receptors and can sense the changes of metabolites like glucose, amino acids and fatty acids (Morton et al., 2006) (**Figure 2**). Furthermore, neonatal ablation of the ARC by peripheral monosodium glutamate administration causes obesity (Dawson et al., 1997) substantiating the role of the ARC in the regulation of energy homeostasis.

The ARC has at least two feeding-related neuronal groups, the medially located neuropeptide Y (NPY) and agouti-related protein (AgRP) expressing neurons that also utilize GABA as transmitter; and the more laterally located α-melanocyte-stimulating hormone (α-MSH) and cocaine-and amphetamine regulated transcript (CART) producing neurons (Dawson et al., 1997). These two cell populations have antagonistic effects on the regulation of energy homeostasis (**Figure 2**).

The peptides of the α-MSH/CART neurons have anorexigenic effects. Both α-MSH and CART exert potent inhibitory effect on the food intake and stimulate energy expenditure (Morton et al., 2006). α-MSH is derived from the proteolytic cleavage of a prohormone, the proopiomelanocortin (POMC) (Corander and Coll, 2011). In the brain, α-MSH exerts its effects primarily via two types of receptors, the melanocortin 3 and 4 receptors (MC3R and MC4R). Genetic mutation of both the POMC gene or the MC4R results in hyperphagia, increased adiposity and markedly increased body weight (Adan et al., 2006; Corander and Coll, 2011). The degree of obesity in these mouse models is similar than that observed in the leptin deficient ob/ob mice. In addition to the obesity, the POMC deficient mice also have altered pigmentation and adrenal insufficiency due

DOI:10.14753/SE.2017.2041

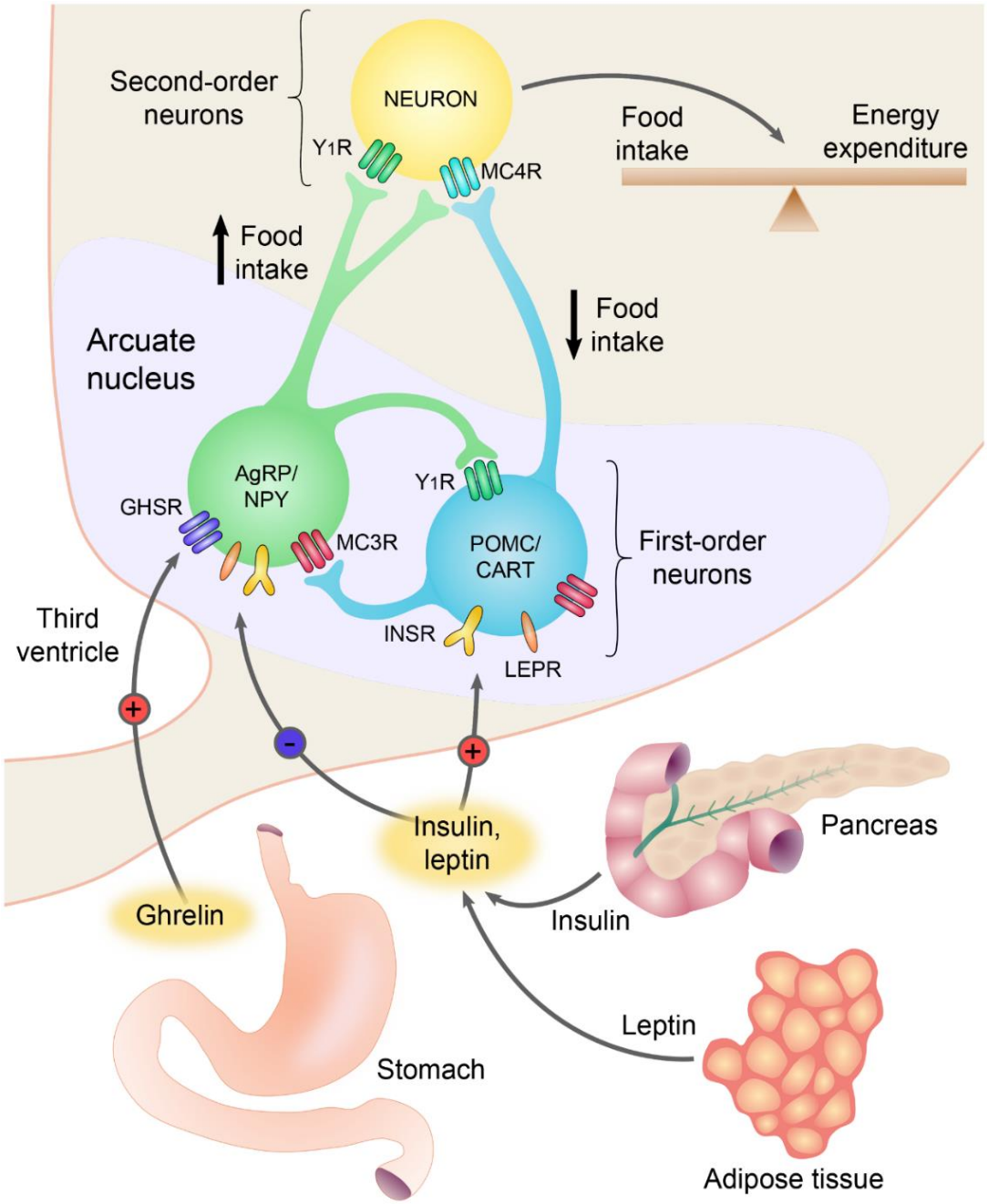

Figure 2 Role of the neurons of the arcuate nucleus (ARC) in the regulation of energy homeostasis. The two main feeding-related neuronal groups of the ARC, the AGRP/NPY and the POMC/CART neurons, are regulated by circulating hormones. AGRP and NPY are neuropeptides that stimulate food intake and decrease energy expenditure, whereas α-melanocyte stimulating hormone (a post-translational derivative of proopiomelanocortin, POMC) and CART are neuropeptides that inhibit food intake and increase energy expenditure. The circulating levels of insulin and leptin are proportional to the size of adipose tissue. These hormones inhibit AGRP/NPY neurons and stimulate the adjacent POMC/CART neurons. During fasting, the lower insulin and leptin levels activate the AGRP/NPY neurons and inhibit the POMC/CART neurons. Ghrelin is a circulating peptide secreted from the stomach, directly activates the AGRP/NPY neurons, thereby, stimulates the food intake. The feeding-related neuronal groups of the ARC transmit these signals to the second order neuronal groups and regulate these cells via activation of NPY and melanocortin receptors. GHSR, growth hormone secretagogue receptor; LEPR, leptin receptor; MC3R/MC4R, melanocortin 3/4 receptor; Y1R, neuropeptide Y1 receptor. Based on work of Barsh and Schwartz, *Nature Reviews* 2002.

to the lack of peripheral melanocortin effect (Yaswen et al., 1999), these effects are independent from the function of POMC neurons in the ARC. Among the obesity syndromes, the phenotype of the MC4R *knockout* (KO) mice has unique features, the MC4R KO mice have increased longitudinal growth and normal lean body mass (Adan et al., 2006). In addition to the increased food intake, the MC4R KO mice also have decreased oxygen consumption and even the pairfed MC4R KO mice develop obesity suggesting that both the hyperphagia and the decreased energy expenditure contribute to this obesity syndrome (Adan et al., 2006). Mutations of the POMC and MC4R are also observed in humans resulting in very similar phenotype than that observed in mice (Farooqi and O'Rahilly, 2008). Indeed, the mutations of the MC4R are the most frequent monogenic causes of morbid obesity in humans (Farooqi and O'Rahilly, 2008).

The CART KO mice also develop obesity, but this phenotype is very mild compared to the phenotypes caused by the genetic alterations of the melanocortin system (Wierup et al., 2005). The lack of CART has no effect on the food intake and causes only 14% increase of body weight that is apparent only after 40 weeks (Wierup et al., 2005). While CART is expressed in the anorexigenic POMC neurons in rodents, this peptide is expressed in orexigenic neurons in humans raising the possibility that CART has different function in the regulation of food intake in rodents and humans (Menyhert et al., 2007). The receptor of CART is still unidentified making the elucidation of the function of CART even more difficult.

The role of the POMC/CART neurons in the regulation of energy homeostasis is further substantiated by the fact that ablation of POMC neurons in adult mice results in hyperphagia and increased body weight (Gropp et al., 2005).

An important signal that regulates the POMC/CART neurons is leptin that stimulates the gene expression of both of these peptides and increases the firing of these neurons (Hill et al., 2008; Morton et al., 2006). Though, the POMC neurons express leptin receptor, the POMC cell specific ablation of leptin receptor causes only mild obesity (Hill et al., 2008) that is in contrast to the morbid obesity of the POMC or MC4R KO mice. These data suggest that the effect of leptin on the POMC neurons is at least partly indirect. Conditional deletion of leptin receptor from GABAergic or glutamatergic neurons demonstrated that leptin responsive GABAergic neurons play critical role in the mediation of leptin effects to the POMC neurons (Vong et al., 2011). Leptin induced

inhibition of the GABA neurons causes disinhibition and therefore stimulation of POMC neurons (Vong et al., 2011).

The POMC neurons are also regulated by insulin and metabolites like glucose, fatty acids and amino acids (Blouet et al., 2009; Fekete et al., 2006; Schwinkendorf et al., 2011). The POMC neurons integrate these humoral and neuronal inputs and transmit these signals toward second order neuronal populations like the hypothalamic paraventricular nucleus (PVN) and hypothalamic dorsomedial nucleus (DMN).

In contrast to the POMC/CART neurons, the NPY/AgRP neurons are orexigenic (Morton et al., 2006). Central administration of both NPY and AgRP stimulates food intake and decreases energy expenditure (Morton et al., 2006). AgRP acts as an endogenous antagonist of the MC3R and MC4R (Dinulescu and Cone, 2000). This peptide is a competitive antagonist of α-MSH on these receptors, but it can also hyperpolarize the target neurons via binding to MC4R and opening a type of K^+ channel (K_{ir} 7.1 channels) (Ghamari-Langroudi et al., 2015). This action of AgRP is independent from the binding of α-MSH to the receptors and also from G proteins (Ghamari-Langroudi et al., 2015). NPY exerts its effect via three Y receptors, the Y1, Y2 and Y5 receptors (Pedragosa-Badia et al., 2013). Among these receptors, Y1 and Y5 are postsynaptic receptors and mediate the orexigenic effects of NPY (Morton et al., 2006; Pedragosa-Badia et al., 2013). However, α-MSH and NPY act through different receptors, NPY can antagonize the action of α-MSH by inhibiting the α-MSH induced cAMP synthesis and cAMP response element-binding protein (CREB) phosphorylation (Sarkar and Lechan, 2003).

Despite the very potent orexigenic effect of these peptides, neither the AgRP nor the NPY KO mice have major phenotype (Morton et al., 2006). In contrast, however, ablation of the NPY/AgRP neurons in adult animals develop severe anorexia (Gropp et al., 2005; Luquet et al., 2005) demonstrating the importance of these neurons in the regulation of food intake. In addition, these data also indicate that transmitter(s) other than NPY or AgRP also play important role in the stimulation of food intake by these neurons. Indeed, the AgRP neuron ablation induced anorexia causes neuronal activation is several neuronal groups and administration of $GABA_A$ receptor agonist can prevent this anorexia demonstrating that GABAergic inhibition of target neurons by the NPY/AgRP neurons is critical for the regulation of food intake (Wu et al., 2009).

The NPY/AgRP neurons are also regulated by metabolic signals, but oppositely than the POMC/CART neurons (Morton et al., 2006). Fasting results in a 4-fold increase of the firing frequency of these neurons, what can be reversed by leptin administration and completely absent in the leptin deficient ob/ob mice (Takahashi and Cone, 2005). Furthermore, fasting stimulates, while leptin administration inhibits the synthesis of both NPY and AgRP in these cells (Morton et al., 2006). The NPY/AgRP neurons are also inhibited by insulin and glucose and stimulated by ghrelin (Fekete et al., 2006; Nakazato et al., 2001).

The projection fields of the NPY/AgRP and POMC/CART neurons highly overlap and in most cases the two neuron populations innervate the very same second order neurons that provide the anatomical basis of the precise regulation of second order neurons by the two feeding-related neuron population of ARC (Fekete et al., 2000; Lechan and Fekete, 2006).

3.3. Peripheral nerves transmitting peripheral metabolic signals to the central nervous system

The visceral organs are innervated by both parasympathetic and sympathetic nerves. The vagus nerve provides the parasympathetic innervation of most of the abdominal organs. Both the parasympathetic and the sympathetic nerves carry primary afferent fibers. Approximately 80% of axons in the vagus nerve are afferent fiber, while this ratio is lower, approximately 20% in the sympathetic nerves (Cervero and Foreman, 1990). The role of this dual sensory innervation of the visceral organs is currently unknown (Cervero and Foreman, 1990).

The cell bodies of the afferent fibers of the vagus nerve are located in the nodose ganglion. These neurons project peripherally to the visceral organs and centrally to the NTS (Cervero and Foreman, 1990). These sensory fibers can sense the passage of food in the gastrointestinal tract, nutrients and gastrointestinal hormones, thus can provide negative feedback signal to the CNS to terminate food intake (de Lartigue and Diepenbroek, 2016).

The presence of food in the stomach and gut is sensed by afferent fibers in the mucosa that are sensitive for mechanical touch, while the amount of food is sensed by the stretch and tension sensitive afferents in the external muscle layers (Berthoud, 2008). In

addition, to mechanical sensing, the sensory vagus neurons are also sensitive to nutrients, therefore can detect the components of food. Long- and medium-chain fatty acids can directly activate the vagal afferent neurons possibly via the fatty acid receptor GPR40 and the nuclear receptor LxR (de Lartigue and Diepenbroek, 2016). These neurons can also directly sense glucose, but currently there is no direct evidence that the vagal afferent neurons can sense amino acids (de Lartigue and Diepenbroek, 2016). The afferent neurons of the vagus nerve are also sensitive to gastrointestinal hormones. Leptin, CCK, and glucagon-like peptide 1 (GLP-1) activates the afferent fibers of vagus nerve, while ghrelin inhibits the firing of these axons (Berthoud, 2008). These hormones can also alter the sensitivity of vagal afferents to mechanic stimuli (de Lartigue and Diepenbroek, 2016). Since these hormones are synthesized in the wall of the stomach and gut, where their synthesis is regulated by the ingested nutrients, the interaction of these hormones can also transmit feeding-related stimuli toward the brain. The vagal fibers are also sensitive for serotonin secreted from the enterochromaffin cells of the stomach after gastric distension (Grill and Hayes, 2012). This serotoninergic signaling is also a critical satiation signal (Grill and Hayes, 2012).

Vagal sensory fibers of the liver and the hepatic portal vessels are also involved in the regulation of energy homeostasis (Warne et al., 2007).

Earlier, the primary function of the sensory fibers of the vagus nerve were thought to be to send feedback information to the brain to terminate the actual meal (de Lartigue and Diepenbroek, 2016). However, selective genetic ablation of the leptin receptor from the sensory neurons of the vagus results in hyperphagia, increased adiposity and increased body weight indicating that afferent signals of the vagus nerve also play role in the long term regulation of food intake (de Lartigue and Diepenbroek, 2016; de Lartigue et al., 2014).

However, the sympathetic afferent fibers give approximately 25% of the sensory innervation of visceral organs currently very little information is available about the role of these fibers in the nutrient sensing.

3.4. The nucleus tractus solitarii as central hub of energy homeostasis-related afferents

The peripheral signals carried by the afferent fibers of the vagus nerve and the sympathetic nerves are relayed through the NTS (**Figure 1**). The termination of the afferents have a viscerotopic organization pattern. The gastrointestinal afferents primarily terminate in the intermediate, medial and commissural subnuclei of the NTS (Loewy, 1990). The NTS also receives taste-related signals via cranial nerves (Loewy, 1990) and can sense humoral signals directly (Grill and Hayes, 2012).

Leptin receptor is expressed by neurons of the NTS (Scott et al., 2009) and intra NTS administration of leptin reduces food intake and body weight (Kanoski et al., 2012) indicating that NTS leptin signaling is involved in the regulation of energy homeostasis. These data are further supported by the finding that siRNA mediated knock down of the leptin receptor in the medial NTS causes hyperphagia and increases body weight (Hayes et al., 2010).

Ghrelin can also act directly on the neurons of the NTS, but in contrast to leptin, ghrelin injection to the NTS increases food intake (Grill and Hayes, 2012). NTS neurons express ghrelin receptor and are directly inhibited by ghrelin (Grill and Hayes, 2012).

In addition to these peripheral inputs, the NTS also receives neuronal inputs from other parts of the CNS. It receives descending inputs from hypothalamic nuclei (Blouet et al., 2009; Singru et al., 2012). An ARC POMC neuron-PVN oxytocin neuron-NTS pathway mediates the stimulatory effect of leucine rich diet on the NTS neurons (Blouet et al., 2009), while an ARC POMC neuron-PVN glutamatergic neuron-NTS pathway mediates the excitatory effect of refeeding (Singru et al., 2012). Serotoninergic neurons also provide an excitatory input to the NTS (Wu et al., 2012).

It is not completely understood, how the NTS neurons integrate these peripheral and central signals, but it is suggested that humoral and neuronal inputs alter the sensitivity of the NTS neurons to the vagus mediated inputs (Grill and Hayes, 2012). Indeed, direct effect of leptin on NTS neurons increases the effect of gastric distension on food intake, while NTS specific siRNA mediated knockdown of leptin receptor prevents the anorexigenic effect of CCK that is known to be mediated by the vagus nerve (Grill and Hayes, 2012). In contrast, ghrelin inhibits the activation of NTS neurons induced by stimulation of vagal afferents (Cui et al., 2011).

After integration of energy homeostasis-related signals, the NTS neurons transmit these signals toward other hindbrain and forebrain nuclei involved in the regulation of energy homeostasis. Since many aspects of ingestive behavior are intact in decerebrated rodents or in anencephal infants, the hindbrain seems to be the primary site of the premotor control of food ingestion (Grill and Hayes, 2012). In addition to these hindbrain nuclei, the NTS also sends feeding-related inputs to forebrain regions that are involved in the regulation of food intake. Recent genetic and optogenetic studies demonstrated that projection of glutamatergic neurons to the PBN has important role in the regulation of food intake (Wu et al., 2012). For example, activation of a NTS-PBN-CEA pathway has been shown to inhibit food intake (Carter et al., 2013; Roman et al., 2016; Wu et al., 2012).

3.5. Involvement of the parabrachial nucleus in the regulation of food intake

One of the major projection fields of the NTS is the PBN. The gustatory regions of the NTS project to the medial part of the PBN, while the visceroreceptive portions project to the lateral PBN (Loewy, 1990).

The involvement of the medial PBN in the taste perception was discovered in 1971 when its connections with the NTS and the thalamic taste area was described (Scott and Small, 2009). Later, series of electrophysiological studies mapped and characterized the taste sensitive neurons of the PBN (**Figure 3**)(Tokita and Boughter, 2016). Similarly to the NTS, the taste sensitive neurons also have topographic distribution in the PBN. Studies focusing on the mapping of neuronal activation in the PBN after different taste stimuli demonstrated that activated neurons after taste with negative or positive hedonic value segregate within the PBN suggesting that PBN starts the hedonic processing of taste information (Yamamoto et al., 1994). In addition, lipids in the small intestine can very rapidly alter the responsiveness of PBN neurons to different taste stimuli (Hajnal et al., 1999) and nutritional status can also alter the neuronal activation pattern induced by tastes (Yamamoto et al., 2009). These data indicate that the PBN not only relay the taste stimuli toward forebrain sites, but the PBN is also involved in the processing of taste information and integrates it with the effect of other inputs.

DOI:10.14753/SE.2017.2041

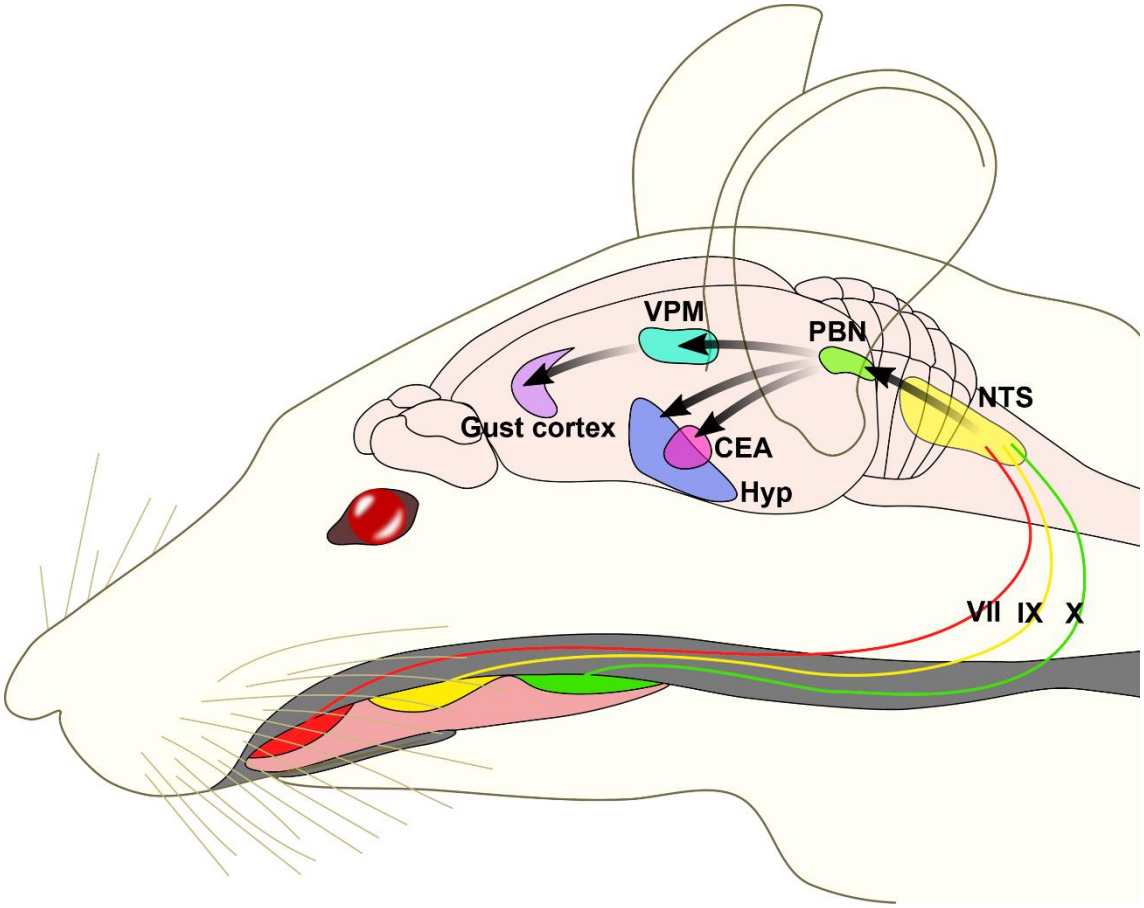

Figure 3 Neuroanatomy of the rodent taste pathways. Taste buds in the mouth are innervated by the chorda tympani branch of facial nerve, greater superficial petrosal facial nerve (VII), glossopharyngeal (IX) cranial nerves and branches to epiglottis and taste buds of vagus nerve (X). Taste signals are conveyed to NTS in the medulla and from the NTS to the medial PBN in rodents. From the PBN, parallel projections reach the ventral posteriomedial nucleus of the thalamus (VPM) and forebrain limbic areas, including the amygdala and hypothalamus. Projection of VPM to the insular cortex define the gustatory aspect of the cortex. From this cortical region the taste-related information is conveyed to higher order regions, including the orbital cortex. NTS, nucleus tractus solitarii; PBN, parabrachial nucleus; VPM, ventral posterior medial thalamic nucleus; CEA, central nucleus of amygdala; Hyp, hypothalamus. Based on work of Fernstrom et al. *Journal of Nutrition* 2012.

An important function of taste perception is to discriminate among foods and poisonous substances. If consumption of a novel taste is followed by sickness, the animals develop avoidance behavior for foods with similar taste. This behavior is called conditioned taste aversion. In contrast, if the novel taste is followed by pleasure, seeking behavior, conditioned taste preference develops. Lesions of PBN prevents the acquisition of both the conditioned taste aversion (Trifunovic and Reilly, 2002) and preference (Reilly and Trifunovic, 2000; Yamamoto et al., 2009). PBN also mediates anorexia associated with malaise induced by intraperitoneal injection of lithium chloride or lipopolysaccharide treatment that are used to mimic the effects of toxic or rancid foods

and bacterial infections, respectively (Elmquist and Saper, 1996; Paues et al., 2006; Rinaman and Dzmura, 2007; Yamamoto et al., 1992). Lithium chloride-induced anorexia results in robust c-Fos expression widely in the brain including the PBN (Andre et al., 2007; Lamprecht and Dudai, 1995; Swank and Bernstein, 1994). This neural activity is particularly observed within the PBel, the lateral external subdivision of PBN, in the calcitonin gene-related peptide expressing (CGRP) neurons. Activation of these CGRP neurons is necessary and sufficient to produce conditioned taste aversion (Carter et al., 2015).

The critical role of the PBN and its connection with the ARC in the regulation of food intake was recently demonstrated by Dr. Palmiter's group (Wu and Palmiter, 2011). They observed that after ablation of the ARC AgRP neurons, a population of PBN neurons are strongly activated, therefore, they hypothesized that loss of GABA release from the AgRP terminals is responsible for the activation of PBN neurons and these cells cause the anorexia of AgRP neuron ablated animals (Wu and Palmiter, 2011). Indeed, they demonstrated that administration of $GABA_A$ receptor agonist into the PBN can prevent the anorexia in these animals (Wu and Palmiter, 2011). Within the PBN, primarily the inhibition of the CGRP neurons is critical for the AgRP neuron induced hyperphagia (Campos et al., 2016). These neurons receive excitatory input from the NTS and relay the information toward the CEA (Carter et al., 2013).

3.6. The central amygdala and the regulation of feeding

Lesions of CEA results in increased food intake and promote body weight gain (Rollins and King, 2000). In contrast, optogenetic activation of the laterocapsular part of CEA (CEAlc) decreases food intake (Carter et al., 2013) demonstrating the importance of this nucleus in the regulation of feeding behavior.

The CEA plays important role in the integration of homeostatic and non-homeostatic signals involved in the regulation of food intake. It plays role in the development of stress induced anorexia, and mediates the effect of social emotions and learned cues on the regulation of food intake (Baxter and Murray, 2002; Callahan et al., 2013). Furthermore, the PBN CGRP neuron-CEAlc pathway was shown to play critical role in the development of taste aversion induced by gastrointestinal illness (**Figure 4**)(Carter et al., 2015).

DOI:10.14753/SE.2017.2041

Currently, however, little information is available, how the CEA is involved in the homeostatic regulation of food intake and how this nucleus is connected in the network of feeding-related neuronal groups.

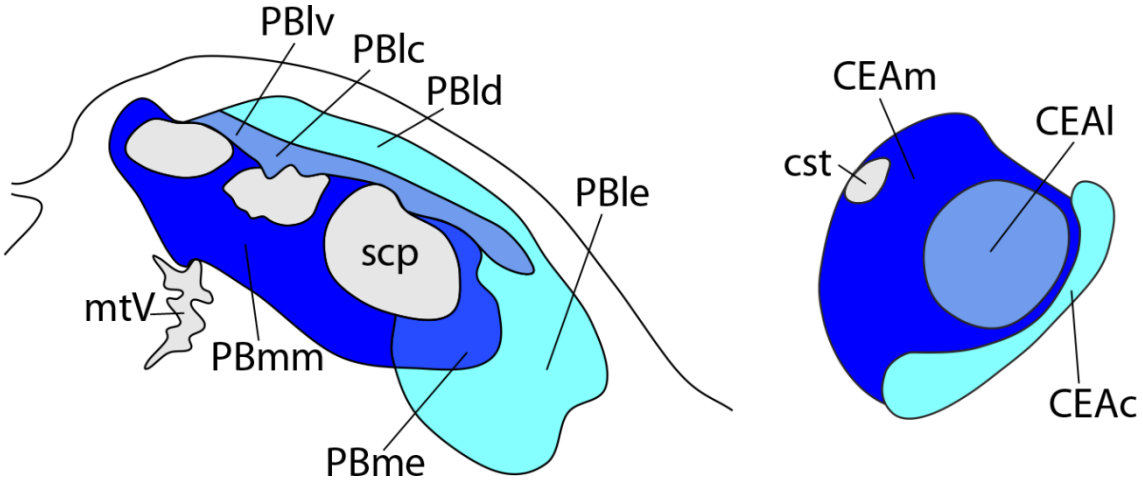

Figure 4 Schematic drawings illustrate the projection pattern from the pontine parabrachial nucleus (PBN) onto the central amygdala (CEA). There are three main pathways between the PBN and CEA. The PBm-CEAm pathway (dark blue), the PBl-CEAl pathway (bright blue) and PBl-CEAc pathway (cyan). Based on work of Bernard et al. *Journal of Comparative Neurology* 1993.

3.7. Fasting and refeeding as a satiety model in rodents

Energy homeostasis depends on a tightly controlled balance between food intake and energy expenditure that is regulated by a complex neuronal network in the central nervous system (Schwartz et al., 2000). Under most conditions, these two components are regulated simultaneously, but become uncoupled during refeeding after a prolonged period of fasting (Ji and Friedman, 1999; Rothwell et al., 1983).

After a long period of fasting, satiety is observed within the first 2 h of food intake, accompanied by characteristic c-Fos activation pattern in many brain regions, however, these changes are not complemented by the increase of energy expenditure (Ji and Friedman, 1999; Timofeeva et al., 2005). During refeeding, the energy expenditure is only increased 24h after the onset of food intake (Rothwell et al., 1983). It is likely that the lack of upregulation of energy expenditure during the first period of refeeding facilitates the refilling of energy stores that are depleted during fasting. Therefore, refeeding provides a unique model when neuronal pathways regulating satiety can be studied independently from the energy expenditure regulating circuits.

However, some of the refeeding-activated neuronal groups including the NTS, PVN, DMN, PBN and CEA, were identified by others and by our laboratory (Singru et al., 2007; Singru et al., 2012; Timofeeva et al., 2005), we hypothesized that detailed mapping of refeeding-activated neuronal groups and their connections can yield identification of novel feeding-related neuron groups and/or neuronal pathways. Similar approach by our group led to the identification of a novel neuronal pathway that mediates the effect of refeeding from the ARC to the NTS (Singru et al., 2012).

One of the neuronal groups that are activated during refeeding is the POMC neurons of the ARC (Singru et al., 2007). These neurons were primarily thought to play role in the long term regulation of food intake (Schwartz et al., 2000), however, inhibition of melanocortin signaling increases the food intake during refeeding suggesting that activation of the POMC neurons are also important for the meal size determination during refeeding (Singru et al., 2007). Since the vagus nerve and the NTS are known to play crucial role in the meal size determination, we hypothesized that the POMC neurons are activated by the vagus nerve (Singru et al., 2007)-NTS-ARC pathway during refeeding.

DOI:10.14753/SE.2017.2041

4. AIMS

Due to the very high incidence of obesity in western countries and the lack of efficient and side effect free therapy, elucidation of the neuronal circuits regulating the food intake has crucial importance. Therefore, the goal of my PhD work was to better understand the neuronal network involved in the development of satiety in refed rats. To reach this goal, our specific goals were:

1. To map the refeeding-activated neuronal groups in the rat brain.

2. To determine whether refeeding-induced activation of POMC neurons in the ARC is dependent upon the vagus nerve and/or ascending brainstem pathways.

3. To map the connections of the PBN with other refeeding-activated neuronal groups.

4. To map the connections of CEA with other refeeding-activated neuronal groups.

5. To elucidate the role of the CEA subnuclei in the development of satiety during refeeding.

DOI:10.14753/SE.2017.2041

5. METHODS

5.1. Animals

The experiments were carried out on adult male Wistar rats (TOXI-COOP KKT, Budapest, Hungary) weighing 270–310 g or Sprague–Dawley rats (230–250 g body weight) purchased from the Charles River Hungary Ltd (Isaszeg, Hungary). The animals were housed under standard environmental conditions (lights on between 06.00 and 18.00 h, temperature 22±1 °C, rat chow and water *ad libitum*). All experimental protocols were reviewed and approved by the Animal Welfare Committee at the Institute of Experimental Medicine of the Hungarian Academy of Sciences. (License numbers: PEI/001/1550-10/2014; 22.1/3891/003/2009).

5.2. Anesthesia

The anesthesia of the animals was performed by intraperitoneal injection of a mixture of ketamine (50 mg/kg body weight) and xylazine (10 mg/kg body weight).

5.3. Transcardial perfusion with fixative and tissue preparation

As a final step of all experiments, the animals were anesthetized and then perfused transcardially with 20 ml 0.01M phosphate buffered saline (PBS; pH 7.4), followed by 150 ml of 4% paraformaldehyde (PFA) in 0.1M phosphate buffer (PB, pH 7.4). The brains were rapidly removed, postfixed in the same fixative for 2 hours and cryoprotected by immersion in 30% sucrose in PBS overnight. The brains were frozen in powdered dry ice and then coronal, 25 μm thick sections were cut through the forebrain and brainstem with a freezing microtome (Leica Microsystems, Wetzlar, Germany). Four series of sections, obtained at 100 μm intervals, were collected into antifreeze solution (30% ethylene glycol; 25% glycerol; 0.05M PB) and stored at -20°C until used for immunohistochemistry.

5.4. Section pretreatment for immunohistochemistry

Free-floating tissue sections were pretreated with 0.5% H_2O_2 and 0.5% Triton X-100 in PBS for 15 min to reduce the endogenous peroxidase activity and increase the permeability of cell membranes, respectively. To reduce nonspecific antibody binding, the sections were treated with 2.5% normal horse serum in PBS for 20 min.

5.5. Preparation of experimental animals for mapping the refeeding-activated brain areas

5.5.1. Animal and tissue preparation

The mapping of the brain areas activated after two hours of refeeding was performed using 10 adult male Wistar rats. The rats were fasted for 40 hours. During this time, they had free access to water. After the fasting period, food was reintroduced to 5 of the 10 animals and they were allowed to eat *ad libitum* for 2 hours. At the completion of the refeeding interval, the food intake was weighed, both the fasted and the fasted+refed animals were deeply anesthetized and perfused transcardially as described above.

5.5.2. Immunohistochemical detection of c-Fos-immunoreactivity

One series of sections from each animal was pre-treated and then the sections were incubated in rabbit anti-c-Fos serum (Ab5; Oncogene Science, Cambridge, MA) at 1:10,000 dilution in PBS containing 2% normal horse serum and 0.2% sodium azide (antibody diluent) for 1 day at room temperature. After washing in PBS, the sections were incubated in biotinylated donkey anti-rabbit IgG (Jackson ImmunoResearch, West Grove, PA) at 1:500 dilution for 2 hours at room temperature, and after further rinsing in PBS, incubated in avidin-biotin-peroxidase complex (ABC Elite Kit, Vector Laboratories, Inc. Burlingame, CA, USA) at 1:1000 dilution for 1 hour. Following further rinses in PBS, the peroxidase activity was visualized with Ni-DAB developer (0.05% diaminobenzidine, 0.15% nickel ammonium sulfate, 0.005% H_2O_2 in 0.05 M Tris buffer at pH 7.6) (**Table 1**), and the sections were mounted on gelatin coated slides, air dried, counterstained with 1% cresyl violet and coverslipped with DPX mounting medium (Sigma-Aldrich Inc., St. Louis, MO, USA).

5.5.3. Mapping the refeeding-activated brain areas

To map the distribution of neurons containing c-Fos-immunoreactivity in fasted and refed animals, large mosaic images of the entire brain sections were taken by Zeiss AxioImager M1 bright field microscope equipped with an AxioCam MR digital camera and AxioVision software (Carl Zeiss AG., Oberkochen, Germany). The identification of brain regions was facilitated by Nissl counterstaining and was based on the rat brain atlas of Paxinos and Watson (Paxinos and Watson, 1998) and the rat brain atlas of Swanson

(Swanson, 2004). Images were imported into the Corel Draw 11 (Corel Corporation, Ottawa, Canada) software to draw the maps.

To identify the areas of the brain that may play role in the development of satiety during refeeding, the differences of neuronal activation in fasted and refed rats were identified by comparing the number of c-Fos-immunoreactive (IR) nuclei in each region.

5.6. Examination of the involvement of the vagus nerve and/or the ascending brainstem pathways in the refeeding-induced activation of POMC neurons in the arcuate nucleus

5.6.1. Surgical procedure of vagotomy

Bilateral subdiaphragmatic vagotomy was performed on 10 adult, male, Sprague–Dawley rats. In addition, 16 adult male rats from the same strain were sham-operated. After anesthesia, the animals were placed in a dorsal recumbent position and a laparotomy was performed to expose the stomach and the lower oesophagus at the subdiaphragmatic level. Anterior and posterior trunks of the vagus nerve were isolated on the surface of the subdiaphragmatic part of the oesophagus and transected with iridectomy scissors. To remove small vagal branches embedded in the connective tissue, all connective tissue was removed from the surface of the subdiaphragmatic part of the oesophagus. Buprenorphine (0.1 mg/kg body weight, subcutaneously) was administered immediately after the surgery and as required until the animals were fully recovered. Sham surgery was performed in a similar way, except that the vagal trunks were not cut and the connective tissue was not removed. One day after surgery, the vagotomized animals were divided into two groups and the sham-operated animals were divided into three groups. The first group was fasted for 40 hours (Fasted Vagotomized, n=5; Fasted Sham, n=5), whereas the second group was fasted for 40 hours and then given free access to food for 2 hours before perfusion (Refed Vagotomized, n=5; Refed Sham, n=5). The third group of the sham-operated rats was fasted for 40 hours and then refed with the same amount of food that was consumed by the refed, vagotomized rats (pairfed group, n=6). Food and water intake was monitored daily and during the 2 hours refeeding period. To verify the completeness of the vagotomy, the vagus nerve, the surrounding tissues and the stomach were visually inspected at the time of euthanasia. Criteria for complete vagus nerve transection were

the lack of continuity in the nervous tissue along the subdiaphragmatic part of the oesophagus together with the presence of gastric distension.

5.6.2. Surgical procedure of unilateral brainstem transection and tissue preparation

Adult male Sprague-Dawley rats (n=19) were deeply anesthetized, and under stereotaxic guidance, a 3mm-wide glass knife was lowered into the brain at the level of mesencephalon, parallel with the coronal plane. The coordinates of the medial edge of the knife were: anterior–posterior, −5.6mm from the Bregma; lateral, 0mm; and dorsoventral, −9.1mm from the surface of the skull. Additional four animals were operated the same way, although the glass knife was not lowered into the brain (sham-transected animals). After 2 weeks of survival, the animals with transection were divided into two groups: the first group was fasted for 40 hours (n=12), whereas the second group and the sham-transected animals were fasted for 40 hours and then given free access to food for 2 hours before perfusion (n=7).

5.6.3. Determination of the effectiveness of brainstem transections by double-labelling immunofluorescence for dopamine β-hydroxylase (DBH) and POMC

Since the catecholaminergic, DBH containing axons originate exclusively in the brainstem, the effectiveness of the unilateral brainstem transections was verified by comparison of the DBH-IR innervation of the POMC neurons in the transected and intact side of ARC. After pretreatment, free-floating tissue sections of rats with unilateral transection were incubated in a mixture of mouse monoclonal antibodies against DBH (dilution 1:1000; Millipore, Billerica, MA, USA) and rabbit antiserum against POMC (dilution 1:2000; Phoenix Pharmaceuticals INC., Burlingame, CA, USA) for 2 days at 4 °C. After washing, the sections were immersed in a mixture of Alexa 555-conjugated donkey anti-mouse IgG (dilution 1:500; Invitrogen, Carlsbad, CA, USA) and fluorescein isothiocyanate (FITC)-conjugated donkey anti-rabbit IgG (dilution 1:50; Jackson ImmunoResearch) for 2 hours at room temperature (**Table 1**, end of this chapter). After additional washing, the sections were mounted on glass slides and coverslipped with Vectashield mounting medium (Vector Laboratories Inc.).

5.6.4. Image acquisition and analysis for determination of the effectiveness of transections

The sections were examined and images were taken using a Radiance 2100 confocal microscope (Bio-Rad Laboratories, Hemel Hempstead, UK). At least two sections were analyzed from each brain from different rostro-caudal levels of the ARC. With a 60X oil immersion objective. Serial optical sections of 180×180 μm areas covering the ARC were recorded on both sides of each section. The sections were scanned in one step for FITC and Alexa 555 using laser excitation lines 488 nm for FITC and 543 nm for Alexa 555, and dichroic/emission filters 560/500–530 nm for FITC and 560–610 nm for Alexa 555. Pinhole sizes were set to obtain optical slices < 0.7 μm thick, and the series of optical slices were recorded with a 0.75-μm Z-step. The series of optical sections were merged and displayed with Laservox (Media Cybernetics Inc., Bethesda, MD, USA) software. Perikarya and proximal dendrites of the POMC neurons were traced through the optical slices, and the DBH boutons juxtaposed to the POMC neurons were counted. Only brains with more than 60% reduction of the DBH innervation of POMC neurons on the transected side were used for double-labelling immunofluorescence of c-Fos and POMC (n=5 in each group).

5.6.5. Determination of the refeeding-induced activation of the ARC POMC neurons using double-labeling immunofluorescence for c-Fos and POMC in vagotomized animals and in rats with unilateral transection of ascending brainstem pathways

Free-floating sections of fasted and refed vagotomized rats and animals with unilateral transection of ascending brainstem pathways were pretreated and were then incubated in rabbit c-Fos antiserum (dilution 1:10000; Calbiochem, San Diego, CA, USA) followed by biotinylated donkey anti-rabbit IgG (dilution 1:500) and ABC (dilution 1:1000). After amplification with the tyramide signal amplification (TSA) kit (Perkin Elmer Life and Analytical Sciences, Waltham, MA) according to the manufacturer's instructions, sections were incubated in streptavidin-labelled FITC (dilution 1:250; Vector Laboratories Inc.) and rabbit POMC antiserum (dilution 1:2000). After additional washing, the sections were incubated in Alexa 555 conjugated donkey anti-rabbit IgG (dilution 1:500) (**Table 1**).

To determine the percentage of POMC-containing neurons of the ARC that contain c-Fos, images of the double-labelled preparations were taken using Zeiss AxioPlan2 or

AxioImager epifluorescent microscopes (Carl Zeiss). The same field was double-exposed when switching the filter sets for each fluorochrome and superimposed using Adobe Photoshop (Adobe Systems Inc., San Jose, CA, USA) to create composite images for analysis. The number of single and double-labelled POMC-IR neurons was counted and the percentage of double-labeled neurons was calculated.

5.6.6. Statistical analysis

Comparison of the data was performed with two-way ANOVA and one-way ANOVA followed by a Newman–Keuls multiple comparisons post-hoc test. Food and water intake of the vagotomized and sham-vagotomized rats was analyzed using Student's t-test. $P<0.05$ was considered statistically significant. Results are presented as the mean±SEM.

5.7. Mapping the connections of parabrachial nucleus and the central nucleus of amygdala with other refeeding-activated neuronal groups

5.7.1. Retrograde tract tracing experiments

The retrograde tracer cholera toxin β subunit (CTB; List Biological Laboratories, Campbell, CA) was injected by iontophoresis into the region of PBN in 3 adult, male Wistar rats and into the region of CEA of 23 animals. Rats were anesthetized and their head positioned in a stereotaxic apparatus with the Bregma and lambda in the horizontal plane. Through a burr hole in the skull, a glass micropipette (17.5-20 μm outer tip diameter) filled with 0.5% CTB in 0.01M PB at pH 8.0 was lowered into the brain at stereotaxic coordinates corresponding to the PBN (anteroposterior, -9.3 mm from the Bregma; lateral,- 2.0 mm; and dorsoventral, -7.0 mm from the surface of the skull), and to the CEA (anteroposterior: -2.4 mm, mediolateral: -4.2 mm, dorsoventral: -8.2 mm) based on the atlas of Paxinos and Watson (Paxinos and Watson, 1998). The CTB was deposited for 10 min (6 μA (PBN) or 5 μA (CEA) positive current, pulsed on—off at 7s intervals) using a constant-current source (Stoelting, Wood Dale, IL). Seven-ten days after tracer deposition, rats were fasted for 48 h and then given free access to food for 2 hours. Immediately after refeeding, the animals were perfused with fixative and sections were prepared as described above.

5.7.2. Anterograde tract tracing experiments

The anterograde tracer, Phaseolus vulgaris leucoagglutinin (PHAL; Vector Laboratories Inc.) was injected into the PBN of 5 Wistar rats, and an additional 11 Wistar rats received PHAL injection into the region of CEA. The animals were anesthetized intraperitoneally with ketamine-xylazine and their head mounted in a stereotaxic apparatus as described above. Using the same stereotaxic coordinates as for the retrograde tract tracing experiment described above, 2.5% PHAL in 0.01M PB at pH 8.0 was injected by a glass micropipette into the PBN using iontophoresis (6 μA positive current, pulsed on—off at 7 s intervals) for 15-20 min. Following a 10-day transport time, the animals were fasted for two days and then refed for two hours. Perfusion of the animals with fixative, sectioning of the tissue, and the pretreatment of the sections for immunohistochemistry were performed as described above.

5.7.3. Localization of the CTB injection sites

CTB immunohistochemistry was performed to identify the core of the injection site in the PBN. One of the four series of sections was pre-treated as described above. The sections were then incubated in goat anti-CTB serum (1:10,000, List Biological Laboratories) for 48 hours. Following washes in PBS, the sections were immersed in biotinylated donkey anti-sheep IgG (1:500; Jackson ImmunoResearch) and incubated for 2 hours at room temperature. After rinsing with PBS, the sections were incubated in ABC at 1:1000 dilution for 1 hour. The peroxidase activity was visualized by Ni-DAB developer. The sections were mounted on gelatin coated slides, air dried, counterstained with 1% cresyl violet and coverslipped with DPX mounting medium (Sigma-Aldrich Inc.).

To facilitate the localization of the injection sites in the CEA, the core of the CTB injection sites were assessed after double-labeling of the sections for CTB and c-Fos. The early gene, c-Fos, was used to mark the CEA, since neurons of CEA are activated by refeeding, while the surrounding regions do not show c-Fos-immunoreactivity in refed animals. Sections pre-treated as described above were incubated in a mixture of primary antisera: goat anti-CTB serum (1:5000, List Biological Laboratories) and rabbit anti-c-Fos serum (1:1500, Oncogene, MA, USA) for 48 hours. After washing in PBS, the sections were incubated in biotinylated donkey anti-sheep IgG (Jackson ImmunoResearch) at 1:500 for 2 h at room temperature. After further rinsing in PBS, the

sections were incubated in ABC (1:1000) for 1 h. Following rinses in PBS, the immunoreaction was intensified with biotinylated tyramide using the TSA kit. Finally, the sections were incubated in the cocktail of dichlorotriazinylamino fluorescein (DTAF)-conjugated streptavidin (1:250) and Alexa555-conjugated donkey anti-rabbit IgG (1:500, Invitrogen) for 2 hours, mounted onto glass slides and coverslipped with Vectashield mounting medium (**Table 1**).

5.7.4. Immunohistochemistry for localization of the PHAL injection sites

To determine the location of the PHAL injection sites, single labeling immunohistochemistry was performed on one series of sections incubated in rabbit anti-PHAL serum (Vector Laboratories, Inc.) at 1:10,000 dilution in antibody diluent for 1 day at room temperature. After washing in PBS, the sections were incubated in biotinylated donkey anti-rabbit IgG (Jackson ImmunoResearch) at 1:500 for 2 h at room temperature, rinsed in PBS, and incubated in ABC solution at 1:1000 dilution for 1 h. Following rinses in PBS, peroxidase activity was visualized with Ni-DAB developer. Sections were mounted on gelatin coated slides, air dried, counterstained with 1% cresyl violet and coverslipped with DPX mounting medium (Sigma-Aldrich Inc.).

Evaluation of PHAL injection sites in the CEA was performed using double-labeling fluorescent immunohistochemistry for PHAL and c-Fos to reveal the location and extent of injection sites using refeeding-induced c-Fos activation as a marker for the CEA. Following standard pre-treatment as described above, sections were incubated in a mixture of primary antisera: goat anti-PHAL serum (1:1000, Vector Laboratories, Inc.) and rabbit anti-c-Fos serum (1:1500), diluted in PBS containing 2% normal horse serum and 0.2% sodium azide (antibody diluent) for 1 day at room temperature. After washing in PBS, sections were incubated in biotinylated donkey anti-sheep IgG (1:500) for 2 h at room temperature. After further rinsing in PBS, the sections were incubated in ABC (1:1000) for 1 h, and then subjected to biotinylated tyramide amplification using the TSA kit. After further washes, the sections were incubated in the cocktail of DTAF-conjugated streptavidin (1:250) and Alexa555-conjugated donkey anti-rabbit IgG (1:500) for 2 h, mounted onto glass slides and coverslipped with Vectashield mounting medium (**Table 1**).

5.7.5. Immunohistochemistry to identify of the sources of the refeeding-activated inputs of the PBN and CEA

Double-labeling, light microscopic immunohistochemistry was performed to map the location of the refeeding-activated neurons projecting to the CEA. Following pretreatment, the sections were incubated in rabbit antiserum against c-Fos (1:10,000), followed by washing in PBS and incubation in biotinylated donkey anti-rabbit IgG (1:500, Jackson ImmunoResearch) for 2h. After further rinsing in PBS, the sections were incubated in ABC (1:1000) for 1 h. The tissue-bound peroxidase activity was visualized by Ni-DAB developer followed by silver-gold intensification (Liposits et al., 1984). In the second step, the sections were incubated in goat anti-CTB (1:5000) serum for two days at 4ºC, followed by biotinylated donkey anti-sheep IgG (1:500) for 2h and ABC (1:1000) for 1h. The CTB-IR sites were visualized with brown DAB developer (0.05% diaminobenzidine and 0.005% H_2O_2 in 0.05 M Tris buffer). The sections were mounted onto glass slides and coverslipped with DPX mounting medium.

To map the refeeding-activated inputs of the PBN and CEA and determine whether the POMC neurons of the ARC are also among the refeeding-activated inputs of these nuclei, triple-labeling immunofluorescence was performed for POMC, CTB and c-Fos on sections from animals with CTB injection positioned into the PBN or CEA. After the pre-treatment, the sections were incubated in a mixture of goat anti-CTB serum at 1:10,000 dilution and rabbit anti-c-Fos serum at 1:2000 dilution for 2 days at 4 °C. Following washes in PBS, the sections were immersed in biotinylated donkey anti-sheep IgG (1:500, Jackson ImmunoResearch) and incubated for 2 h at room temperature. After rinsing with PBS, sections were incubated in ABC solution at 1:1000 dilution for 1 h, rinsed in PBS and the immunoreaction amplified with the TSA kit. After further washes, the sections were incubated in a cocktail of streptavidin-conjugated FITC at 1:250 dilution (Vector Laboratories, Inc.) and Alexa 555-conjugated anti rabbit IgG at 1:500 dilution, and then incubated in rabbit antiserum against POMC at 1:2000 dilution for 2 days at 4 °C. Following washes in PBS, the sections were incubated in Cy5-conjugated anti-rabbit IgG for 2 hours at room temperature, mounted onto glass slides, air dried, and coverslipped with Vectashield mounting medium (**Table 1**).

5.7.6. Identification of the refeeding-activated targets of the PBN and CEA using triple-labeling immunofluorescence for PHAL, c-Fos and the neuronal marker HuC/HuD

To identify the brain regions where refeeding-activated neurons are contacted by axons of PBN and CEA neurons, triple-labeling immunofluorescence for PHAL, c-Fos and HuC/HuD was performed on sections of animals with a PHAL injection site confined within the area of the PBN or CEA. HuC/HuD-immunoreactivity was used to label the cytoplasm of neurons. Following pre-treatment, the sections were incubated in anti-PHAL serum at 1:5000 dilution for 2 days at room temperature, followed by biotinylated donkey anti-rabbit IgG (Jackson ImmunoResearch) diluted to 1:500 and then ABC (1:1000) for 1 hour after rinses in PBS. The immunoreaction was amplified with TSA kit, and after further washes, the sections were incubated in streptavidin-conjugated Alexa 555 (1:500; Vector Laboratories, Inc.). Then, the sections were incubated in a mixture of rabbit antiserum against c-Fos at 1:2000 dilution and mouse antiserum against HuC/HuD (Molecular Probes, Eugene, Oregon) at 1:500 dilution for 2 days at 4°C. After washes in PBS, the sections were immersed in a cocktail of FITC-conjugated donkey anti-rabbit IgG (Jackson ImmunoResearch) at 1:250 dilution and Cy5-conjugated donkey anti-mouse IgG (Jackson ImmunoResearch) at 1:100 dilution for 2 hours at room temperature (**Table 1**). The sections were then mounted onto glass slides and coverslipped with Vectashield mounting medium.

5.7.7. Image acquisition and analysis for the PBN and CEA tract-tracing studies

The DAB- and Ni-DAB-labeled immunohistochemical preparations were examined and imaged using a Zeiss AxioImager M1 microscope equipped with an AxioCam MR digital camera (Carl Zeiss AG). The fluorescent preparations were examined with a Nikon A1R Confocal System (Nikon Instruments Ltd.). Confocal images were taken using line by line sequential scanning with laser excitation lines 488 nm for FITC, 561.6 nm for Alexa 555 and 641.8 for Cy5, dichroic mirror 405/488/561/640, emission filters 525/50 for FITC, 595/50 for Alexa 555 and 700/50 for Cy5 fluorophores were used. For 20x and 60x oil lenses, pinhole sizes were set to obtain optical slices of 2 and 1 μm thickness, respectively, and the series of optical sections were recorded with 2.0 and 1.0 μm Z steps. To enhance visibility of triple-labeled PHAL/c-Fos/ HuC/HuD and CTB/c-Fos/POMC cell bodies, consecutive optical sections (from 3

to 10) were projected into one image with ImageJ image analysis software (public domain at http://rsb.info.nih.gov/ij/download/src/). Adobe Photoshop 7.0 (Adobe Systems Inc.) was used to create composite images and to modify brightness and contrast of the images. Line drawings representing the distribution of c-Fos of fasted and refed rats were made using Corel Draw 11 (Corel Corporation, Ottawa, Canada).

5.8. Elucidation of the role of the CEA subnuclei in the development of satiety during refeeding

5.8.1. Stereotaxic injection of hSyn-hM3D(Gq)-mCherry adeno-associated virus (AAV)

The hSyn-hM3D(Gq)-mCherry AAV virus was injected into the CEA of 24 Wistar rats. The surgeries were performed in a biosafety level 2 virus injection facility. The rats were anesthetized and their head positioned in a stereotaxic apparatus with the bregma and lambda in the horizontal plane. Through a burr hole in the skull, a glass pipette (20-μm outer tip diameter) connected to a Nanoject II/Nanoliter 2000 microinjector (Drummond Scientific Co. or WPI Inc.) was lowered into the brain at stereotaxic coordinates corresponding to the medial part of CEA (CEAm) (anteroposterior: -2.4 mm, mediolateral: -3.9 mm, dorsoventral: -8.2 mm), or CEAlc (anteroposterior: -2.4 mm, mediolateral: -4.45 mm, dorsoventral: -8.25 mm) based on the atlas of (Paxinos and Watson, 1998). The virus containing solution (80-100nl; 4.5 $x10^{12}$ virus/ml) was injected unilaterally into the CEA with 5nl/sec speed. Five minutes after the injection, the pipette was removed slowly, the scalp was sutured and the rats were housed in biosafety level 2 quarantine for 2 weeks before experimentation.

5.8.2. Examination of the effects of the chemogenetic activation of CEA

Experimental animals were transferred to the biosafety level 1 room 2 days before the beginning of the experiment to let the animals habituate to the metabolic cages. Each cage had calibrated food sensor that recorded food eaten to a sensitivity of 0.01 g. Food spillage was minimized by a catch tray.

Half of the animals were injected intraperitoneally with clozapine-N-oxide (CNO; RD-4936/50, Tocris Bioscience (Bristol, UK)) dissolved in saline (3mg/kg BW) and the other half were treated with saline alone after 40 hours fasting. Fifteen min after the injection, rats received food and the food intake was monitored during the 20 hours

refeeding period. One week later, the experiment was repeated as follows: rats that were injected with CNO in the first experiment received saline injection, and the saline treated rats received CNO injection after 40 hours fasting. The food intake was monitored using the PhenoMaster system (TSE Systems GmbH, Bad Homburg, Germany). Food was measured by highly reliable sensors. The food intake was recorded at intervals of 1 min, and the cumulative food intake was calculated from these data.

One week after the second treatment, the rats were fasted for 40 hours and then the first injection protocol was repeated with the difference that the animals did not receive food. Two hours after the treatment, the animals were deeply anesthetized with ketamine-xylazine and perfused transcardially with fixative.

5.8.3. Statistical analysis of the food intake data

The food intake of CEAm and CEAlc injected rats was compared after saline or CNO injection. Data were analyzed by repeated measures ANOVA followed by Tukey HSD test.

5.8.4. Localization of the virus injection sites

The virus injection site was detected based on the fluorescence of hM3D(Gq)-mCherry fusion protein. Sections were mounted onto glass slides and coverslipped with Vectashield mounting medium. Only animals with virus injection site confined within the CEA were included in the studies.

5.8.5. Identification of brain areas activated by the chemogenetic stimulation of CEA neurons using triple-labeling immunofluorescence for c-Fos, RFP and HuC/HuD

To identify the brain areas activated by the stimulation of the CEA, triple immunofluorescent labeling was carried out on sections obtained from the chemogenetic activation experiment as described above to detect c-Fos expressing neuronal groups directly contacted by axons of CEA neurons. Following standard pre-treatment as described above, sections were incubated in a mixture of the following primary antisera: rabbit anti-c-Fos serum (1:10,000) and mouse anti-HuC/HuD serum (1:500). After incubation in biotinylated donkey anti-rabbit IgG (1:500, 2h), the sections were rinsed in PBS followed by the ABC and biotinylated tyramide amplification using the TSA kit. C-Fos immunoreactivity was detected with FITC-conjugated streptavidin (1:250) and the

sections were than incubated in DyLight 649-conjugated anti-mouse IgG (1:100, Jackson ImmunoResearch). Then, the sections were incubated in rabbit anti-RFP serum (1:3000, Rockland Immunochemicals Inc. Limerick, PA) for 48 hours. After rinsing in PBS, the immunoreaction was visualized with Alexa555-conjugated donkey anti-rabbit IgG (1:500) for 2 hours, mounted onto glass slides and coverslipped with Vectashield mounting medium (**Table 1**). In this experiment, c-Fos-immunoreactivity labeled the activated neurons, HuC/HuD-immunoreactivity labeled the cytoplasm of neurons, while the RFP antiserum detected the mCherry part of the hM3D(Gq)-mCherry fusion protein and therefore labeled the axons of the CEA neurons. The HuC/HuD labeling of neuronal cytoplasm enabled us to examine the RFP-IR contacts on the surface of c-Fos-IR neurons.

5.8.6. Image acquisition and analysis

To localize the injection site of the hM3D(Gq)-mCherry expressing AAV virus, the fluorescence of mCherry was examined with a Zeiss AxioImager M1 epifluorescent microscope (Carl Zeiss AG). Sections were examined under fluorescent illumination through Zeiss Filter Set 43 DsRed RL: Images were captured with the Zeiss AxioImager M1 microscope using AxioCam MRc 5 digital camera (Carl Zeiss AG) and AxioVision 4.6 software (Carl Zeiss AG).

To identify the brain regions directly activated by the CEA neurons, the triple-labeled fluorescent sections were analyzed by a ZEISS LSM 780 confocal microscope with Plan-Apochromat 10x0.45 M27, 20x 0.8 M27, 40x1.40 Oil DIC M27, 63x1.40 Oil DIC M27 objectives (Carl Zeiss AG). The sections were sequentially scanned for FITC, Alexa 555 and DyLight 649 using laser excitation lines 488 nm for FITC, 561 nm for Alexa 555 and 633 nm for DyLight 649 and dichroic/emission filter wavelength 488/493–556 nm for FITC, 561/570-624 nm for Alexa 555 and 633/638-759 nm for DyLight 649. Pinhole sizes were set to obtain the minimal thickness of optical slices.

The number of the c-Fos-IR cell nuclei in the different brain regions was counted with ImageJ software (http://rsbweb.nih.gov/ij/) using automatic particle analysis. The color images were converted to black and white images. The monochrome images were thresholded. The threshold range was set to differentiate the c-Fos containing nuclei apart from the background.

The association of CEA axons and the activated neurons were studied in the activated regions.

5.8.7. Statistical analysis of the CEA activation induced neuronal activation in refeeding-related areas

The number of c-Fos containing cells in the distinct brain areas of the CEAm and CEAlc injected rats were compared after saline or CNO treatment by one-way ANOVA followed by Tukey HSD post hoc test.

Table 1 Summary of antibodies, fluorochromes and chromogens used for immunohistochemical studies.

Detected Antigen	Primary antibody	Detection
c-Fos	rabbit antiserum against c-Fos (Oncogen; 1:10000)	biotinylated-anti-rabbit IgG (Jackson), ABC biotinylated tyramide amplification, Ni-DAB
		Nissl-staining
DBH/ POMC	mouse antiserum against DBH (oncogene; 1:1000)	Alexa 555-conjugated donkey anti-mouse IgG (Invitrogen)
	rabbit antiserum against POMC (Phoenix; 1:2000)	FITC-conjugated donkey anti-rabbit IgG (Jackson)
c-Fos/ POMC	rabbit antiserum against c-Fos (Oncogen; 1:10000)	biotinylated donkey anti-rabbit IgG (Jackson), ABC, biotinylated tyramide amplification, streptavidin-labeled FITC (Vector)
	rabbit antiserum against POMC (Phoenix; 1:2000)	Alexa 555-conjugated donkey anti-rabbit IgG (Jackson)
CTB	goat antiserum against CTB (Listlab; 1:10000)	biotinylated donkey anti-sheep IgG (Jackson), ABC, Ni-DAB
		Nissl-staining
PHAL	goat antiserum against PHAL (Vector; 1:10000)	biotinylated donkey anti-sheep IgG (Jackson), ABC, Ni-DAB
		Nissl-staining
CTB/ c-Fos	goat antiserum against CTB (Listlab; 1:5000)	biotinylated donkey anti-sheep IgG (Jackson), ABC, DAB
	rabbit antiserum against c-Fos (Oncogen; 1:10000)	biotinylated donkey anti-rabbit IgG (Jackson) ABC, Ni-DAB
CTB/ c-Fos/ POMC	goat antiserum against CTB (Listlab; 1:10000)	biotinylated-anti-sheep IgG (Jackson), ABC, biotinylated tyramide amplification, streptavidin-labeled FITC (Vector)
	rabbit antiserum against c-Fos (Oncogen; 1:2000)	FITC-conjugated donkey anti-rabbit IgG (Jackson)
	rabbit antiserum against POMC (Phoenix; 1:2000)	Cy5 donkey anti-rabbit IgG (Jackson)
PHAL/ c-Fos/ HuC/HuD	goat antiserum against PHAL (Vector; 1:5000)	biotinylated donkey anti-sheep IgG (Jackson), ABC, biotinylated tyramide amplification, streptavidin-labeled Alexa 555 (Vector)
	rabbit antiserum against c-Fos (Oncogen; 1:2000)	FITC-conjugated donkey anti-rabbit IgG (Jackson)
	mouse antiserum against HuC/HuD (Molecular probes; 1:500)	Cy5-anti-mouse IgG (Jackson)
c-Fos/ RFP/ HuC/HuD	rabbit antiserum against c-Fos (Oncogen; 1:10000)	biotinylated-anti-rabbit IgG (Jackson), ABC, biotinylated tyramide amplification, streptavidin-labeled FITC (Vector)
	rabbit anti-RFP (1:3000, Rockland)	Alexa 555-conjugated donkey anti-rabbit IgG (Jackson)
	mouse antiserum against HuC/HuD (Molecular probes; 1:500)	DyLight 649-conjugated anti-mouse IgG (Jackson)

DOI:10.14753/SE.2017.2041

6. RESULTS

6.1. Refeeding-activated neuronal groups in the rat brain

Brain areas showing altered number of c-Fos-containing neurons in refed compared to fasted rats are summarized in **Figure 5**, **Figure 6** and **Table 2**. In the forebrain, the highest density of c-Fos-containing cells was detected in antero-posterior direction in the following areas: the prelimbic area (Prl), the bed nucleus of stria terminalis (BST), primarily the medial subdivision including the anterior and ventral parts, DMN, lateral preoptic area (LPO), CEAm, CEAlc (**Figure 18**), the ventral and lateral parvocellular subdivisions of the PVN (PVNv, PVNl), ARC and the parasubthalamic nucleus (PSTN). In the brainstem, a large number of c-Fos-IR neurons was observed in the medial and lateral parts of the PBN (PBm, PBl) (**Figure 11**), in the medial, intermediate and commissural subdivisions of the NTS and the area postrema. Moderate to weak neuronal activation was found in the somatosensory cortex representing the oral surface, jaw and upper lip region, medial orbital cortex, lateral olfactory tract, piriform-amygdalar area, olfactory tubercle, posterolateral cortical amygdaloid nucleus, agranular insular area (AIA) and secondary motor cortex. Moderate neuronal activation was seen in the amygdaloid complex in the medial nucleus of amygdala and the cortical amygdaloid nucleus and in the diencephalon including the anterior hypothalamic area, lateral hypothalamic area (LH), lateral and dorsomedial posterior arcuate nucleus (ARCdmp), zona incerta, paraventricular thalamic nucleus and paratenial thalamic nucleus. In the metencephalon, moderate to weak c-Fos activation was present in the dorsal raphe nucleus. There was also a redistribution in the pattern of c-Fos containing neurons in the ventrolateral part of the periaqueductal grey (PAGvl). In the fasted rats, the c-Fos containing nuclei were concentrated in the lateral part of PAGvl, while the number of c-Fos-IR nuclei decreased in this region and a diffuse neuronal activation was apparent in the lateral and ventrolateral periaqueductal grey. Nevertheless, intense neuronal activation was seen in the fasted rats in the nucleus reuniens, midbrain reticular nucleus and pontine gray. Moderate to weak activation was found in fasted rats compared to the refed rats in the lateral septal nucleus.

DOI:10.14753/SE.2017.2041

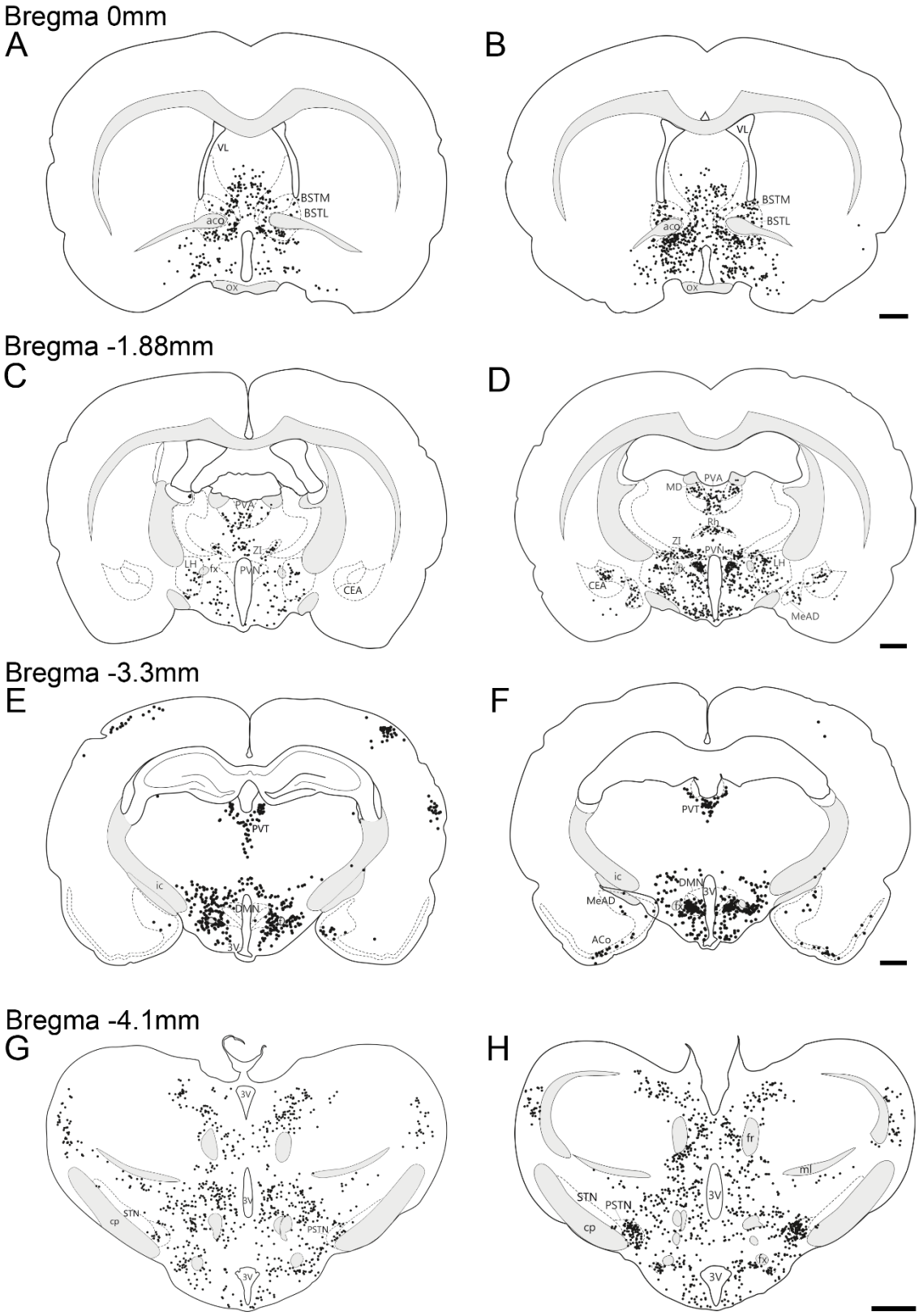

DOI:10.14753/SE.2017.2041

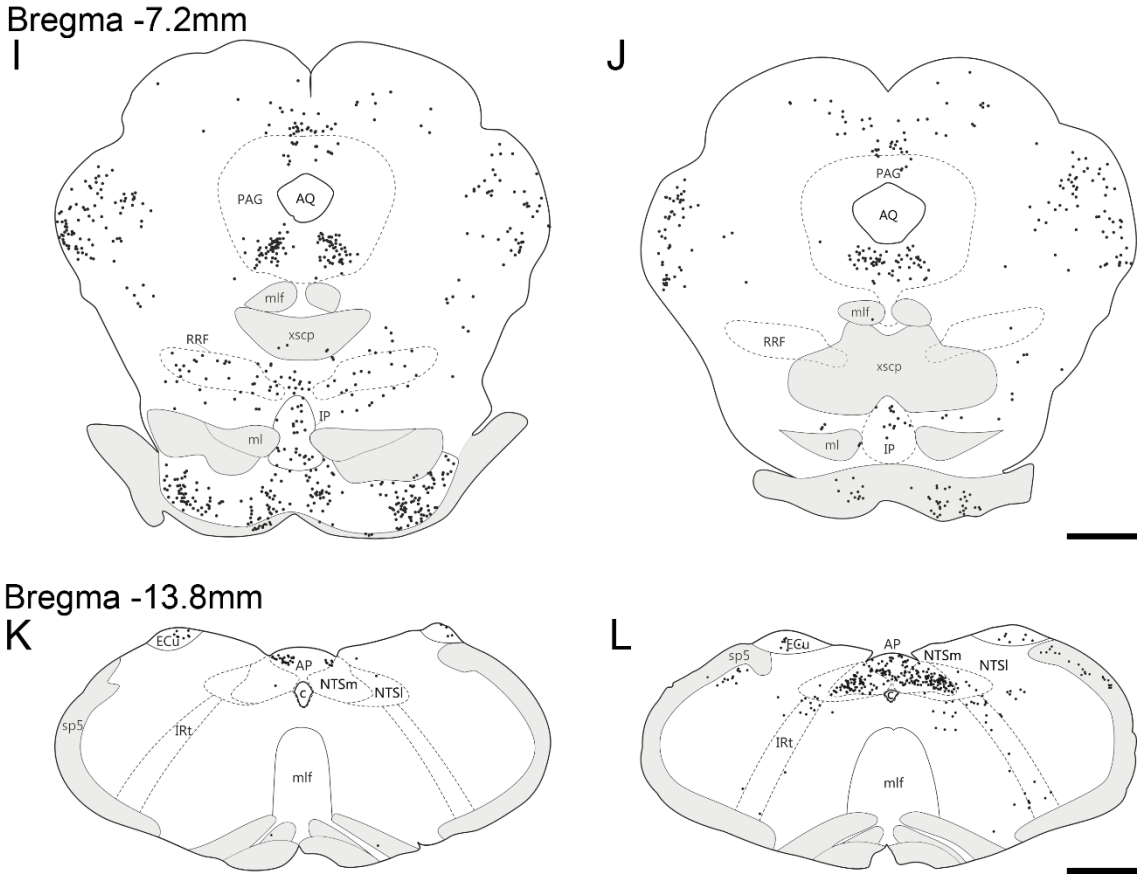

Figure 5 Schematic drawings illustrate the distribution of c-Fos-immunoreactive (IR) neurons in representative coronal sections of the rat brain. Drawings of the left column (**A, C, E, G, I, K**) show the distribution of c-Fos-IR nuclei after two days of fasting, while drawings in the right column (**B, D, F, H, J, L**) illustrate the pattern of c-Fos-immunoreactivity in rats refed for 2h after 2 days of fasting. The c-Fos-containing neurons are visualized by black dots. Scale bar=1mm

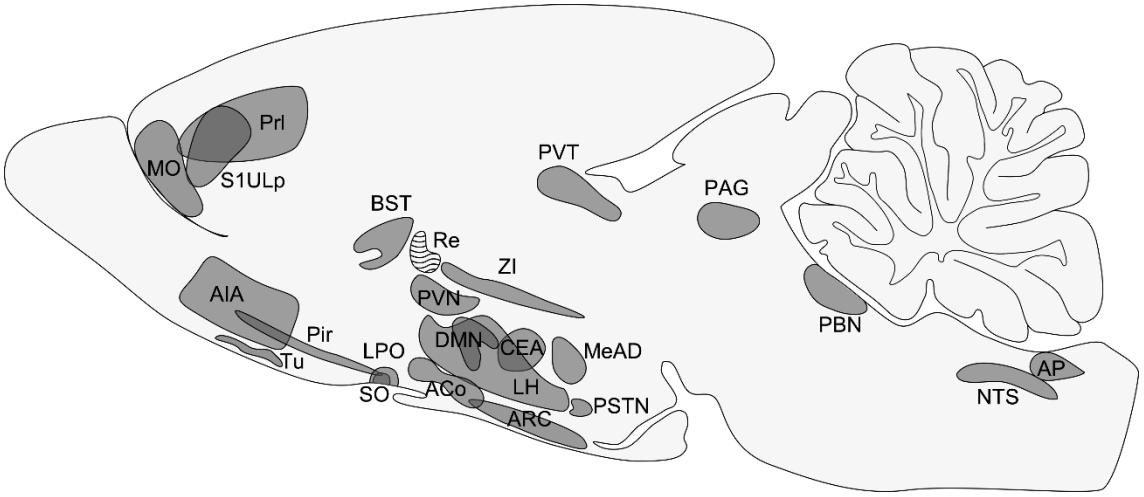

Figure 6 Schematic drawing illustrates the areas showing the most pronounced changes in the number of c-Fos-containing nuclei in refed rats compared to the fasted rats. The dark gray color indicates increase, the white area with waves indicates decrease of the number of c-Fos-IR nuclei.

DOI:10.14753/SE.2017.2041

Table 2 c-Fos-immunoreactivity (c-Fos-ir) in brains from fasted and refed rats mapped to Swanson (2004)

	Density of c-Fos-ir[(1)]	
Cell Group or Region (Abbreviation, *Swanson Atlas Level*)	**Fasted**	**Refed**
Cerebrum (CH)		
Cerebral Nuclei		
Pallidum		
Globus pallidus (GP)		
Medial globus pallidus (GPi, *27*)	(+)	(+)
Lateral globus pallidus (GPe, *27*)	(-)	(-)
Substantia innominata (SI, *27*)	(-)	(-)
Medial septal complex (MSC)		
Medial septal nucleus (MS, *18*)	++++	+++*
Bed nuclei of terminal stria (BST)		
Anteromedial area (BSTam, *18*)	+++	++++*
Striatum		
Lateral septal nucleus (LS)		
rostral (rostroventral) part (LSr, *18*)	+	+*
ventral part (LSv, *18*)	++++	+++
Caudoputamen (CP, *27*)	(-)	(-)
(CP, *30*)	(-)	(+)
Central amygdalar nucleus (CEA)		
Medial part (CEAm, *27*)	(-)	(+++)
Lateral part (CEAl, *27*)	(-)	(++)
(CEAl, *30*)	(-)	(-)
Intercalated amygdalar nuclei (IA, *27*)	(-)	(-)
(IA, *30*)	(-)	(-)
Medial amygdalar nucleus (MEA)		
Anteroventral part (MEAav, *27*)	(+)	(++)
Anterodorsal part (MEAad, *27*)	(+)	(+)
Posterodorsal part, *sublayer c* (MEApd.c, *30*)	(-)	(++)
Cerebral Cortex (CTX)		
Cortical Plate (CTXpl)		
Limbic region		
Olfactory region (OLF)		
Piriform area (PIR)		
molecular layer (PIR1, *27*)	(-)	(+)
(PIR1, *30*)	(-)	(+)
pyramidal layer (PIR2, *27*)	(-)	(-)
(PIR2, *30*)	(-)	(+)
polymorph layer (PIR3, *27*)	(-)	(-)
(PIR3, *30*)	(-)	(++)

DOI:10.14753/SE.2017.2041

Cell Group or Region (Abbreviation, *Swanson Atlas Level*)	Density of c-Fos-ir[(1)] Fasted	Refed
Cortical amygdalar complex		
Cortical amygdalar area (COA)		
Anterior part (COAa, *27*)	(+)	(++)
Posterior part (COAp, *30*)		
Medial zone (COApm, *30*)		
layer 1	(-)	(+)
layer 3	(+)	(+)
Lateral zone (COApl, *30*)		
layer 1	(-)	(-)
layer 2	(-)	(+)
layer 3	(+)	(+)
Piriform-amygdalar area (PAA, *30*)		
layer 1	(-)	(+++)
layer 3	(-)	(-)
Retrohippocampal region (RHP)		
Entorhinal area (ENT)		
Lateral part (ENTl)		
layer 1 (ENTl1)	(-)	(-)
layer 2 (ENTl2)	(-)	(-)
layer 3 (ENTl3)	(-)	(-)
layer 4 (ENTl4)	(-)	(-)
layer 5 (ENTl5)	(-)	(-)
layer 6 (ENTl6)	(-)	(-)
Cingulate region (CNG)		
Prelimbic area (PL)		
layer 1 (PL1, *8*)	-	+*
layer 2 (PL2, *8*)	-	++*
layer 3 (PL3, *8*)	-	+*
layer 5 (PL5, *8*)	-	++++*
layer 6a (PL6a, *8*)	-	+++*
Anterior cingulate area, dorsal part (ACAd)		
layer 1 (ACAd1, *8*)	-	+*
layer 5 (ACAd5, *8*)	+	+
layer 6a (ACAd6a, *8*)	+	+
layer 6b (ACAd6b, *8*)	-	-
Frontal region (FRO)		
Somatomotor areas (MO)		
Secondary somatomotor areas (MOs)		
layer 1 (MOs1, *8*)	-	+*
layers 2/3 (MOs2/3, *8*)	-	+*
layer 5 (MOs5, *8*)	+	+
layer 6a (MOs6a, *8*)	++*	+
layer 6b (MOs6b, *8*)	-	-

DOI:10.14753/SE.2017.2041

Cell Group or Region (Abbreviation, *Swanson Atlas Level*)	Density of c-Fos-ir[1] Fasted	Refed
Temporal region (TE)		
Perirhinal area (PERI)		
layer 1 (PERI1)	(-)	(-)
layer 3 (PERI3)	(-)	(-)
layer 5 (PERI5)	(+)	(-)
Ectorhinal area (ECT)		
layer 1 (ECT1)	(-)	(+)
layer 3 (ECT3)	(-)	(+)
layer 5 (ECT6)	(-)	(+)
Temporal association areas (TEa)		
layer 1 (TEa1)	(-)	(-)
layer 3 (TEa2)	(-)	(-)
layer 4 (TEa4)	(-)	(+)
layer 5 (TEa5)	(-)	(+)
Cortical subplate (CTXsp)		
Basolateral amygdalar complex		
Basomedial amygdalar nucleus (BMA)		
Anterior part (BMAa, *27*)	(-)	(+)
Posterior part (BMAp, *27*)[2]	(-)	(-)
(BMAp, *30*)	(-)	(+)
Basolateral amygdalar nucleus (BLA, *30*)		
Anterior part (BLAa, *27*)	(-)	(-)
Posterior part (BLAp, *30*)	(-)	(-)
Lateral amygdalar nucleus (LA, *27*)	(-)	(-)
(LA, *30*)	(-)	(-)
Posterior amygdalar nucleus (PA, *30*)	(+)	(-)
(PA, *33*)	-	-
Endopiriform nucleus (EP)		
Ventral part (EPv, *27*)	(-)	(-)
(EPv, *30*)	(-)	(-)
Dorsal part (EPd, *27*)	(-)	(-)
(EPd, *30*)	(-)	(-)
Interbrain (IB)		
Hypothalamus (HY)		
Periventricular hypothalamic zone		
Terminal lamina (lam)		
Median preoptic nucleus (MEPO, *18*)	+	+
Internuclear area, hypothalamic periventricular part (I, *30*)	++*	+
Anterodorsal preoptic nucleus (ADP, *18*)	++++	++++
Medial preoptic area (MPO, *18*)	++*	+++
Parastrial nucleus (PS, *18*)	++	++++*
Subparaventricular zone (SBPV, *26*)	+*	+
(SBPV, *27*)	+*	+

DOI:10.14753/SE.2017.2041

Cell Group or Region (Abbreviation, *Swanson Atlas Level*)	Density of c-Fos-ir[(1)] Fasted	Refed
Paraventricular hypothalamic nucleus, magnocellular division (PVHm)		
Posterior magnocellular part (PVHpm)		
lateral zone (PVHpml, *26*)	+	+++*
Paraventricular hypothalamic nucleus, parvicellular division (PVHp)		
Periventricular part (PVHpv, *27*)	+	+
Medial parvicellular part, dorsal zone (PVHmpd, *27*)	+	!!!!
[Lateral parvicellular part] (PVHlp, *27*)	++++	!!!!
[Forniceal part] (PVHf, *27*)	+*	++++
Supraoptic nucleus (SOg)		
retrochiasmatic part (SOr)	-	-
Neurohypophysis		
Infundibulum (INF)		
Median eminence (ME, *30*)	-	+
Arcuate hypothalamic nucleus (ARH, *30*)	-	++++
Periventricular hypothalamic nucleus intermediate part (PVi)	-	++
Dorsomedial hypothalamic nucleus (DMH)		
Anterior part (DMHa, *30*)	+	+
Posterior part (DMHp, *30*)	+	++
Ventral part (DMHv, *30*)	++*	!!!!!
Posterior hypothalamic nucleus (PH, *30*)	++*	+*
(PH, *33*)	!!!!	!!!!
Periventricular hypothalamic nucleus, posterior part (PVp, *33*)	+++*	++
Medial hypothalamic zone		
Anterior hypothalamic nucleus (AHN)		
Central part (AHNc, *27*)	+*	++*
Posterior part (AHNp, *27*)	++*	+++
Dorsal part (AHNd, *27*)	-	+
Ventromedial hypothalamic nucleus (VMH)		
Ventrolateral part (VMHvl, *27*)	+	+
(VMHvl, *30*)	++*	++
Central part (VMHc, *27*)	+*	++*
(VMHc, *30*)	+*	++
Dorsomedial part (VMHdm, *27*)	+*	+*
Ventral premammillary nucleus (PMv, *33*)	+++*	-
Dorsal premammillary nucleus (PMd, *33*)	+	++*
Mammillary body (MB)		
Tuberomammillary nucleus (TM)		
ventral part (TMv, *33*)	+	+
Medial mammillary nucleus (MMg)		
median part (MMe, *33*)	-	-
Supramammillary nucleus (SUM)		
lateral part (SUMl, *33*)	+++*	+

DOI:10.14753/SE.2017.2041

Cell Group or Region (Abbreviation, *Swanson Atlas Level*)	Density of c-Fos-ir[(1)] Fasted	Refed
Lateral hypothalamic zone		
Lateral preoptic area (LPO, *18*)	+*	++++
Lateral hypothalamic area (LHA)		
Anterior group (LHAag)		
Anterior region (LHAa)		
intermediate zone (LHAai, *26*)	+++	++++
dorsal zone (LHAad, *26*)	+	++++
Middle group (LHAmg)		
Medial tier (LHAm)		
Juxtaventromedial region (LHAjv)		
Ventral zone (LHAjvv, *27*) [(3)]	++	++
(LHAjvv, *30*)	++++*	+++
Dorsal zone (LHAjvd, *27*) [(3)]	+	++*
Juxtaparaventricular region (LHAjp, *26*)	+	++++
Juxtadorsomedial region (LHAjd, *27*)	+	+
(LHAjd, *30*)	++++*	++++
Perifornical tier (LHApf)		
Subfornical region (LHAsf)		
Anterior zone (LHAsfa, *27*)	+++*	!!!!*
Posterior zone (LHAsfp, *30*)	++	+++*
Premammillary zone (LHAsfpm, *33*)	++++	+++*
Suprafornical region (LHAs, *30*)	++++*	++
Lateral tier (LHAl)		
Tuberal nucleus (TU)		
Subventromedial part (TUsv, *27*)	-	++++
(TUsv, *33*)	-	-
Intermediate part (TUi, *27*) [(3)]	+*	-
(TUi, *33*)	-	+
Terete part (TUte, *33*)	-	+
Lateral part (TUl, *33*)	+	-
Ventral region (LHAv)		
Medial zone (LHAvm, *30*)	++++*	++++*
Lateral zone (LHAvl, *30*)	+	+
(LHAvl, *33*)	+	+
Parvicellular region (LHApc, *27*)	+	+
Magnocellular nucleus (LHAma, *30*)	+	-
Dorsal region (LHAd, *27*)	!!!!	!!!!
(LHAd, *30*)	++++	++++
Posterior group (LHApg)		
Posterior region (LHAp, *33*)	!!!!*	!!!!*
Parasubthalamic nucleus (PSTN, *33*)	++	!!!!*
Subthalamic nucleus (STN, *30*)	-	-
(STN, *33*)	+++	!!!!

DOI:10.14753/SE.2017.2041

Cell Group or Region (Abbreviation, *Swanson Atlas Level*)	Density of c-Fos-ir[(1)] Fasted	Refed
Thalamus (TH)		
Ventral part of thalamus (VNT)		
Zona incerta, general (ZIg)		
Zona incerta (ZI, *26*)	+++*	++++
(ZI, *27*)	+++*	!!!!!
(ZI, *30*)	++++	+++*
(ZI, *33*)	+++*	++*
Fields of Forel (FF, *33*)	++++	+
Dorsal part of thalamus (DOR)		
Midline thalamic nuclei (MTN)		
Nucleus reuniens (RE)		
Rostral division (REr, *26*) [(4)]	++++*	+++
Caudal division (REca, *27*) [(4)]	++	+++
Paraventricular thalamic nucleus (PVT, *25*)	++	++++
Paratenial nucleus (PT, *25*)	++	++++
Anterior thalamic nuclei (ATN)		
Anteromedial thalamic nucleus (AM, *25*)		
Dorsal part (AMd)	+	-
Intralaminar thalamic nuclei (ILM)		
Central medial thalamic nucleus (CM, *25*)	+	++
(CM, *33*)	+	-
Medial thalamic nuclei (MED)		
Perireuniens nucleus (PR, *27*)	+*	+*
(PR, *30*)	-	+
Submedial thalamic nucleus (SMT, *30*)	-	-
Mediodorsal nucleus of the thalamus (MD)		
Medial part (MDm, *25*)	-	+*
Ventral thalamic nuclei		
Ventral medial thalamic nucleus (VM, *30*)	-	-
Ventral posterior thalamic nucleus (VP)		
Ventral posteromedial thalamic nucleus, general (VPMg)		
Parvicellular part (VPMpc, *33*)	-	+*
Ventral posterolateral thalamic nucleus, general (VPLg)		
Parvicellular part (VPLpc, *33*)	-	-
Subparafascicular nucleus (SPF)		
Magnocellular part (SPFm, *33*)	+*	++*

DOI:10.14753/SE.2017.2041

Cell Group or Region (Abbreviation, *Swanson Atlas Level*)	Density of c-Fos-ir[(1)] Fasted	Refed
Midbrain (MB)		
Tegmentum (TG)		
Interpeduncular nucleus (IPN)		
apical subnucleus (IPNa, *43*)	+++	+
dorsomedial subnucleus (IPNd, *43*)	+	++
lateral subnucleus (IPNl, *43*)		
dorsal part (IPNld)	-	-
intermediate part (IPNli)	+	-
ventral part (IPNlv, *43*)	+	-
intermediate subnucleus (IPNi, *43*)	+	-
central subnucleus (IPNc, *43*)	+	-
Central linear raphe nucleus (CLI, *43*)	+	-
Superior central raphé nucleus (CS)		
medial part (CSm, *43*)	+	-
Dorsal raphe nucleus (DR, *43*)	+	-
(DR, *49*)	!!!!	+++
Ventral tegmental area (VTA, *43*)	-	+
Midbrain reticular nucleus (MRN)		
Magnocellular part (MRNm, *43*)	++++*	+++
Parvicellular part (MRNp, *43*)	++*	-
Retrorubral area (RR, *43*)	++++*	+
Periaqueductal gray (PAG)		
Medial division (PAGm, *43*)	-	+
Ventrolateral division (PAGvl, *43*)	!!!!	!!!!
Dorsolateral division (PAGdl, *43*)	-	-
Dorsal division (PAGd, *43*)	++	++
Midbrain nucleus of trigeminal nerve (MEV, *49*)	+	++
(MEV, *50*)	+	!!!!
(MEV, *69*)	-	-
Nucleus sagulum (SAG)	-	+
Parabigeminal nucleus (PBG, *43*)	-	-
Nucleus of brachium of inferior colliculus (NB)	+++*	!!!!
Tectum (TC)		
Superior colliculus (SC)		
zonal layer (SCzo, *43*)	-	+
superficial gray layer (SCsg, *43*)	-	-
sublayer a of intermediate gray layer (SCig.a, *43*)	-	++*
sublayer b of intermediate gray layer (SCig.b, *43*)	++*	++++*
sublayer c of intermediate gray layer (SCig.c, *43*)	++*	+++*
Inferior colliculus (IC)	-	-
Central nucleus (ICc, *49*)	!!!!!*	-
(ICc, *50*)	-	-
Dorsal nucleus (ICd, *49*)	!!!!	-
(ICd, *50*)	-	-

External nucleus (ICe, *43*)	+++*	++++
	Density of c-Fos-ir[(1)]	
Cell Group or Region (Abbreviation, *Swanson Atlas Level*)	**Fasted**	**Refed**
Rhombic Brain (RB)		
Hindbrain (HB)		
Pons (P)		
Motor nucleus of trigeminal nerve (V)		
Magnocellular part (Vma, *49*)	+	!!!!*
(Vma, *50*)	+++	!!!!!*
Parvicellular part (Vpc, *49*)	+*	-
(Vpc, *50*)	-	+
Pontine nuclei, general (PGg)		
Pontine nuclei (PG, *43*)	!!!!!	+
Tegmental reticular nucleus (TRN, *49*) [(5)]	++	+
(TRN, *50*) [(5)]	+++	++
Magnus raphe nucleus (RM, *49*)	+	+
(RM, *50*)	+	+
Pontine raphe nucleus (RPO, *49*)	+++	+++*
(RPO, *50*)	+++*	+*
Pontine reticular nucleus, Caudal part (PRNc, *49*)	!!!!*	++++
(PRNc, *50*)	!!!!*	++++*
Pedunculopontine nucleus (PPN, *43*)	+++	++*
Supratrigeminal nucleus (SUT, *49*)Pontine central gray, general (PCGg)		
Pontine central gray (PCG, *49*)	!!!!	++++*
(PCG, *50*)	+++*	++*
Nucleus incertus (NI)		
compact part (NIc, *50*)	++++	++++
diffuse part (NId, *50*)	++++	++*
Lateral tegmental nucleus (LTN, *49*)	+	+++*
Dorsal tegmental nucleus (DTN, *49*)	+++*	+
(DTN, *50*)	!!!!*	++++*
Sublaterodorsal nucleus (SLD, *49*) [(5)]	++++*	+
(SLD, *50*)	++*	+
Laterodorsal tegmental nucleus (LDT, *49*)	++++	+++
(LDT, *50*)	!!!!*	+++*
Barrington's nucleus (B, *49*)	+	+*
(B, *50*)	++++*	!!!!*
Locus ceruleus (LC, *49*)	-	++++
(LC, *50*)	++	++++
Parabrachial Nucleus (PB)		
Medial division (PBm)		
Ventral medial part (PBmv, *50*)	+*	++++*
Medial medial part (PBmm, *49*)	+	!!!!
(PBmm, *50*)	+	++++*

DOI:10.14753/SE.2017.2041

Cell Group or Region (Abbreviation, *Swanson Atlas Level*)	Density of c-Fos-ir[(1)] Fasted	Refed
Kölliker-Fuse subnucleus (KF, *49*)	+*	!!!!!*
Lateral division		
Ventral lateral part (PBlv, *49*)	+	!!!!*
(PBlv, *50*)	-	!!!!*
Central lateral part (PBlc, *49*)	++	!!!!*
(PBlc, *50*)	++*	!!!!!*
External lateral part (PBle, *49*)	-	++*
(PBle, *50*)	-	!!!!*
Dorsal lateral part (PBld, *49*)	+*	+++*
Principal sensory nucleus of trigeminal nerve (PSV, *49*)	!!!!*	++++*
(PSV, *50*)	!!!!*	+++*
Nucleus of lateral lemniscus (NLL)		
ventral part (NLLv, *43*)	+	+
Superior olivary complex (SOC)		
medial part (SOCm, *49*) [(5)]	+*	-
(SOCm, *50*) [(5)]	+	+
lateral part (SOCl, *50*) [(5)]	++*	+++*
periolivary region (POR, *49*) [(5)]	!!!!*	!!!!*
(POR, *50*) [(5)]	!!!!*	!!!!*
Nucleus of trapezoid body (NTB, *49*)	+	!!!!
(NTB, *50*)	+	+++*
Medulla (MY)		
Hypoglossal nucleus (XII, *69*)	-	+
Ambiguus nucleus, dorsal division (AMBd, *69*)	-	-
Ambiguus nucleus, ventral division (AMDv, *69*)	-	+
Dorsal motor nucleus of vagus nerve (DMX, *69*)	-	+*
Obscurus raphe nucleus (RO, *69*)	-	-
Pallidal raphe nucleus (RPA)	+	-
Parvicellular reticular nucleus (PARN, 69)	+	+
Medullary reticular nucleus (MDRN)		
Ventral part (MDRNv, *69*)	+	+*
Inferior olivary complex (IO)		
Medial accessory olive (IOma, *69*)	+	+
Lateral reticular nucleus (LRN, 69)		
Magnocellular part (LRNm)	++	+
Cochlear nuclei (CN)		
Ventral cochlear nucleus, anterior part (VCOa, *49*)	!!!!*	++*
(VCOa, *50*)	++*	+
Subpeduncular granular region (CNspg, *49*)	-	-
(CNspg, *50*)	!!!!*	++*
Parvicellular part (LRNp)	-	+
Paramedian reticular nucleus (PMR, *69*)	-	-
Parasolitary nucleus (PAS, *69*)	-	+*

DOI:10.14753/SE.2017.2041

Cell Group or Region (Abbreviation, *Swanson Atlas Level*)	Density of c-Fos-ir[(1)] Fasted	Refed
Nucleus of solitary tract (NTS)		
Medial part (NTSm)		
Caudal zone (NTSm, *69*)	-	!!!!!
Gelatinous part (NTSge, *69*)	-	+++*
Lateral part (NTSl, *69*)	-	++*
Commissural part (NTSco, *69*)	-	++++*
Area postrema (AP, *69*)	++++	!!!!
Dorsal column nuclei (DCN, *69*)		
Gracile nucleus, general (GRg)		
gracile nucleus, principal part (GR)	+	+
Cuneate nucleus (CU, *69*)	-	-
External cuneate nucleus (ECU, *69*)	++	++
Paratrigeminal nucleus (PAT, *69*)	-	+++*
Spinal nucleus of the trigeminal nerve (SPV)		
Interpolar part (SPVI, *69*)	+	++*
Caudal part (SPVC, *69*)	-	+

Fos Scattered in White Matter Tracts (Abbreviation, *Atlas Level*)	Density of c-Fos-ir[(1)] Fasted	Refed
Cerebrospinal Axis		
Spinal tract of the trigeminal nerve (sptV, *69*)	++	+++
Tegmentum		
Brachium of inferior colliculus (bic, *43*)	+++*	!!!!
Pons		
Middle cerebellar peduncle (mcp, *43*)	+++	-
Ventral spinocerebellar tract (sctv, *49*)	!!!!	!!!!*
(sctv, *50*)	!!!!*	+++
Pyramid (py, *49*)	++	!!!!!
(py, *50*)	+++	!!!!*

Scale (c-Fos-IR cells):

-:	0
+:	1-5 cells
++:	6-10 cells
+++:	11-20 cells
++++:	20-30 cells
!!!!:	31-99 cells
!!!!!:	>100 cells

6.2. Activation of anorexigenic pro-opiomelanocortin neurons during refeeding is independent of the inputs mediated by the vagus nerve and the ascending brainstem pathways

6.2.1. Food and water intake

Sham-vagotomized animals consumed significantly more food (Sham versus Vagotomized 2-h food intake: 8.1 ± 0.7 g versus 2.7 ± 0.6 g; $P < 0.001$) and water (Sham versus Vagotomized 1-h water intake: 7.6 ± 0.9 g versus 2.4 ± 0.6 g; $P < 0.001$; 2-h water intake: 13.2 ± 2.5 g versus 6.5 ± 5.0 g; $P < 0.05$) than the vagotomized animals during the 2 h refeeding period after the fast. The sham-vagotomized, pairfed group consumed 2.7 g of food during the refeeding period. Animals with unilateral transection of ascending brainstem pathways ate the same amount of food as the sham-operated animals (Sham versus Transected: 8.7 ± 0.9 g versus 8.7 ± 0.6 g) during the 2-h refeeding period.

6.2.2. Effect of vagotomy on refeeding-induced activation of POMC neurons in the ARC

Only a few POMC-IR neurons containing c-Fos-immunoreactivity were seen in the ARC of fasting animals, without apparent differences between sham-operated and vagotomized rats. Refeeding of sham-operated animals led to a marked increase in the number of double-labelled neurons in the ARC (**Figure 7** and **Figure 8**). Refeeding also resulted in an increased number of double-labelled POMC neurons in vagotomized rats (**Figure 7** and **Figure 8**), although the increase was less pronounced. The number of double-labelled POMC neurons also increased in the pairfed sham-operated group compared to fasting controls, although it appeared to be lower than both the intact and vagotomized rats. Two-way ANOVA of the image analysis of sham fasted, sham refed, sham pairfed, vagotomized fasted and vagotomized refed groups revealed a significant main effect of both vagotomy and refeeding ($P < 0.01$). By one-way ANOVA, sham pairfed animals showed a significant increase in the c-Fos response compared to sham fasted and vagotomized fasted animals, but also a significant decrease compared to sham refed animals (percentage of c-Fos-containing POMC neurons, Sham-Fasted versus Sham-Refed versus Sham-Pairfed: 2.1 ± 1.5% versus 48.7 ± 3.7% versus 13.5 ± 2.4%; $P < 0.05$; Vagotomized Fasted versus Vagotomized Refed: 2.9 ± 0.7% versus 27.6 ± 2.4%; $P < 0.001$).

DOI:10.14753/SE.2017.2041

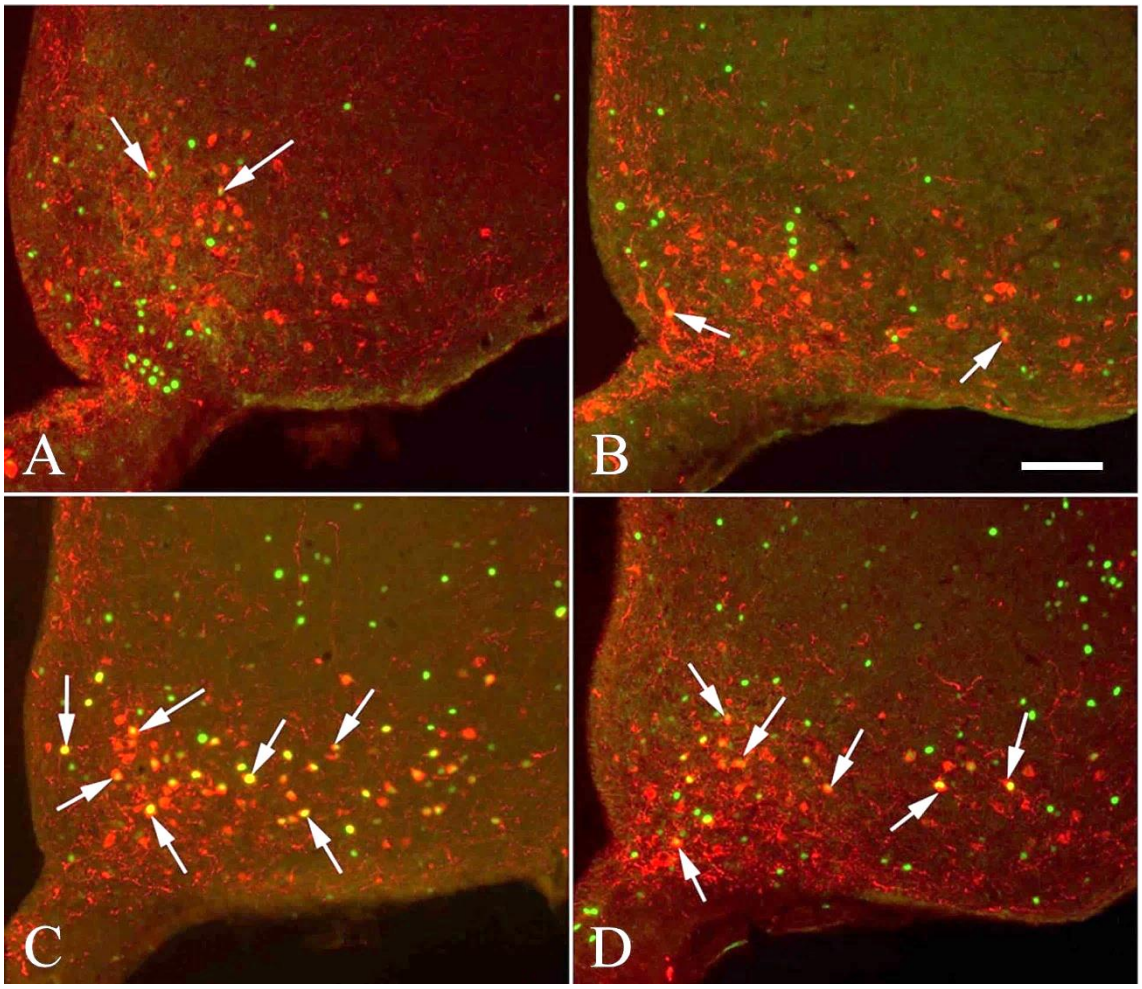

Figure 7 Effect of vagotomy on the refeeding-induced activation of the pro-opiomelanocortin (POMC) neurons in the arcuate nucleus (ARC). c-Fos (green) and POMC (red) immunofluorescence in the ARC of Sham/Fasted (**A**), Sham/Refed (**C**), Vagotomized/Fasted (**B**) and Vagotomized/Refed (**D**) animals. Only scattered c-Fos-immunoreactive POMC neurons are seen in the ARC of fasting animals without any apparent differences after vagotomy (**A, B; arrows**). Refeeding of fasted sham-operated animals led to a significant increase in the number of double-labelled neurons in the ARC (**C**). Refeeding also increased the number of double-labelled POMC neurons in vagotomized rats (**D**), although this increase was less than in sham-operated animals. Scale bar = 50 μm.

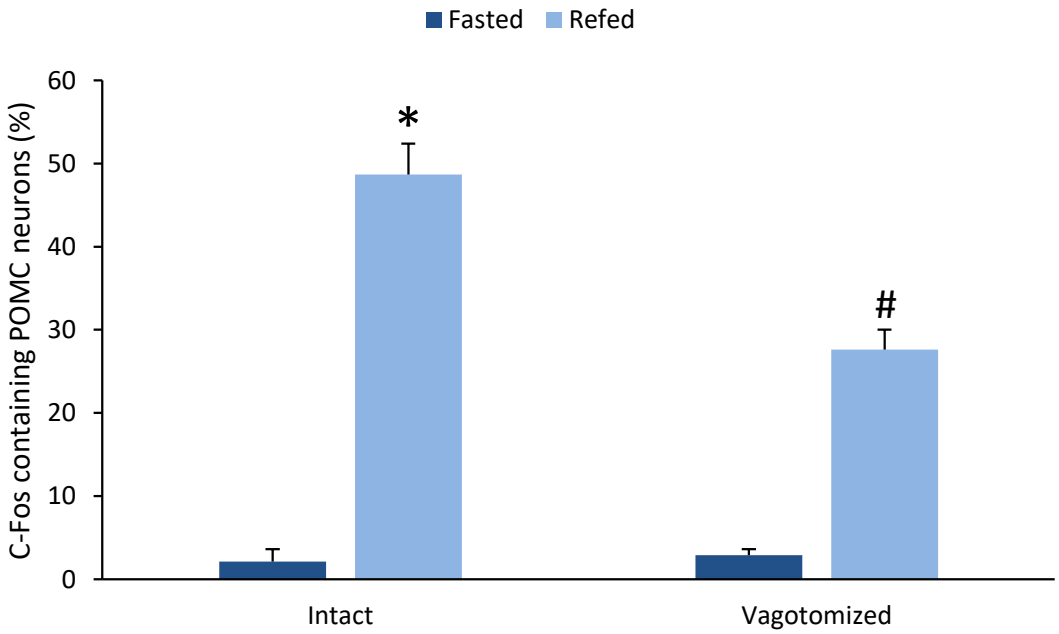

Figure 8 Effect of vagotomy on the refeeding-induced activation of pro-opiomelanocortin (POMC) neurons in the arcuate nucleus. By image analysis, the number of c-Fos-containing POMC neurons was significantly increased in the vagotomized refed animals compared to both of vagotomized fasted and intact fasted animals. However, the number of double-labeled neurons is 43% lower in the Vagotomized/Refed rats compared to Sham/Refed animals. *: significantly different compared to Intact/Fasted and Vagotomized/ Fasted and Vagotomized/Refed animals. #: significantly different compared to Intact/Fasted, Vagotomized/ Fasted, and Intact/ Refed animals.

6.2.3. Effect of transection of ascending brainstem pathways on the DBH-IR innervation of POMC neurons in the ARC

An intense network of DBH-IR fibers was observed within the ARC on the intact side, whereas animals with successful transection of the ascending brainstem pathways showed a marked reduction in DBH-immunoreactivity on the transected side (**Figure 9A**, **B**). POMC-IR neurons were contacted by DBH-IR varicosities in both the intact and transected sides, but in the ten animals (five fasted and five refed) included in the present study, the number of DBH-IR varicosities on the surface of POMC neurons in the ARC was reduced by a mean of 74.05 ± 3.55% on the side of the knife cut. In addition, quantitative analysis of the number of POMC neurons receiving contacts by DBH-IR varicosities showed a marked reduction on the transected side in both the fasted and refed animal groups (intact side versus transected side in fasted animals: 93.1 ± 3.1% versus 50.8 ± 13.1%; in refed animals 91.8 ± 2.9% versus 56.2 ± 2.8%; $P < 0.05$).

DOI:10.14753/SE.2017.2041

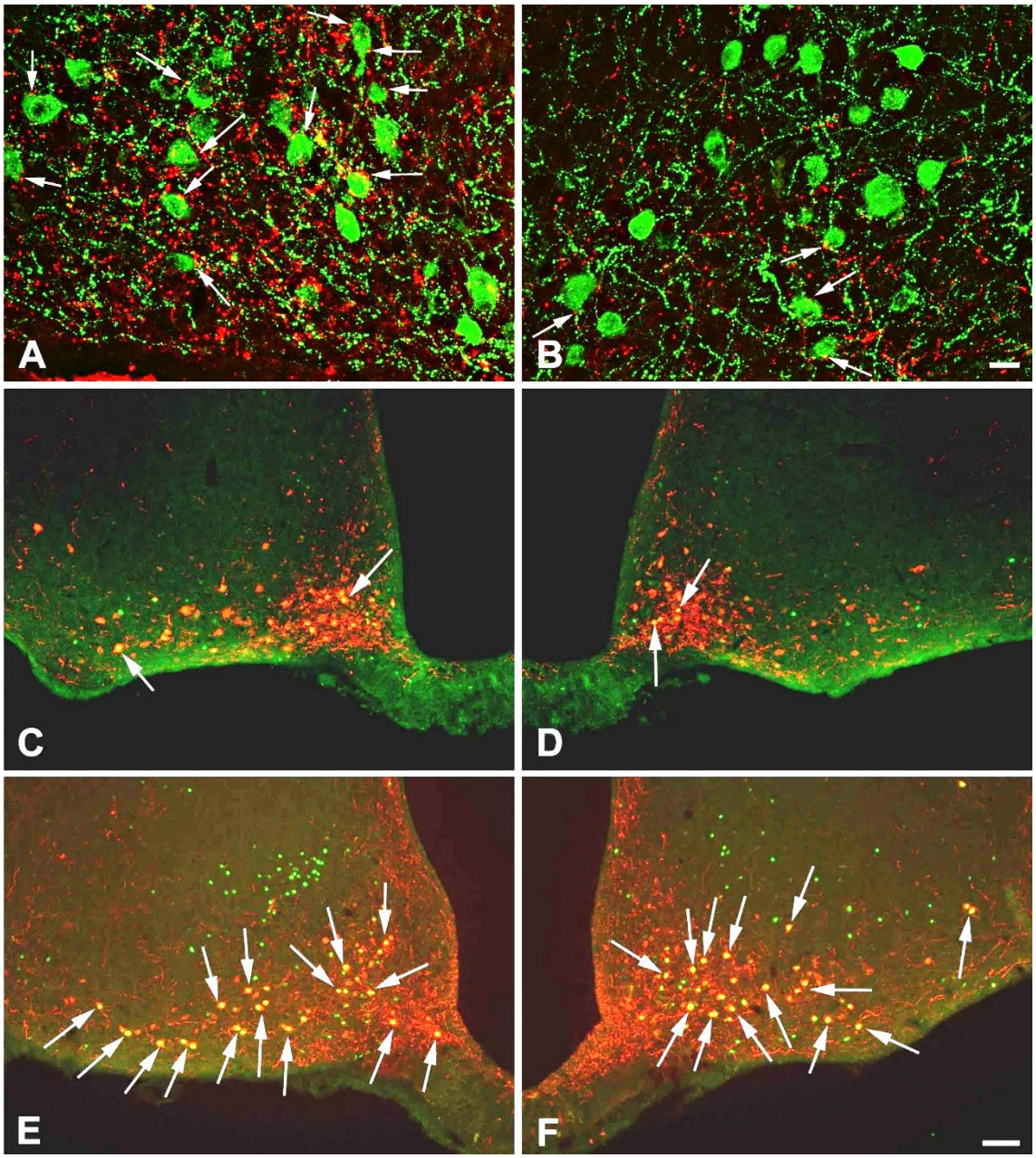

Figure 9 Effect of the unilateral transection of the ascending brainstem pathways on the dopamine β-hydroxylase (DBH)-immunoreactive (-IR) innervation and refeeding induced activation of the pro-opiomelanocortin (POMC) neurons in the arcuate nucleus (ARC). A large number of DBH-IR (red) varicosities are in contact with POMC-IR (green) neurons in the ARC on the intact side (**A**), although this is markedly reduced on the surface of POMC neurons on the side of the transection (**B**). Arrows indicate DBH-IR varicosities in juxtaposition to POMC-IR neurons. In fasted animals (**C, D**), only scattered double-labelled neurons (arrows) containing both c-Fos- (green) and POMC-immunoreactivity (red) are present in the ARC. The number of these cells is similar on the intact (**C**) and the transected (**D**) sides. In contrast, the number of double-labelled neurons (**arrows**) is markedly increased on both the intact (**E**) and the transected sides (**F**) of the refed animals. Scale bar in (**B**) = 20 μm, corresponds to (**A**) and (**B**). Scale bar in (**F**) = 100 μm, corresponds to (**C**) to (**F**).

DOI:10.14753/SE.2017.2041

6.2.4. Effect of the transection of ascending brainstem pathways on the refeeding-induced activation of POMC neurons in the ARC

In fasted animals, only few c-Fos-IR POMC neurons were observed in both the intact and the transected sides of the ARC (**Figure 9C, D** and **10**). Refeeding-induced a marked and significant increase in the number of c-Fos-labelled POMC neurons in the sham-operated animals (not shown) and also on both sides of the ARC in the transected animals (**Figure 9E**, **F** and **10**) (percentage of double-labelled POMC neurons, Intact Side Fasted versus Intact Side Refed: 6.5 ± 2.6% versus 28.0 ± 3.4%; $P < 0.001$; Transected Side Fasted versus Transected Side Refed: 7.4% ± 2.3 versus 25.2 ± 3.81%; $P < 0.001$). Transection had no influence on the effect of refeeding on the number of double-labelled neurons ($P = 0.37$). The number of c-Fos-IR POMC neurons was similar in the sham operated refed and in either side of the refed transected animals (23.4 ± 4.6; Sham versus Transected Side Refed, $P = 0.75$; Sham versus Intact Side Refed, $P = 0.69$).

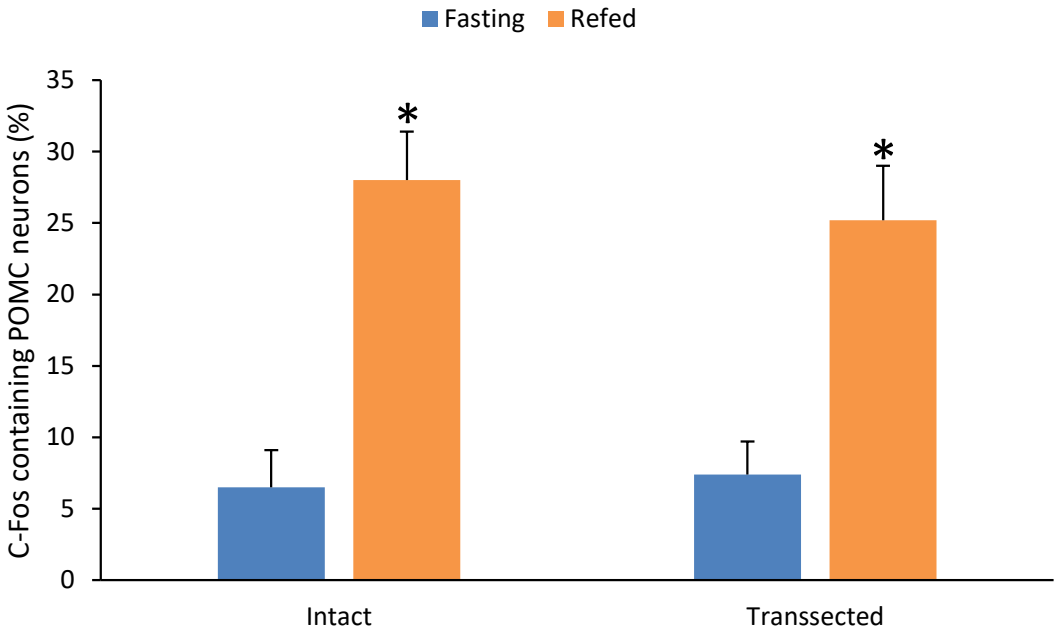

Figure 10 Effect of the transection of the ascending brainstem pathways on the refeeding-induced activation of pro-opiomelanocortin (POMC) neurons in the arcuate nucleus. By image analysis, the number of c-Fos-containing POMC neurons was significantly increased on both the intact and transected sides of the refed animals compared to the fasted animals. *Significantly different compared to both the intact and transected sides of the fasted animals.

DOI:10.14753/SE.2017.2041

6.3. Retrograde and anterograde connections of PBN with other refeeding-activated neuronal groups

After refeeding, marked increase of c-Fos-IR nuclei was observed in the PBN compared to the fasted rats. The examination of PBN subnuclei showed that the number of c-Fos-containing neurons was increased in all parts of the PBN including the medial and lateral parts of PBN and their subnuclei (**Figure 11**).

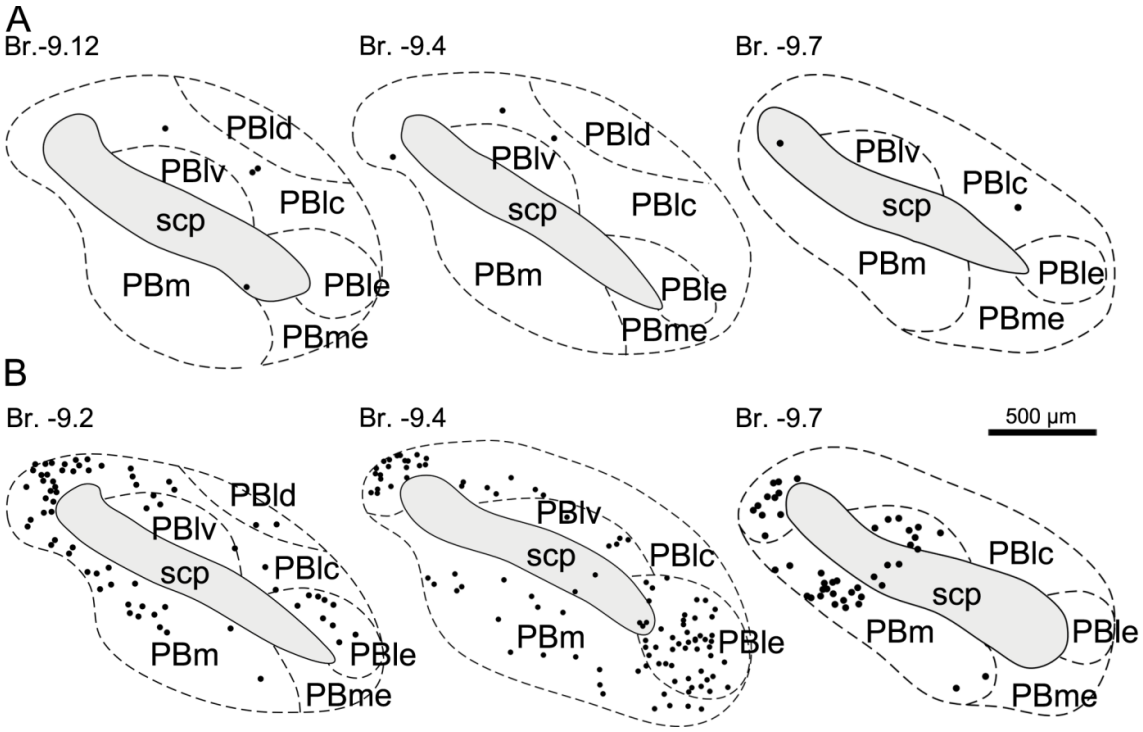

Figure 11 Schematic drawings illustrate the distribution of activated neurons in the PBN of fasted (**A**) and refed rats in 3 different coronal plains (**B**). C-Fos-containing neurons are visualized by black dots. Only few activated neurons were observed in the PBN of fasted rats. In contrast, numerous c-Fos-IR nuclei were found in all subdivision of PBN in refed rats. Scale bar = 500 µm.

6.3.1. Localization of CTB/PHAL injection sites

The CTB injection site in all three cases spread throughout the entire PBN including the medial and lateral parts, but the injection sites were centered in different parts of the nucleus (**Figure 11A**, **B**, **C**). In animal A, the center of the injection site was in the lateral part of PBN, but the medial part was also covered by the tracer. In animal B, there was intense CTB signal in the medial and lateral parts of the PBN. In animal C, the middle of the injection was in the medial part of PBN and the tracer spread to the lateral part of the PBN. The number of CTB containing neurons in the refeeding-activated areas was higher

in cases where the injection site was centered in the medial part of the PBN (Animals B and C) compared to the animal where the injection was centered into the lateral part of PBN (Animal A), although the distribution of CTB containing cells were similar in all cases.

Of the five animals (D-H) where the PHAL injection sites were centered in the PBN, the localization of injection sites was somewhat different (**Figure 12**). The center of the PHAL injection site in animal D was localized in the medial part of the nucleus and spread only to a small portion of the ventral part of the lateral PBN (**Figure 12D**). In animal E, the PHAL injection site was centered in the external part of the lateral PBN (**Figure 12E**). In animal F, PHAL entered the central and external parts of the lateral PBN and spread into a small part of the medial PBN close to the superior cerebellar peduncle (**Figure 12F**). In animals G and H, PHAL spread into all parts of the PBN (**Figure 12G**, **H**).

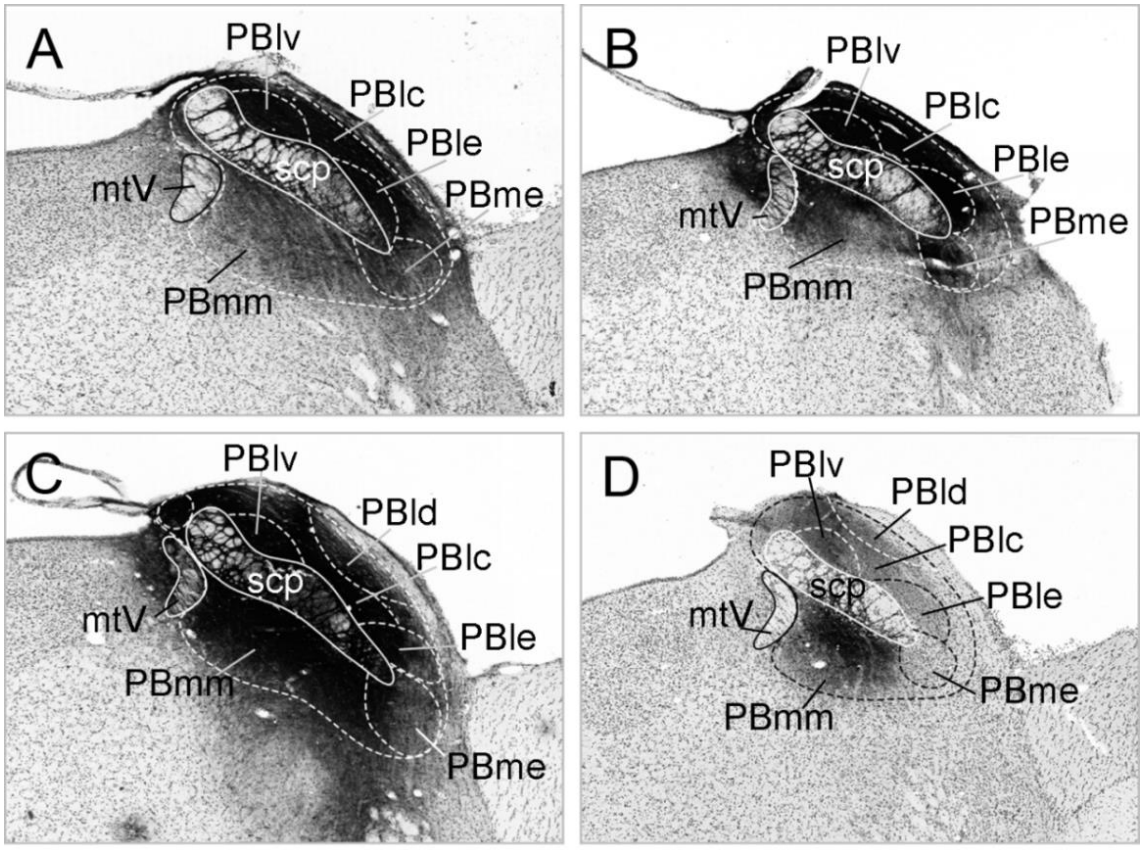

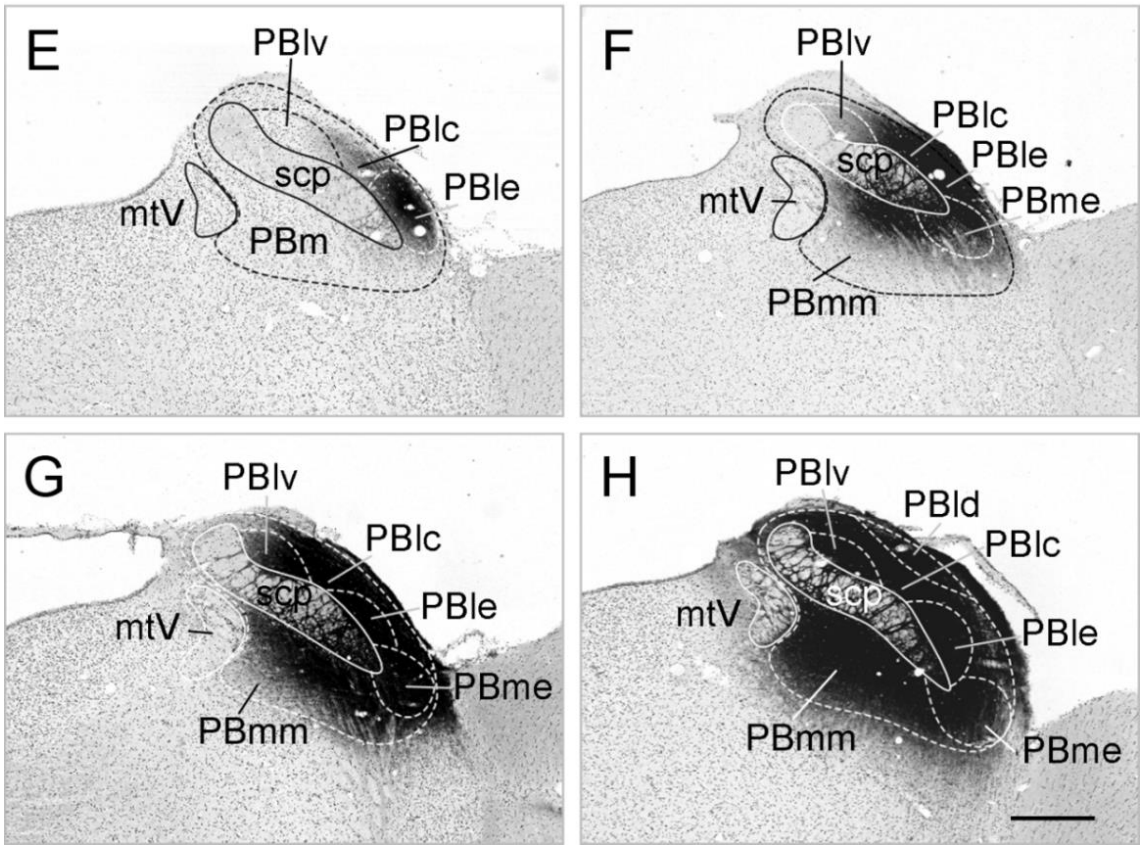

Figure 12 Localization of CTB (**A-C**) and PHA-L (**D-H**) injection sites in the parabrachial nucleus. Scale bar=500 µm PBlc: lateral parabrachial nucleus, central part; PBld: lateral parabrachial nucleus, dorsal part; PBle: lateral parabrachial nucleus, external part; PBlv: lateral parabrachial nucleus, ventral part; PBm parabrachial nucleus, medial part; PBme: medial parabrachial nucleus, external part; PBmm: medial parabrachial nucleus, medial part.

6.3.2. Origins of the refeeding-activated neuronal inputs of the PBN

In refed, CTB-injected animals, the greatest number of refeeding-activated neurons that project to the PBN (CTB and c-Fos-containing) were observed in the PVN, particularly in PVNv and PVNl subdivisions (**Figure 13B**), the PSTN (**Figure 13D**) and in the medial, intermediate and commissural subdivisions of the NTS (**Figure 13E**). A moderate number of double-labeled neurons were observed in the BST, primarily the medial part of this nucleus (**Figure 13A**), the CEA (**Figure 13C**), LH and area postrema (**Figure 13F**). Scattered c-Fos and CTB-containing neurons were detected in the AIA, anterior hypothalamus, ARC, DMN and zona incerta. The localization of c-Fos and CTB double-labelled neurons are illustrated by **Figure 15**, the brain areas are summarized in **Figure 16**.

DOI:10.14753/SE.2017.2041

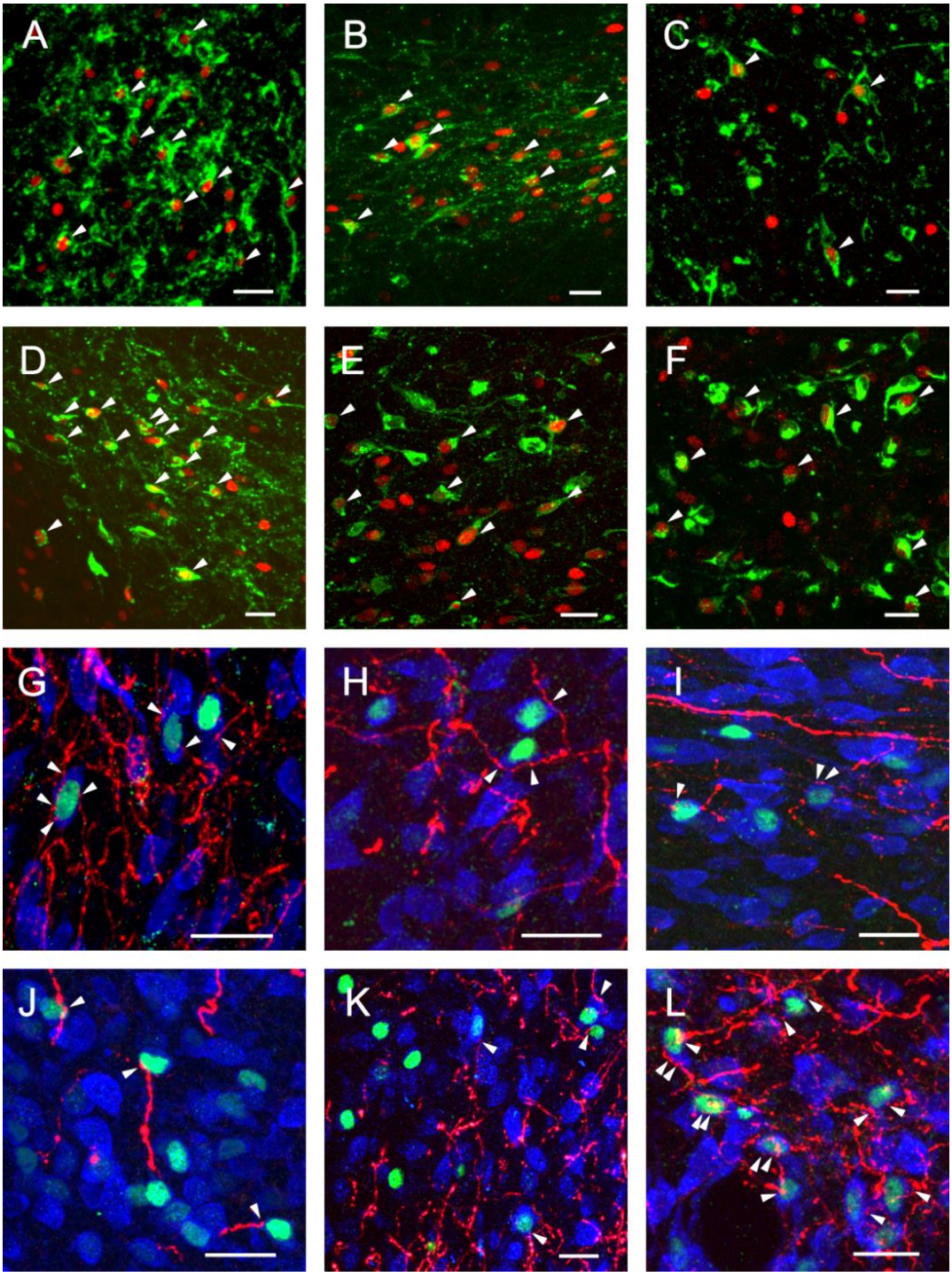

Figure 13 Confocal microscopic images illustrate the connections of the parabrachial nucleus (PBN) with refeeding-activated neuron groups. Double-labeled images show the neurons-containing both c-Fos- (red), and CTB-immunoreactivity (green) cells (**A-F**) in refed rats after injection of retrograde tracer CTB into the PBN. Arrowheads point to double labelled neurons (**A-F**). Triple-labeled images illustrate the connection of PHAL-IR axons (red) with c-Fos-IR neurons (green nucleus) in refed rats after injection of anterograde tracer PHAL into the PBN. The cytoplasm of neurons is labeled with HuC/HuD-immunoreactivity (blue). Arrowheads point to PHAL-IR axons in contact with c-Fos-IR neurons. The majority of c-Fos-containing neurons are contacted by PHAL-IR axon varicosities in the following areas. Bed nucleus of stria terminalis (**A, G**), ventral (**B, H**) and lateral (**I**) parts of hypothalamic paraventricular nucleus, central nucleus of amygdala (**C, K**) parasubthalamic nucleus (**D, L**), Nucleus tractus solitarii (**E**), area postrema (**F**) and dorsomedial nucleus of hypothalamus (**J**). Scale bar = 25 μm.

DOI:10.14753/SE.2017.2041

6.3.3. Identification of the direct and indirect inputs of the PBN from refeeding-activated POMC neurons

Triple-labeling immunocytochemistry for c-Fos, CTB and POMC was used to determine whether the PBN receives direct or indirect refeeding-activated inputs from POMC neurons in the ARC. A large number of POMC neurons in the ARC contained c-Fos-immunoreactivity in their nuclei after refeeding, but only a very small portion of these cells contained also CTB-immunoreactivity (1 or 2 cells/section).

However, POMC-IR axons were seen to heavily innervate refeeding-activated, neurons in the ventral and lateral parvicellular subdivisions of the PVN and in the PSTN (**Figure 14**).

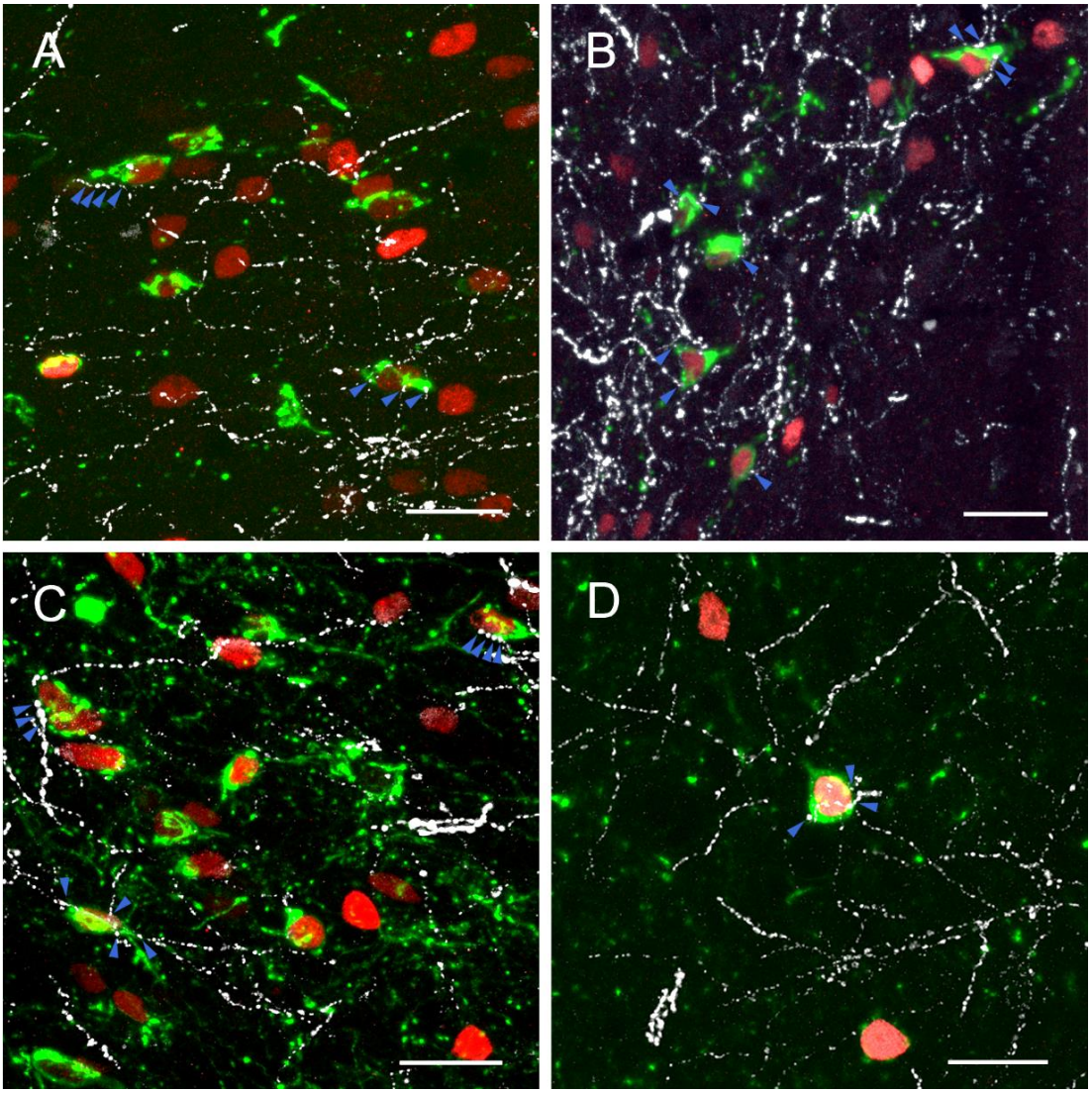

Figure 14 Confocal microscopic images of triple-labeled immunofluorescent sections illustrating the POMC-IR innervation (white) of refeeding activated (c-Fos positive, red) PBN projecting (CTB-containing; green) neurons in the PVNl (**A**) PVNv (**B**), PSTN (**C**) and CEA (**D**). Scale bar = 25 μm.

DOI:10.14753/SE.2017.2041

6.3.4. Identification of the refeeding-activated targets of the PBN

PHAL-IR fibers were found in refeeding-activated areas only in animals D, G and H, where the injection centered or spread into the medial part of the PBN. In animal F, there were only few PHAL-IR fibers in the CEA, whereas in animal E, PHAL-IR axons were not observed in any of the refeeding-activated areas. In animals D, G and H, the pattern of the PHAL-IR axons was similar with a large number of PHAL-IR fibers observed in close association with refeeding-activated neurons in the BST (**Figure 13G**) and CEA (**Figure 13K**), mainly in the medial parts of both nuclei, and in the PSTN (**Figure 13L**). Fewer, but still numerous fibers were observed in association with c-Fos-IR neurons in the anterior hypothalamus, PVNv and PVNl (**Figure 13H, I**), ARC, DMN (**Figure 13J**), LH and zona incerta. Only scattered PHAL-IR fibers were found in association with c-Fos-containing neurons in the AIA and NTS. The brain areas are summarized in **Figure 15** and **17**.

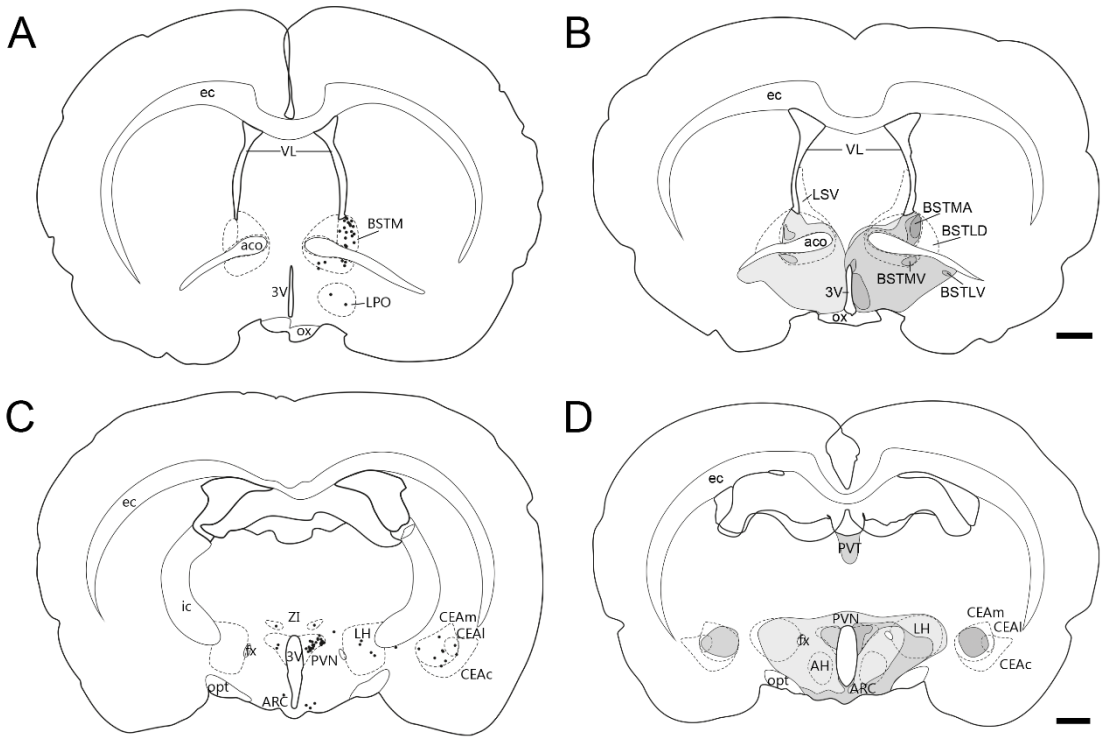

DOI:10.14753/SE.2017.2041

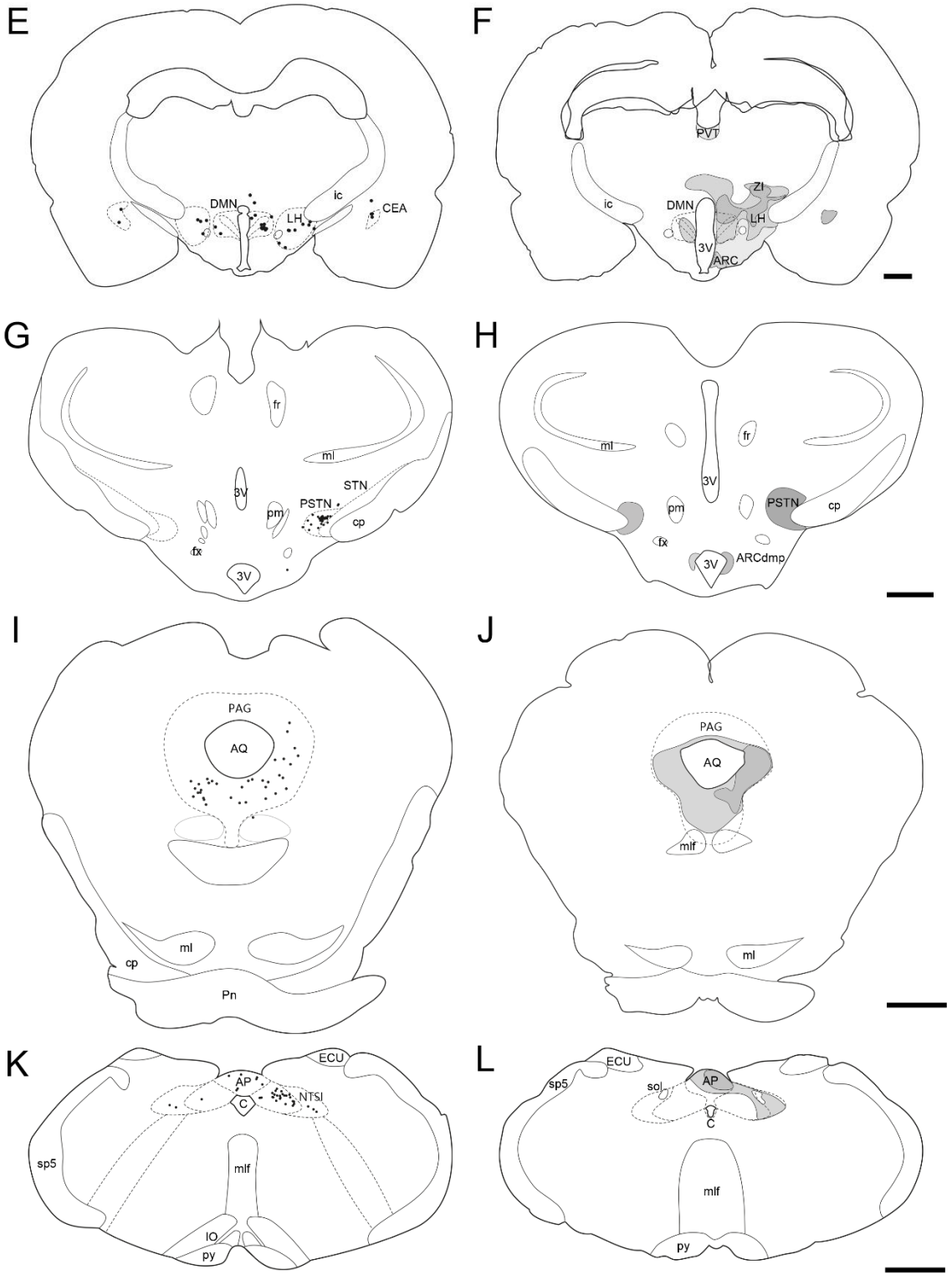

Figure 15 Schematic drawings illustrate the connections of the PBN with refeeding-activated neuronal groups. The distribution of CTB-containing c-Fos- IR neurons in a representative brain injected with CTB into the PBN is shown on **A, C, E, G, I, K**. The c-Fos and CTB-containing neurons are visualized by black dots. The localization of PHAL-IR fibers in refeeding activated areas is presented on **B, D, F, H, J, L**. The darkness of the area corresponds to the density of PHAL fibers. Scale bar=1mm.

DOI:10.14753/SE.2017.2041

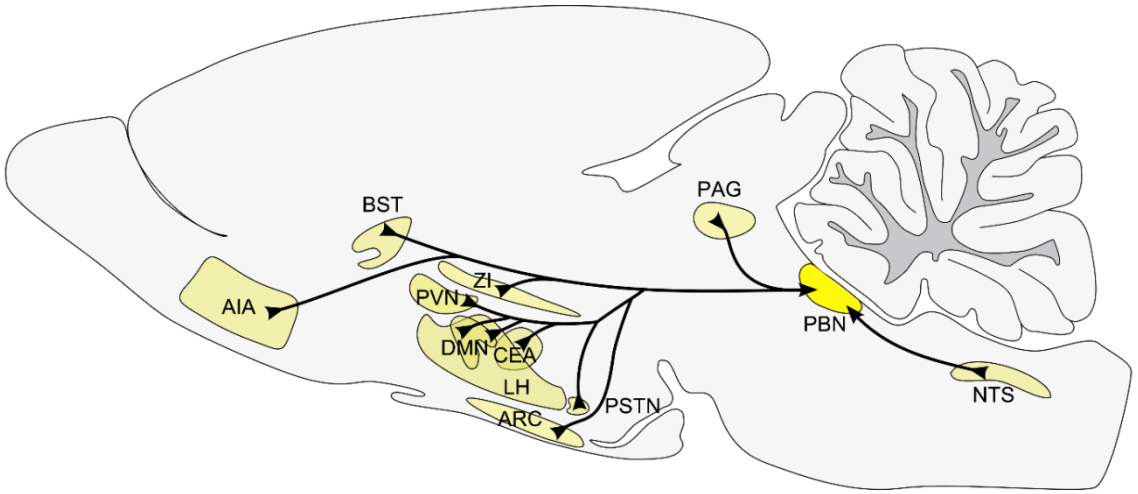

Figure 16 Schematic drawing illustrates the origins of the refeeding activated inputs of the PBN.

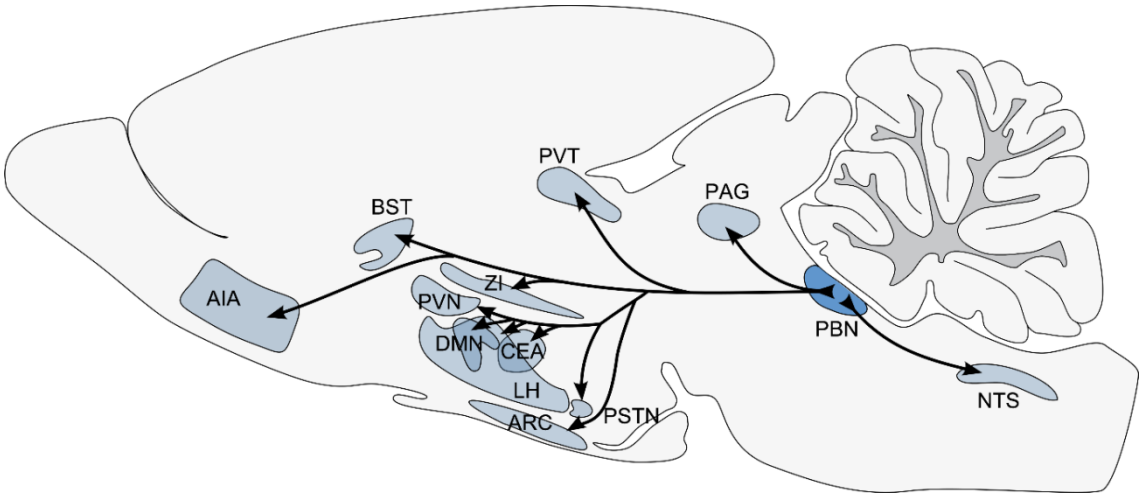

Figure 17 Schematic drawing illustrates the refeeding activated areas innervated by PBN neurons.

6.4. Connections of the central nucleus of amygdala with other refeeding-activated neuronal groups

Both the CEAm and the CEAlc contained activated neurons after refeeding, though the number of c-Fos-containing neurons was higher in the CEAm than in the CEAlc (**Figure 18**).

DOI:10.14753/SE.2017.2041

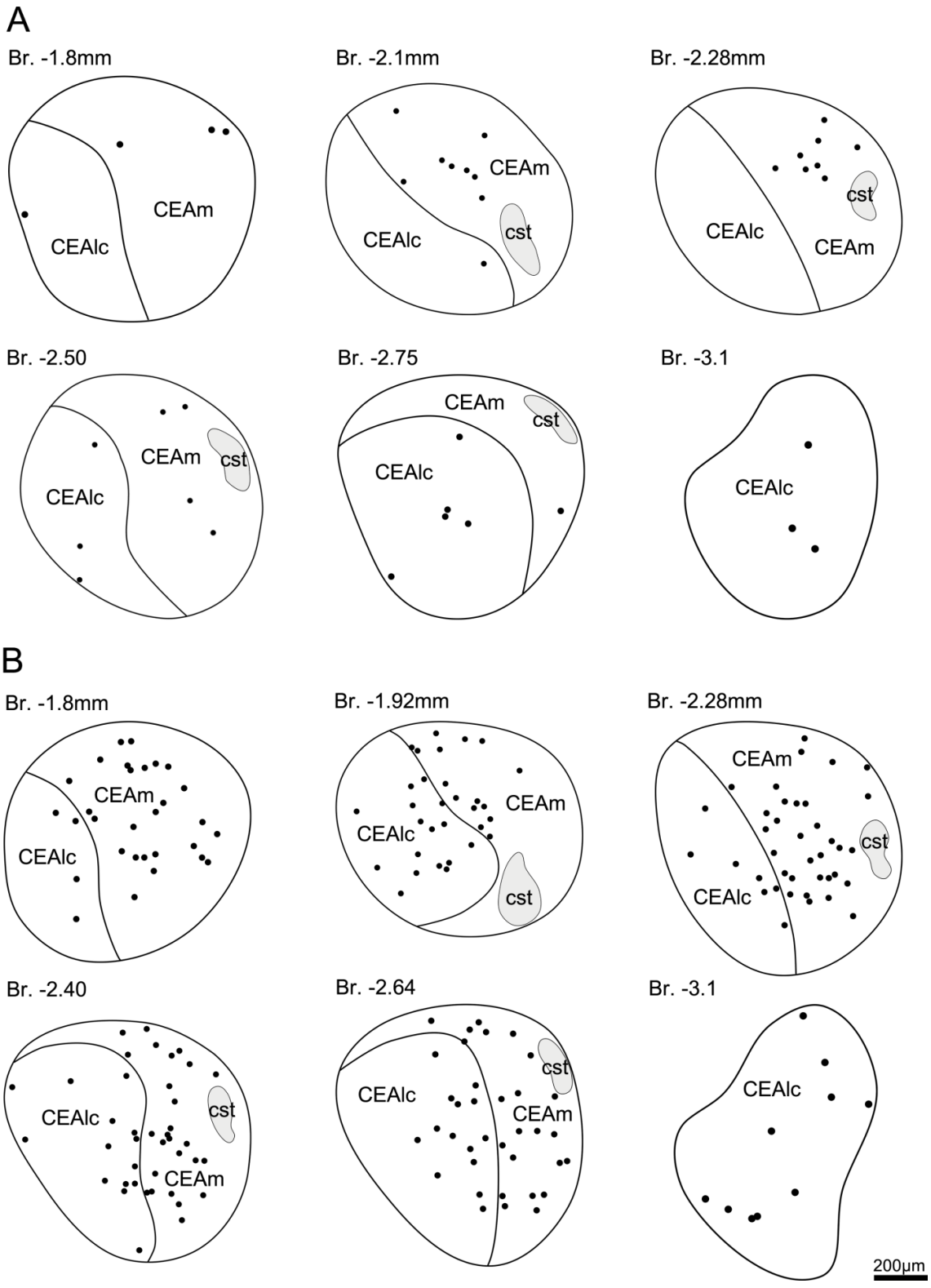

Figure 18 Schematic drawings of fasting (**A**) and refeeding (**B**) induced neuronal activation in the subnuclei of CEA in six different coronal plains. Both the medial (CEAm) and the laterocapsular (CEAlc) subdivisions contain activated (c-Fos-IR) neurons, but the majority of c-Fos-IR nuclei are concentrated rather in the CEAm.

DOI:10.14753/SE.2017.2041

6.4.1. Localization of the CTB/PHAL injection sites in the CEA

In five, CTB-injected and three, PHAL-injected animals, the injection site was centered in the CEA. In these cases, the injection site filled the CEA and did not spread to the surrounding regions. Only these brains were included in the analysis. In all studied brains, the distribution of the CTB-IR neurons and of PHAL-IR fibers was similar. Images of representative injection sites are shown in **Figure 19**, **20**.

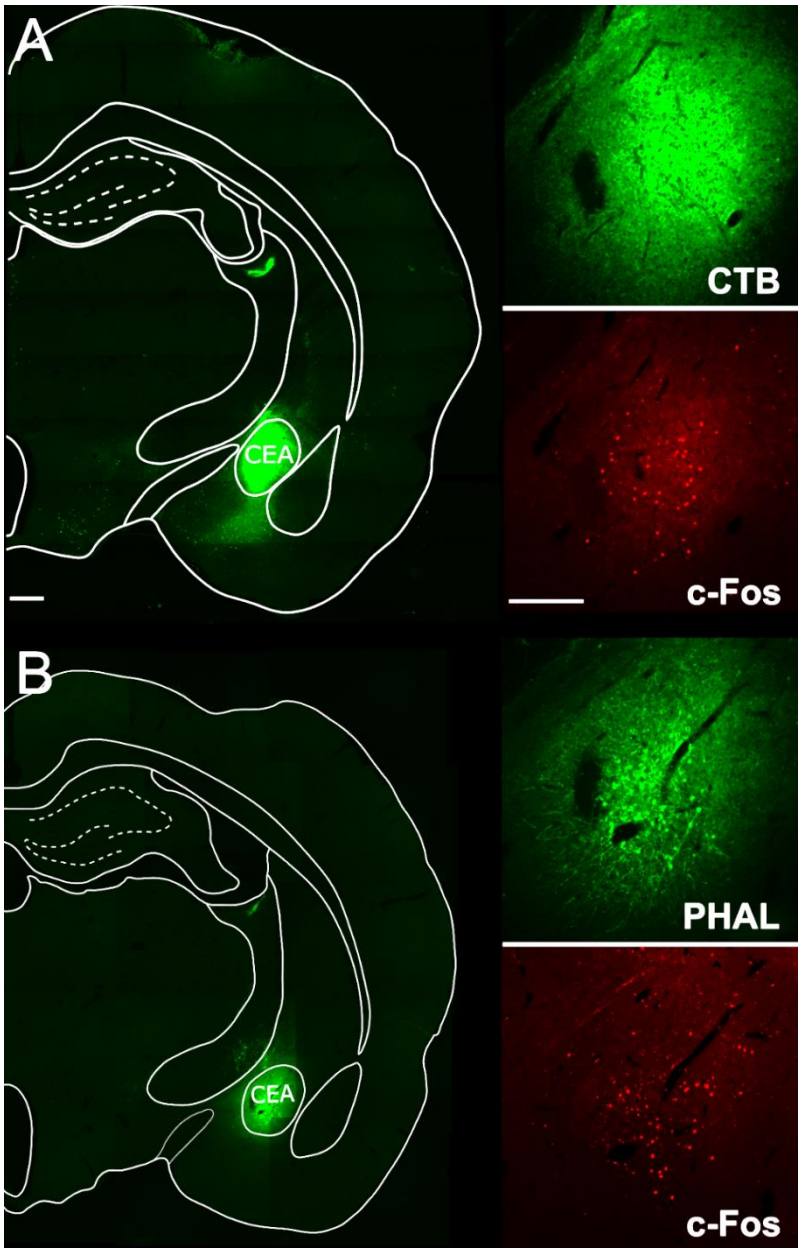

Figure 19 Representative images of CTB and PHAL injection sites in the CEA. **A**: Core of CTB injection site deposited into the CEA. **B**: Core of PHAL injection site centered in the CEA. Higher magnification images of the same fields show the colocalization of CTB (green) and c-Fos (red) or PHAL (green) and c-Fos (red) in the CEA. refeeding induced c-Fos-immunoreactivity was used as a marker of CEA. Scale bars=500μm.

DOI:10.14753/SE.2017.2041

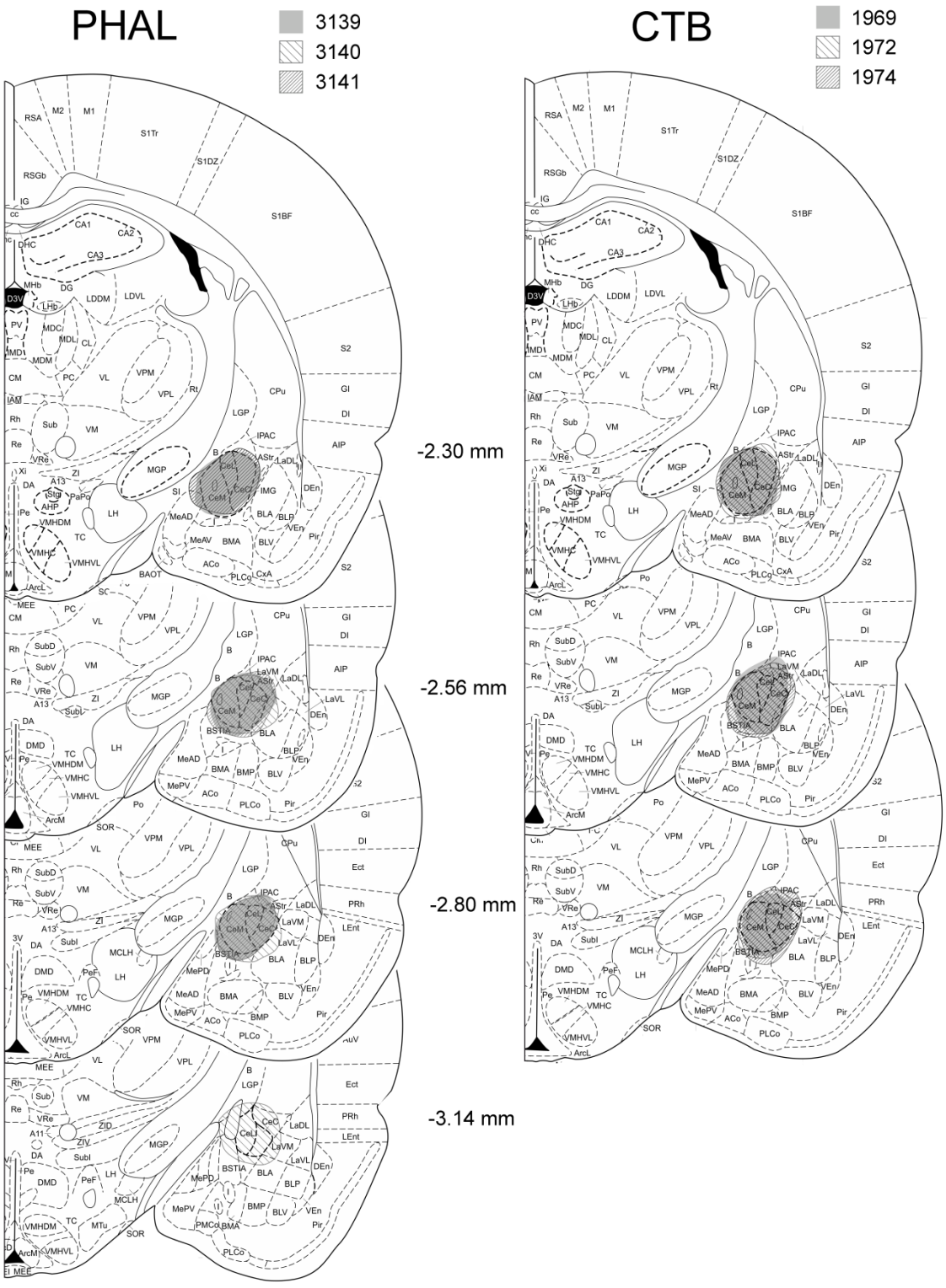

Figure 20 Schematic representation of the core of CTB and PHAL injection sites within the CEA in 3 or 4 anteroposterior levels, respectively. The injection sites were mapped to plans of the Paxinos rat brain atlas (Paxinos and Watson, 1998). Case numbers and the pattern demonstrating the boundaries of each injection core are indicated above the images

DOI:10.14753/SE.2017.2041

6.4.2. Origin of the refeeding-activated inputs of the CEA

After iontophoretic injection of CTB into the CEA, the majority of the double-labeled neurons containing both c-Fos and CTB (**Figure 21**) were detected ipsilateral to the injection site. Large number of double-labeled cells were observed in the PVT, (**Figure 21N**), PSTN (**Figure 21N**, **Q**), PBN (**Figure 21O**, **S**) and in the PAGvl (**Figure 21M**, **P**). Few CTB-c-Fos double-labeled neurons were detected in the Prl, (**Figure 21A**, B), AIA (**Figure 21C**, **D**), visceral (**Figure 21C**), piriform, primary and supplementary somatosensory area (SSs) (**Figure 21C**, **E**), BST (**Figure 21F**, **G**), ARC (**Figure 21N**, **R**) perifornical nucleus (PeF) (**Figure 21H**, **I**), LH, (**Figure 21K**), ZI, and NTS (**Figure 21L**). The brain areas are summarized in **Figure 24**

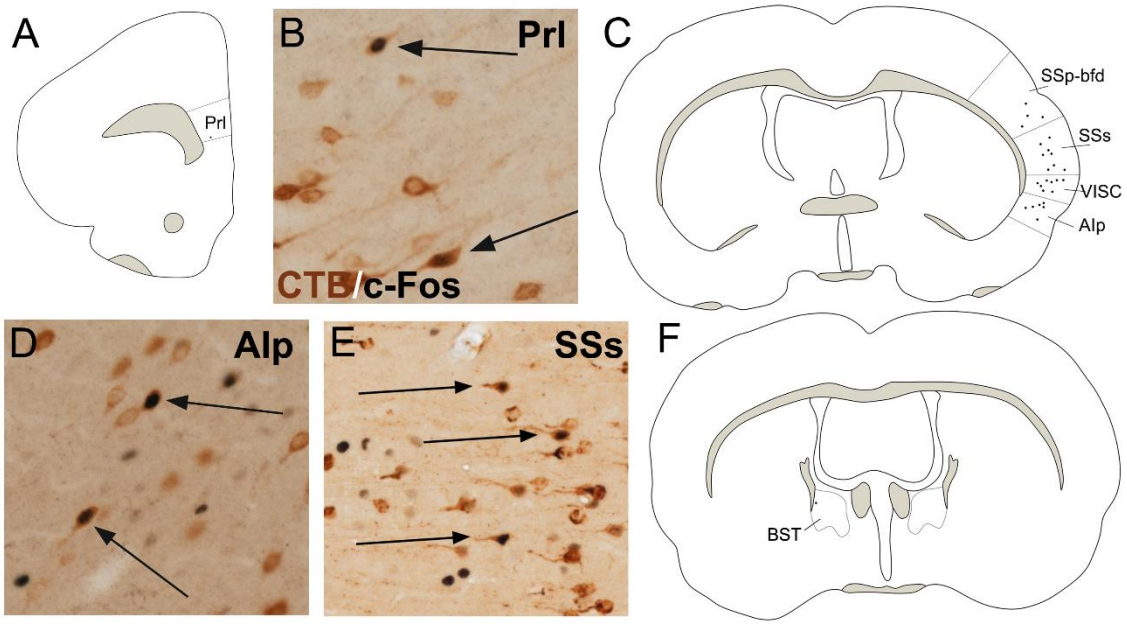

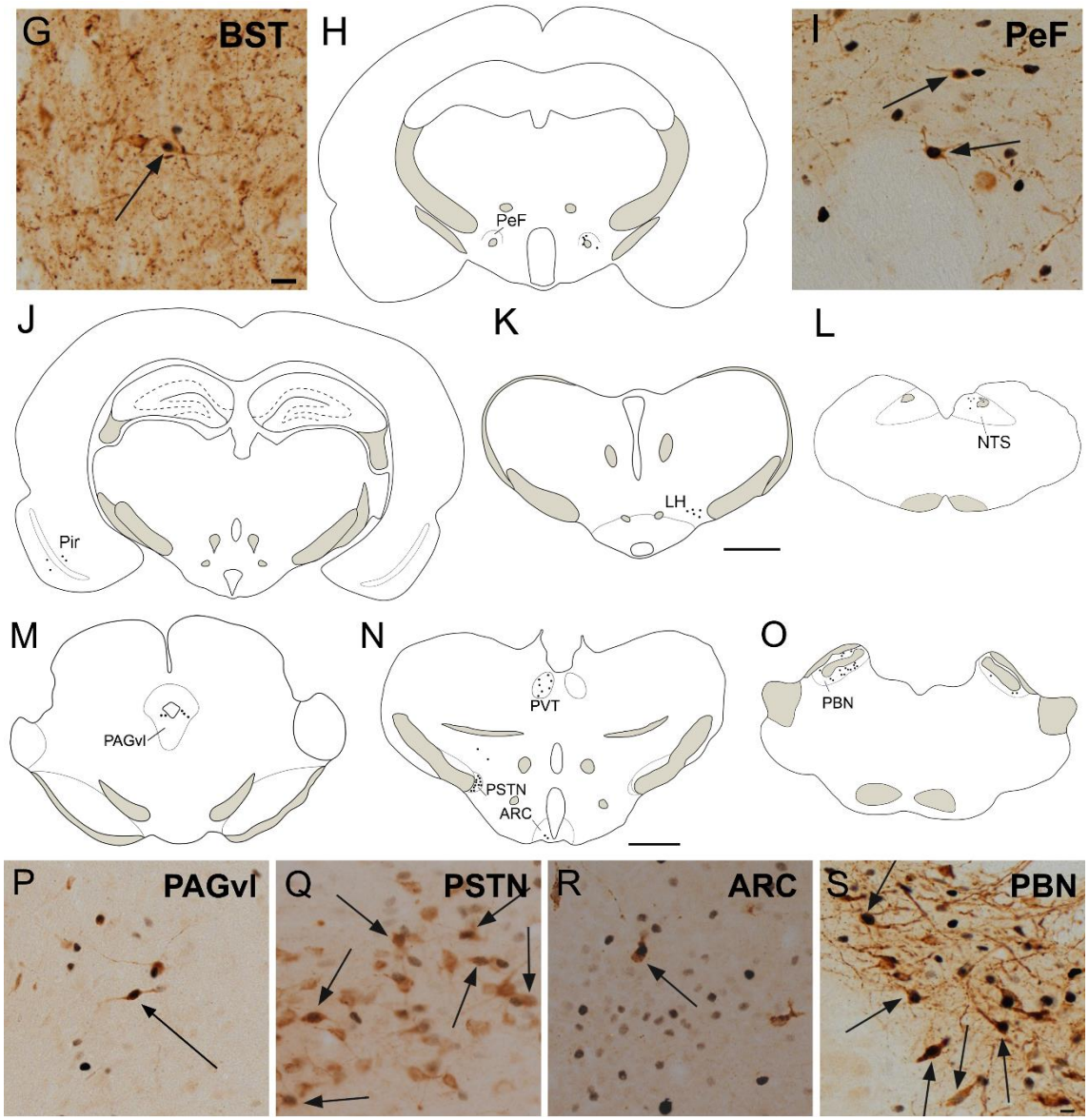

Figure 21 Schematic drawings illustrate the brain regions where the refeeding-activated (c-Fos-positive, black) neurons that projects to the CEA (CTB-immunoreactive perikarya, brown) are located. These double-labeled neurons are present in the prelimbic area (Prl; **A, B**), agranular insular area, posterior part (AIp; **C, D**), visceral area (VISC; **C**), supplementary somatosensory area (SSs; **C, E**), primary somatosensory cortex, barrel field (SSp-bfd; **C**), bed nuclei stria terminalis (BST; **F, G**), perifornical nucleus (PeF; **H, I**), piriform area (Pir; **J**), lateral hypothalamic area (LH; **K**), nucleus of the solitary tract (NTS; **L**), ventrolateral division of the periaqueductal gray (PAGvl; **M, P**), paraventricular thalamic nucleus (PVT; **N**), parasubthalamic nucleus (PSTN; **N, Q**), arcuate hypothalamic nucleus (ARC; **N, R**), Parabrachial nucleus (PBN; **O, S**). Representative images illustrate the distribution of the double labeled neurons in these areas. Arrows indicate examples of double-labeled neurons. Scale bar = 500µm on the schematic drawings and 20µm on the photomicrographs.

DOI:10.14753/SE.2017.2041

6.4.3. Involvement of the anorexigenic arcuate nucleus POMC neurons in the innervation of the CEA and the potential role of the PSTN as a relay nucleus between the ARC and CEA

After iontophoretic injection of CTB into the CEA, confocal microscopic analysis of sections immunolabeled for c-Fos, CTB and POMC revealed that only few (1-3/ section) refeeding-activated POMC-IR neurons were found to project to the CEA (**Figure 22A**). However, sections containing the PSTN revealed that in this nucleus, POMC-IR fibers frequently formed appositions on refeeding-activated neurons projecting to the CEA (**Figure 22B**).

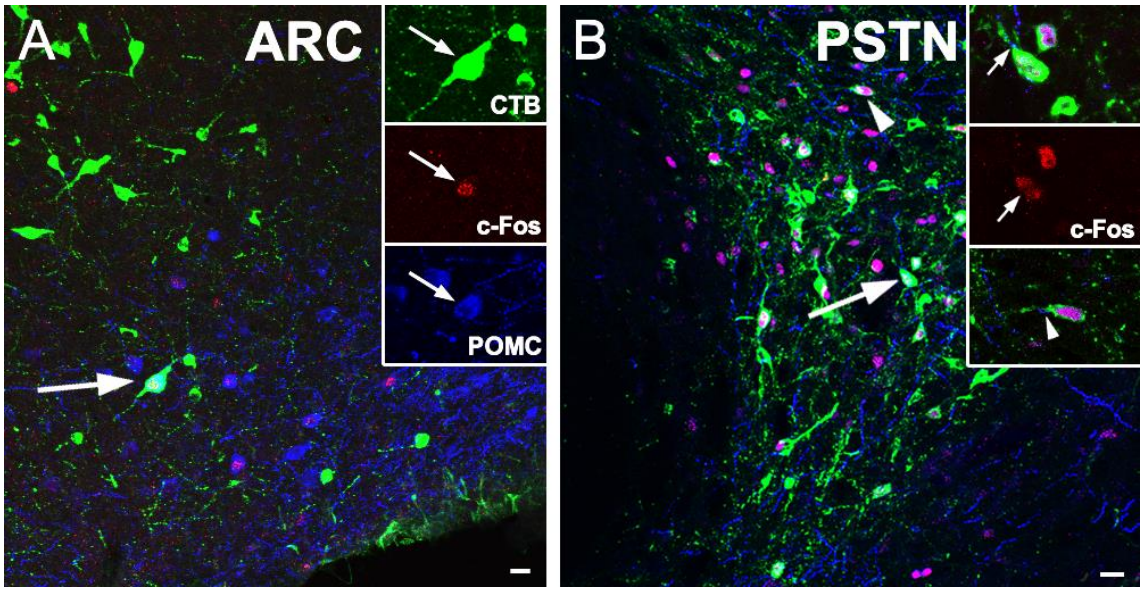

Figure 22 A: Confocal microscopic image of a triple-immunolabeled section indicate the presence of CTB (green) in refeeding-activated (c-Fos-positive, red), POMC-producing (blue) perikarya in the hypothalamic arcuate nucleus of a brain previously injected with CTB into the CEA. Arrows point to a triple-labeled neurons. To facilitate identification of triple-labeled cells, CTB, c-Fos and POMC-labeling of the same cells are shown in separate images in the insets. **B**: Confocal image of a triple-immunolabeled section shows POMC-IR (blue) boutons on refeeding-activated neurons (c-Fos-positive, red) in the parasubthalamic nucleus (PSTN) projecting to the CEA (CTB-immunoreactive, green). Double-labeled neuron indicated by arrowhead is shown with higher magnification in the insets, the arrowhead points to the POMC-IR apposition on the cell. The neuron indicated by arrow in the lower magnification image is in the insets for the better illustration of c-Fos immunoreactivity in the nucleus. Note that primary antibody against c-Fos and POMC was produced in rabbit, thus immunolabeling was performed sequentially, which prevented cross reaction in the cytoplasm, but not in the cell nuclei. Scale bars=20µm.

DOI:10.14753/SE.2017.2041

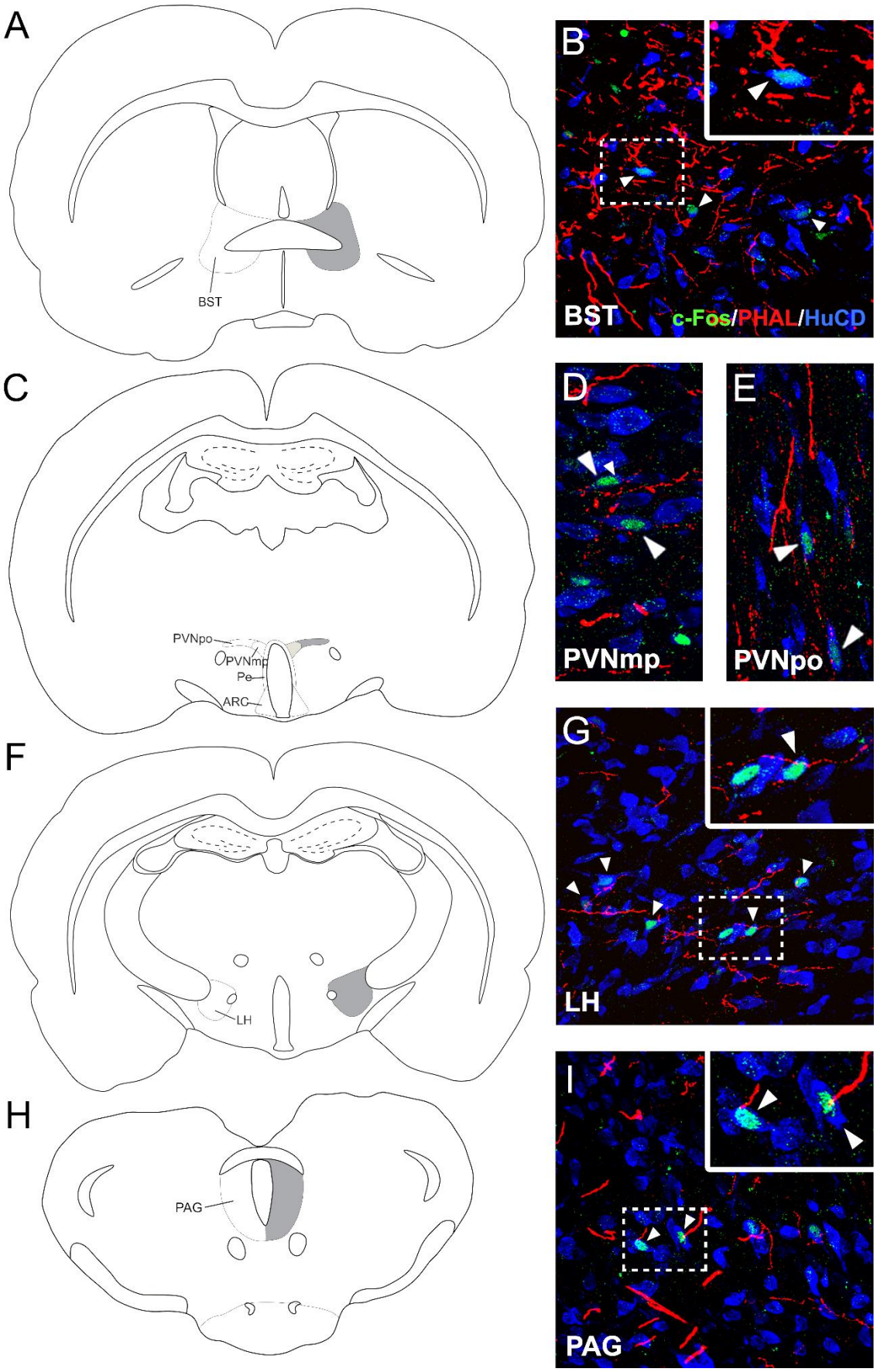

DOI:10.14753/SE.2017.2041

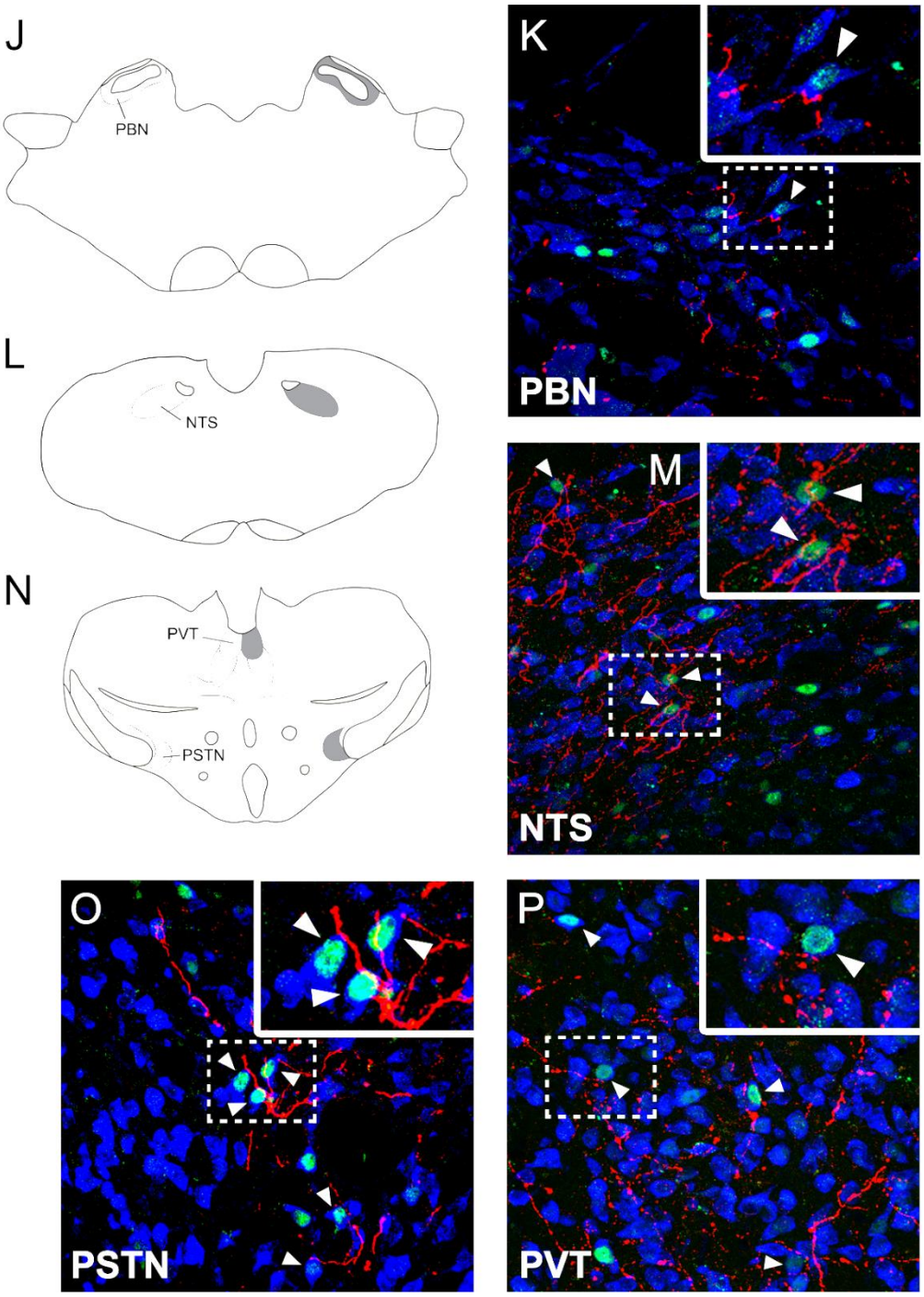

Figure 23 Schematic drawings and representative images illustrate the distribution of PHAL-immunoreactive axons in refeeding-activated areas of rats after injection of the anterograde tracer PHAL into the CEA. The darkness of gray indicates the density of PHAL fibers. The representative confocal images illustrate PHAL (red) fibers on the surface of refeeding-activated neurons (green) in the following areas: the bed nuclei of stria terminalis (BST; **A, B**), paraventricular hypothalamic nucleus, medial parvicellular part (PVNmp; **C, D**), paraventricular hypothalamic nucleus, posterior magnocellular part (PVNpm; **C, E**), lateral hypothalamus (LH; **F, G**), periaqueductal gray (PAG; **H, I**), PBN (PBN; **J, K**), nucleus tractus solitarius (NTS; **L, M**), parasubthalamic nucleus (PSTN; **N, O**), paraventricular thalamic nucleus (PVT; **O, P**). Arrowheads point to PHAL-immunoreactive contacts on c-Fos-containing neurons. The cytoplasm of neurons is labeled by HuC/HuD-immunoreactivity (blue). Higher magnification of framed areas is shown in the insets. Scale bars=500µm in the schematic drawings and 20µm in the confocal images.

DOI:10.14753/SE.2017.2041

6.4.4. Innervation of refeeding-activated neuronal populations by CEA neurons

Numerous PHAL-IR fibers were detected in several refeeding-activated brain regions (**Figure 23A**, **C**, **F**, **H**, **J**, **L**, **N**) on the ipsilateral side of the tracer injection including the BST, LH, posterior magnocellular part of the PVN, PSTN, paraventricular thalamic nucleus, PAG, NTS, and PBN. Only few PHAL-IR fibers were identified in the medial parvicellular part of the PVN (PVNmp). Confocal microscopic analysis of sections immunolabeled for PHAL, c-Fos and a neuronal marker, HuC/HuD, revealed that PHAL-containing axons contact refeeding-activated neurons in all of these areas (**Figure 23B**, **D**, **E**, **G**, **I**, **K**, **M**, **O**, **P**). The brain areas are summarized in **Figure 25**.

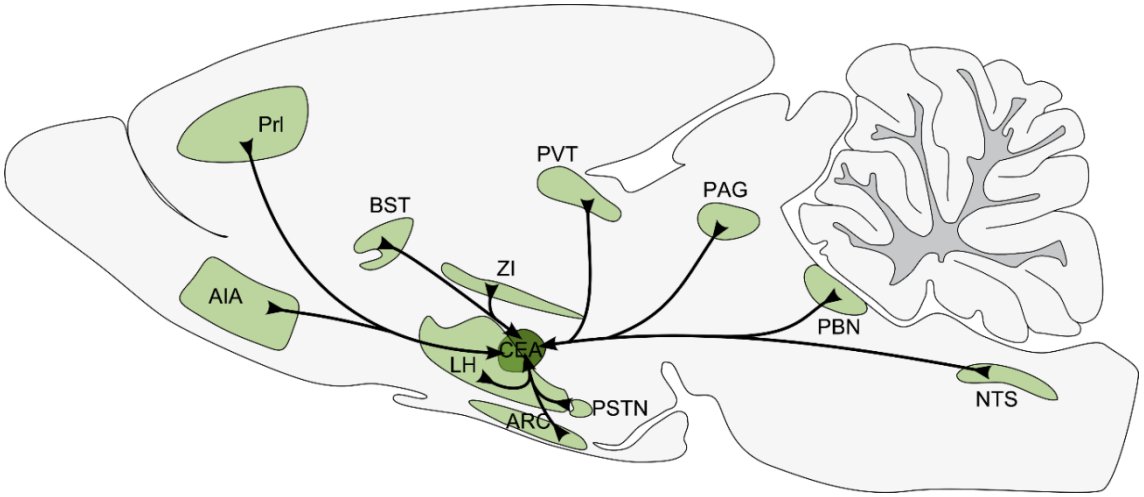

Figure 24 Schematic drawing shows the main origins of the refeeding activated inputs of the CEA.

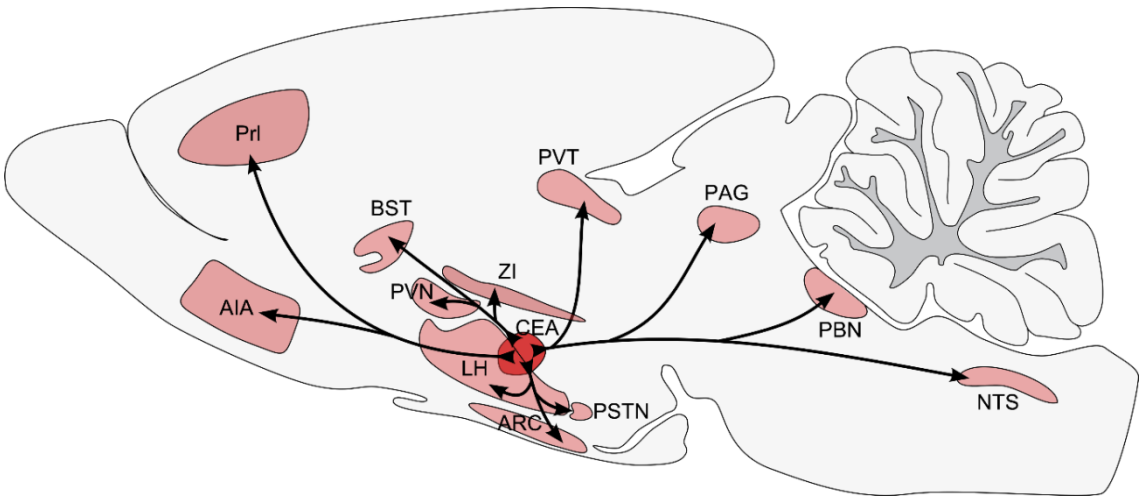

Figure 25 Schematic drawing illustrate main projections of CEA to refeeding activated neuronal groups.

DOI:10.14753/SE.2017.2041

6.5. Role of the subnuclei of the central nucleus of amygdala in the development of satiety during refeeding

6.5.1. Localization of the hSyn-hM3D(Gq)-mCherry AAV injection sites

To selectively activate neurons located in the CEA, hSyn-hM3D(Gq)-mCherry AAV was used to express the hM3Dq receptor-mCherry fusion protein in this nucleus. This receptor has a high affinity for the pharmacologically inert ligand CNO, but could not be activated by endogenous neurotransmitters (Alexander et al., 2009).

The virus injection site in 10 cases was localized within the borders of the CEA. In 6 animals the center of the injection site was in the CEAm, and did not spread into the CEAlc. In the additional 4 cases. the virus spread only the CEAlc, without reaching the medial subnucleus (**Figure 26**). Within the CEA, the CNO induced activation resulted in c-Fos expression only in the region covered by the injection site. In brains where the injection site was confined to the CEAm, the CNO treatment did not result in c-Fos activation in the CEAlc, and in brains with CEAlc injections, the neurons of CEAm were not activated by CNO (**Figure 27**).

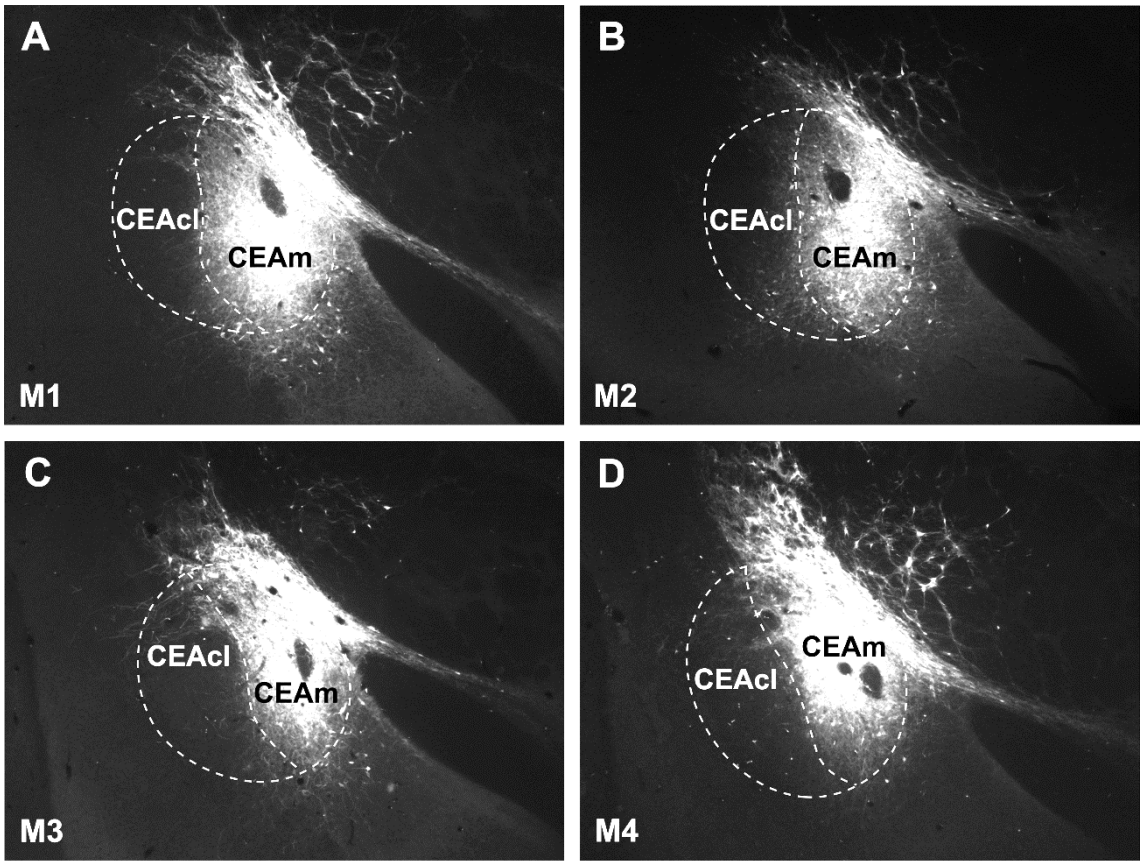

DOI:10.14753/SE.2017.2041

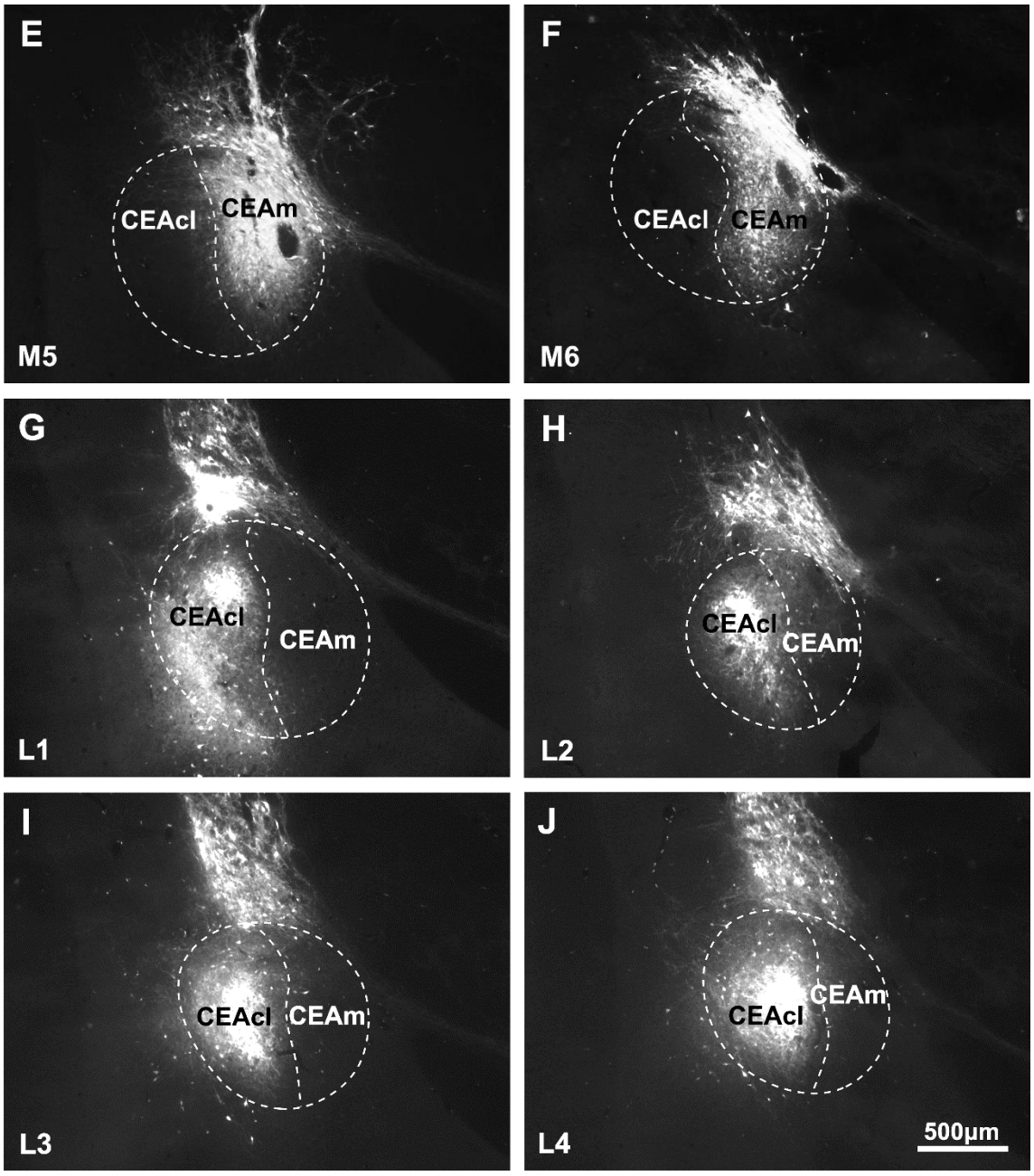

Figure 26 Localization of hSyn-hM3D(Gq)-mCherry AAV injection sites. The animals shown on (**A-F**) are used to study the effects of CEAm activation, while animals shown on (**G-J**) were used in experiments studying the effects of the activation of CEAlc. Scale bar = 500µm.

DOI:10.14753/SE.2017.2041

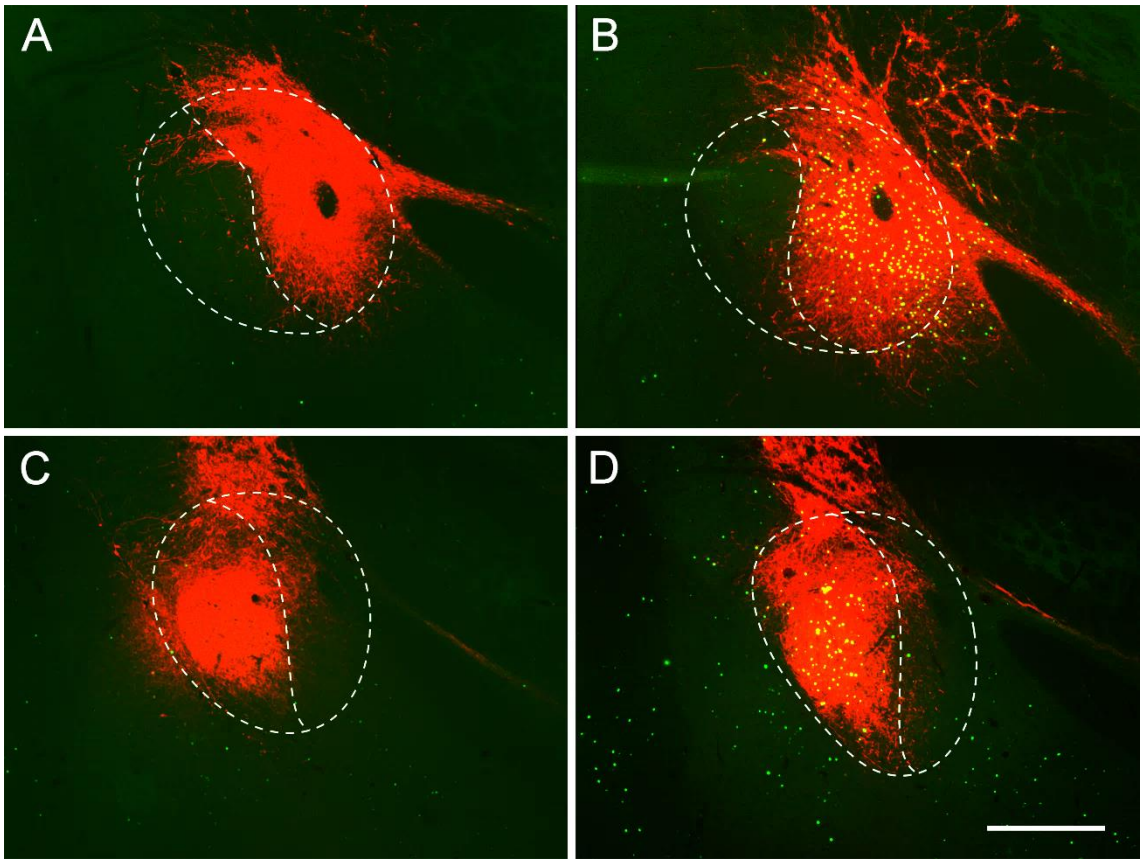

Figure 27 Effect of the chemogenetic activation of CEA subnuclei on the c-Fos expression in this nucleus. Saline treatment did not cause neuronal activation in the CEA of rats injected with hM3D(Gq)-mCherry expressing AAV in the CEAm (**A**) or CEAlc (**C**). The c-Fos-immunoreactivity is labeled with green color, while the red fluorescence of the mCherry labels the injection site. CNO treatment induced marked neuronal activation in the CEAm, but did not influence the c-Fos expression in the CEAlc in the CEAm injected animals (**B**). Conversely, CNO treatment induced marked neuronal activation in the CEAlc, but did not influence the c-Fos expression in the CEAm in the CEAlc injected animals (**D**). Scale bar =500μm.

6.5.2. Effect of chemogenetic activation of CEA subnuclei on the food intake during refeeding

Activation of the CEAm neurons by intraperitoneal CNO administration resulted in significant decrease of food intake, in the first 60 min of refeeding. Animals injected with CNO ate 15.32±1.5mg/g lean body weight whereas saline injected animals ate 23.32±2.1mg/g lean body weight, ($p=0.0035$). In the second hour of refeeding, the CNO injected animals consumed significantly more food (10.514 ±2.05 mg/g lean body weight) than the saline injected animals (2.459±1.05 mg/g lean body weight) ($p=0.006$). Therefore, the first two hours of food intake of the saline and CNO treated animals did not differ significantly ($p=0.98$). In animals with hM3D(Gq)-mCherry expression in the CEAlc, CNO treatment did not cause significant changes of food intake (Saline versus

CNO in the first hour (g/lean body weight): CNO: 24.71±0.7 versus 20.88±1.19 p= 0.24; Saline versus CNO in the second hour (g/lean body weight): 2.33±0.79 versus 3.37±2.23 p= 0.96) (**Figure 28**).

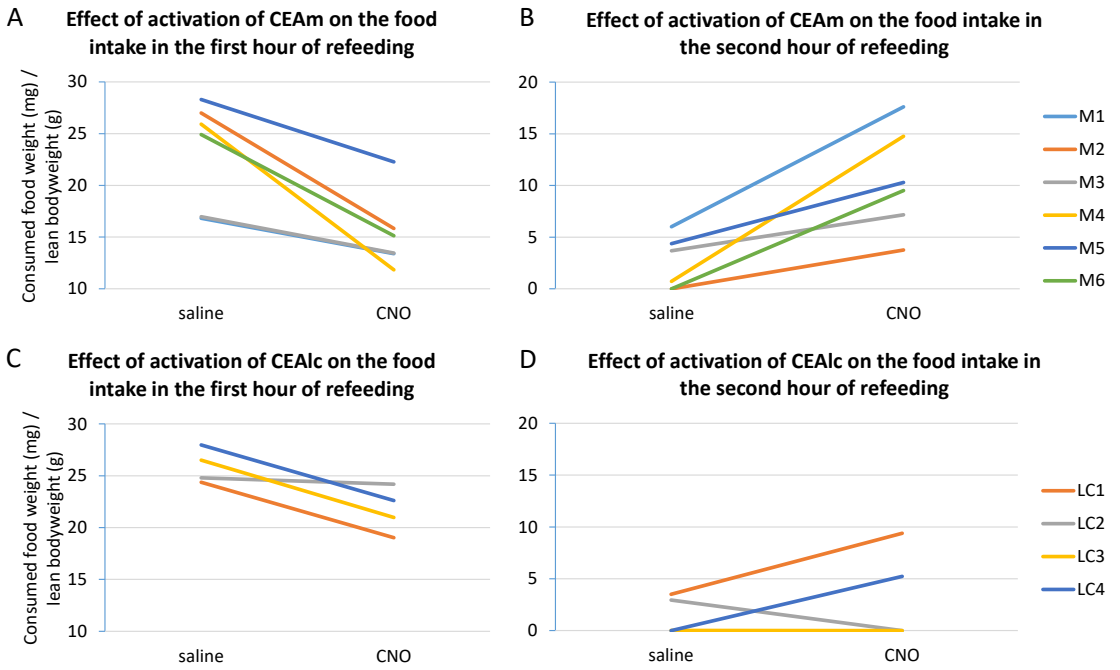

Figure 28 Effect of chemogenetic activation of the subnuclei of CEA on the food intake during refeeding. CNO induced activation of the neurons of CEAm significantly decreased the food intake in the first hour of refeeding compared to the food intake of the same animal after saline injection (**A**; p=0.003). The color lines label the differences of the food intake of the same animal after saline and CNO injection. In the second hour, the animals ate significantly more food when the CEAm was activated by CNO (**B**; p=0.006). Chemogenetic activation of CEAlc did not cause significant change of food intake. First hour food intake is shown in (**C**; p= 0.24). Second hour food intake is shown in (**D**; p= 0.956).

6.5.3. Brain areas activated by chemogenetic activation of CEA and innervated by CEA neurons

To understand which brain areas may be directly activated by CEA neurons during refeeding, the refeeding-activated brain areas were identified where chemogenetic activation of CEA subnuclei induced c-Fos expression and the activated neurons are contacted by the axons of CEA neurons. The chemogenetic activation of CEAm neurons induced significant increase of c-Fos-IR nuclei in the BST, PSTN and PBN compared to virus injected saline treated animals (**Figure 29**, **30**). Axons of CEAm neurons contacted c-Fos-IR neurons in all of these areas at the ipsilateral site.

DOI:10.14753/SE.2017.2041

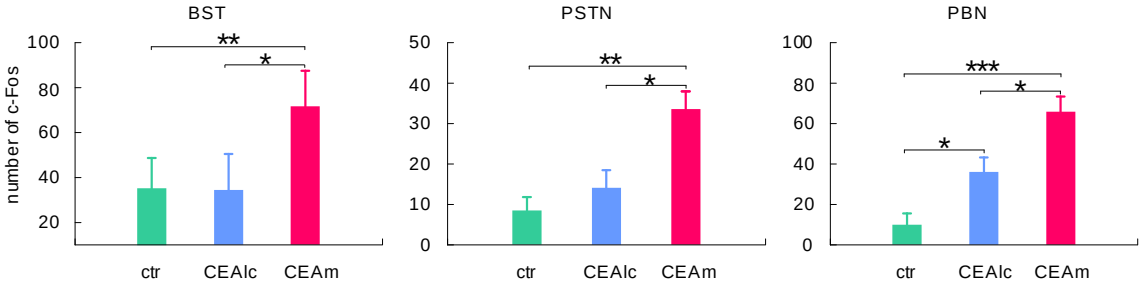

Figure 29 Effects of the chemogenetic activation of CEAlc and CEAm on the number of c-Fos-IR nuclei in brain regions responding to refeeding by neuronal activation. Control animals (ctr) were also injected by hSyn-hM3D(Gq)-mCherry AAV into the CEAlc or CEAm, but received saline treatment instead of CNO injection. (*=p<0.05, **=p<0.01, ***=p<0.001).

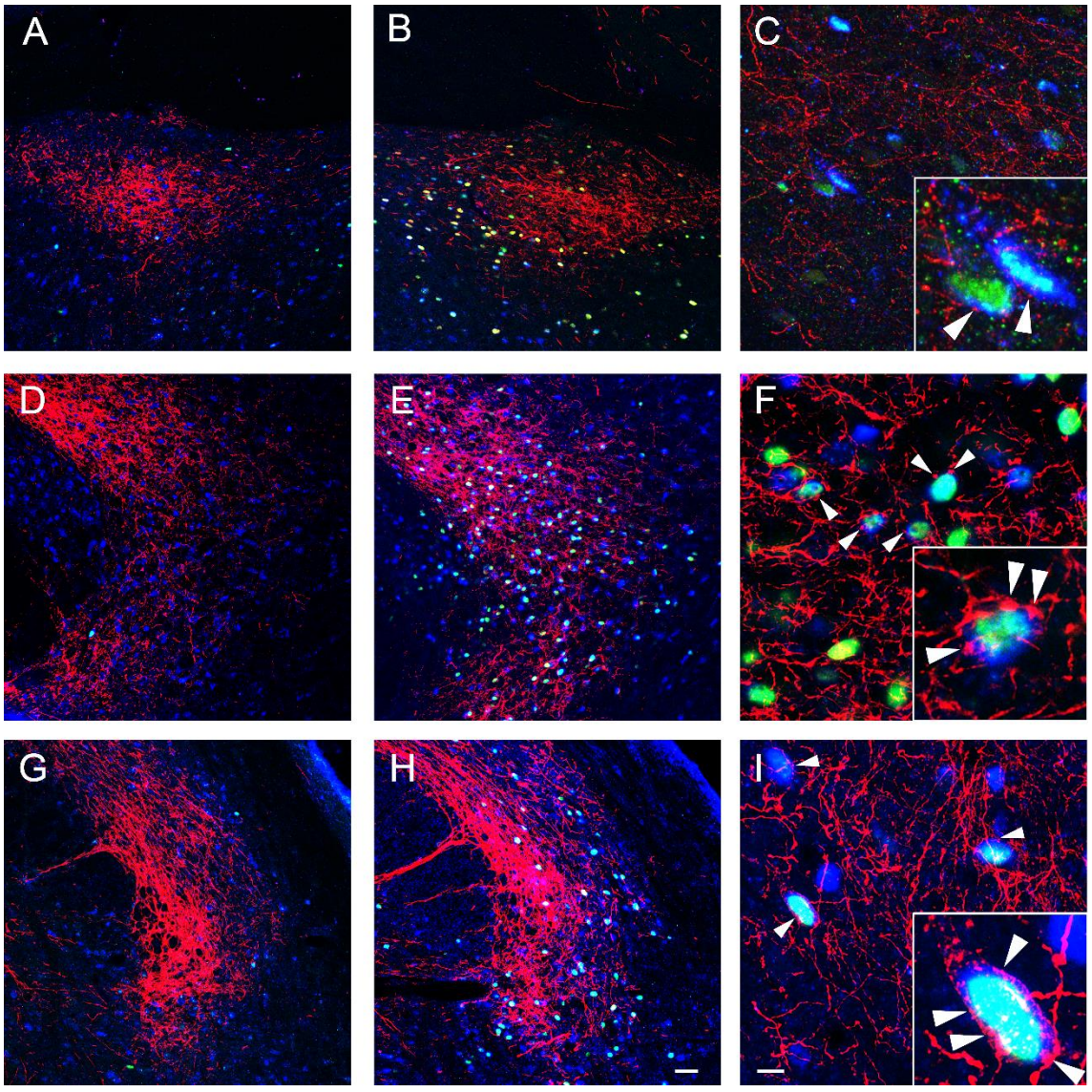

Figure 30 Confocal images of triple-immunolabeled section show mCherry containing axons (red), labeling the axons of CEA origin, activated (c-Fos-positive, green), HuC/HuD-producing neurons in saline (**A, D, G**) and CNO (**B, E, H**), treated rats in the following areas: BST (**A-C**), PSTN (**D-F**), PBN (**G-I**), Arrowhead show the activated neurons which receive inputs by mCherry positive fibers. Scale bar: 50µm on **A, B, D, E, G, H** 10µm on **C, F, I**.

DOI:10.14753/SE.2017.2041

The activation of cealc did not influence the activation of bst and pstn, but it resulted in significant increase of neuronal activation in the pbn. The increase in the number of c-fos-ir nuclei was less than that induced by the activation of ceam (**Figure 29**).

DOI:10.14753/SE.2017.2041

7. DISCUSSION

7.1. Refeeding-activated neuronal groups in the rat brain

During the last decades, an enormous effort has been made to elucidate the central mechanisms governing appetite control and energy homeostasis. While several brain regions have now been implicated, little information is available about how these neuronal groups are interconnected and function together as a network. To better understand the satiety-related neuronal network, as a first step, we took advantage of an experimental model, the refeeding of fasted animals, that we believe has made it possible to separate loci involved in satiety vs energy expenditure, and generated a detailed map of these refeeding-activated neuronal groups. In agreement with previous reports (Fekete et al., 2012; Timofeeva et al., 2002), describing refeeding-activated cell populations, c-Fos-IR neurons were observed in two, well known, major, metabolic sensor areas in the brain, in the area of the NTS and the ARC. The NTS is known to receive feeding-related inputs from the periphery through the vagus nerve, conveying information about the amount and content of the consumed food in response to distension of the esophagus and stomach, and also from the chemosensors in the wall of gastrointestinal tract (Grill and Hayes, 2009; Hayes and Covasa, 2006). Distension of esophagus and stomach results in neuronal activation in the caudal NTS, particularly the medial and commissural parts (Sabbatini et al., 2004) that overlaps the distribution of the refeeding-activated neurons identified in our study. This region of the NTS is also known to receive satiety information from amylin-sensitive neurons in the area postrema and to express leptin receptors (Grill and Hayes, 2012).

The ARC contains POMC neurons that are known to have potent anorectic effects, and regulated primarily by circulating levels of peripheral hormones like leptin, insulin and ghrelin (Schwartz et al., 2000). These neurons play a critical role in the determination of meal size during refeeding, as inhibition of melanocortin signaling markedly increases the amount of food consumed during the first two hours of refeeding (Singru et al., 2007).

In addition to these, known metabolic, sensor areas, refeeding-induced neuronal activation was also observed in second order feeding-related neuronal groups including the PVN, DMN, LH, PBN and limbic structures with a known role in the regulation of food intake including the CEA. A number of other neuronal groups that have not

previously been described as anorectic brain centers were also observed to show c-Fos activation including the PSTN and ARCdmp. The PSTN is primarily known as a preautonomic nucleus with depressor effects on circulation (Ciriello, 2007), but it is of particular interest that it may be involved in conditioned taste aversion (Yasoshima et al., 2006). Furthermore, the neurons of PSTN show increased number of c-Fos-IR neurons in association with anorexia induced by a dehydration or a diet deficient in an amino acid (Watts et al., 1999; Zhu et al., 2012).

Currently, little information is known about the role of the ARCdmp in the regulation of energy homeostasis. This region of the ARC is of particular interest because it has been implicated in seasonal regulation of body weight in the Syberian hamster (Nilaweera et al., 2009). Exposure to short days continuously activates c-Fos in the ARCdmp and induces marked changes in gene expression of energy homeostasis-related genes such as the MC3R, vascular growth factor and serotonin receptors that are associated with decreasing body weight and food intake (Nilaweera et al., 2009). Although the rat is not considered as a seasonal mammal, the apparent increase in neuronal activation of ARCdmp neurons in response to refeeding suggests that this nucleus also has an important role in the regulation of energy homeostasis in this species. Given that the activated neurons of the ARCdmp are contacted by POMC-IR varicosities (Fekete et al., 2012), we presume that the observed refeeding response is secondary to the activation of POMC neurons, suggesting an anorexigenic role of ARCdmp neurons.

The loss of c-Fos activation in the ventrolateral subdivision of the PAG of refed rats requires special mention as the PAG has been recently recognized to have a potential role in appetite regulation (Stachniak et al., 2014). In these studies, evidence for a descending input from feeding-related neurons of the PVN to the PAGvl was observed, and when the activity of this descending input was inhibited in the PAGvl, animals demonstrated a marked increase in feeding behavior. Given the loss of c-Fos in these neurons during the refeeding interval, it is possible that inhibition of this neuronal population contributes the development of satiety in these animals.

7.2. Activation of ARC POMC neurons during refeeding is independent of vagal and brainstem inputs

Experiments using chronically decerebrate rats have established the importance of gastrointestinal inputs reaching the brainstem through the vagus nerve in the regulation of meal size (Grill and Norgren, 1978). Because activation of the melanocortin system also contributes to the determination of the amount of food consumed during the early phase of refeeding (Singru et al., 2007), it could be hypothesized that a vagus nerve-NTS-ARC pathway may contribute to activation of ARC POMC neurons during refeeding. Nevertheless, the results obtained in our study using vagotomized animals, as well as animals in which the ascending input from the brainstem to the ARC had been transected on one side show, that refeeding-induced activation of POMC neurons in the ARC appears even in the absence of ascending inputs. These data indicate that the activation of ARC POMC neurons during refeeding is largely mediated through pathways independent of the vagus nerve. Although vagotomized animals had substantially reduced ARC POMC c-Fos activation compared to sham refed animals, refeeding still caused a significant increase in the number of double-labeled neurons. Thus, however, we cannot exclude the possibility that a component of POMC activation requires vagal activation, we presume, that the difference of the refeeding-induced activation of POMC neurons in the intact and vagotomized rats is related rather to an indirect effect of vagotomy on POMC regulation as a result of the decreased food intake of the vagotomized animals. This is based on the observation that like the vagotomized animals, pairfed, sham-operated rats also had a significantly decreased number of activated POMC neurons at the end of the 2 h refeeding. This is further supported by knowledge that the potential vagal input to ARC POMC neurons must be mediated through ascending brainstem pathways, as well as the observations in the present study showing that unilateral transection of the ascending brainstem pathways did not prevent refeeding-induced activation of POMC neurons and led to a similar increase in the number of POMC neurons expressing c-Fos on both the intact and transected sides. Adequacy of the transection was established by the substantial reduction of approximately 74% in the mean number of DBH-containing axon terminals in contact with POMC neurons, which is a decrease similar to that previously shown to have a profound effect on preventing increase of CRH gene expression in the PVN after endotoxin administration (Fekete et al., 2005). In

addition to the vagus nerve, spinal afferents and gustatory inputs are also involved in relaying information from the gastrointestinal tract and liver to the brain and contribute to the regulation of meal size (Grill and Hayes, 2009; Hokama et al., 2006). All of these pathways terminate in brainstem nuclei, however, and therefore could only influence the ARC through ascending pathways to the forebrain. Given that refeeding-induced similar activation of POMC neurons on both the intact and transected sides of the forebrain, it is unlikely that the vagus nerve (or any of the above mentioned routes) mediates the effect of refeeding on the POMC neurons. Altered levels of circulating hormones and increased levels of the digested and absorbed metabolites in the circulating blood, such as glucose, amino acids and fatty acids, are known to influence the POMC neurons (Schwartz et al., 2000). In the absence of a major influence from the vagus nerve or ascending input from the lower brainstem, it is feasible that one or more of circulating, hormonal or metabolic signals may be responsible for the refeeding activation of POMC neurons. Leptin is also well known to be one of the most important regulators of POMC neurons in the ARC (Morton et al., 2006). In the fed state (Elias et al., 1999), the peripheral administration of leptin results in c-Fos expression in POMC neurons in the ARC and increased expression of POMC and its derivatives (Fekete et al., 2006; Schwartz et al., 2000). After a prolonged fast, however, there is a delay in the rise of leptin levels in the circulating blood, with an increase being observed only 4 h after the onset of refeeding (Iritani et al., 2000). In addition, the administration of leptin to fasted rats does not cause c-Fos expression in the ARC (Wang et al., 1998), suggesting that leptin is unlikely to be the mediator for refeeding-induced activation of these cells. Further studies will be necessary to determine circulating mediators responsible for refeeding-induced activation of this anorexigenic cell type. Given that the lower brainstem is known to be involved in the determination of meal size (Grill and Norgren, 1978) but may not have a major role in refeeding-induced activation of POMC, as suggested by the data obtained in the present study, it is likely that a dual mechanism may be involved in regulating satiety after fasted animals have been refed. Recently, we demonstrated that one of the major projection fields of POMC-producing neurons in the ARC is a discrete population of neurons in the PVNv, which neurons are simultaneously activated by the feeding stimulus via the activation of POMC neurons (Singru et al., 2007). The PVN is considered to be an important appetite-regulating center in the hypothalamus and, on the basis of studies by Balthasar et al.

(Balthasar et al., 2005) showing that selective reactivation of the MC4-R in the PVN restores most of the satiety signals induced by melanocortin signaling, it is likely to be the primary locus in the brain that mediates the effects of α-MSH on food intake. Given that refeeding-activated neurons of the PVN project to the NTS (Fuzesi et al., 2008), focal administration of α-MSH into the PVN activates the neurons of the NTS (Singru et al., 2012), and injection of a melanocortin antagonist into the PVN attenuates the effect of peripherally administered CCK on the food intake that is known to be mediated through the vagus nerve and the NTS (Blevins et al., 2009), we hypothesized that POMC neurons through an arcuate–PVNv–NTS pathway modulate the sensitivity of the neurons of the NTS innervated by the vagus nerve. A similar pathway has been reported to mediate the effects of leucine intake on the NTS (Blouet et al., 2009). In addition, the POMC neurons may also directly influence the NTS (Zheng et al., 2010). We conclude that refeeding activates anorexigenic POMC neurons in the ARC, although this is largely independent of vagal and brainstem inputs. The data obtained in the present study raise the possibility that direct effects of circulating hormones and/or metabolites may be the primary mechanism necessary for refeeding-induced activation of POMC neurons, although cooperation between ARC and brainstem nuclei may be necessary for the regulation of meal size during refeeding.

7.3. Connections of PBN with other refeeding-activated areas

To begin to untangle the complicated circuitry involved in appetite regulation, we focused on the c-Fos-activated cells in the PBN. The PBN is a central relay nucleus in rodent taste and viscerosensory pathways (Cho et al., 2002). PBN has crucial role in the regulation of food intake. Chronic activation of PBN by ablation of orexigenic AgRP neurons leads to anorexia, because cease the inhibitory inputs of the AgRP neurons (Wu et al., 2012). Connecting to this findings, a question, which areas are the sources of excitatoric input of PBN remains. Retrograde tract tracing experiments revealed that the largest number of refeeding-activated neurons that project to the PBN reside in the NTS, PVN and PSTN. The NTS relays vagal and humoral inputs toward the PBN using glutamate as the major, anorexic neurotransmitter (Roman et al., 2016; Wu et al., 2012), indicating its important role in the mediation of feeding-related peripheral signals toward the PBN. The PVN, especially, the PVNv and PVNl, contains a large number of PBN

projecting refeeding-activated neurons that show glutamatergic phenotype and densely innervated by POMC neurons in the ARC (Singru et al., 2012). Since only few refeeding-activated POMC neurons project directly to the PBN, the PVNv and PVNl appear to serve as the major relay center between the anorexigenic ARC POMC neurons and the PBN. Particularly interesting that MC4R expressing neurons in the PVN project to the PBN and establish a dense innervation on PBN neurons. Optogenetic activation of PVN MC4R neurons which project to the PBN increased latency to feed and decreased total time spent feeding, as well as number and duration of individual feeding bouts, consistent with the promotion of satiety, but do not have effect on PBl CGRP neurons (Garfield et al., 2015), which neurons mediate the anorexigenic effects of the gastrointestinal illness and involved in conditioned taste aversion (Carter et al., 2015). Therefore, it is likely that the ascending NTS-PBN anorexigenic pathway and the descending ARC-PVN-PBN/NTS pathway interact at multiple levels that result in multimodal integration of hypothalamic and brainstem signals.

The third major source of the refeeding-related inputs of the PBN is the PSTN. The majority of PSTN neurons are glutamatergic (Ciriello et al., 2008), suggesting that the PSTN neurons may mediate the excitatory effect of refeeding on the PBN neurons. In addition, anorexigenic stimuli have been shown to induce CRH expression in the PSTN (Zhu et al., 2012), and CRH neurons in the PSTN are known to project to the PBN (Magableh and Lundy, 2014). In addition to glutamate, therefore, CRH may also be involved in the inhibition of food intake in the PSTN-PBN pathway. Since, like the PVN, the PSTN is densely innervated by POMC-containing axons, the PSTN may also serve as a relay station between ARC POMC neurons and the PBN similar to that observed for the ARC-PVN-PBN pathway. The PBN was also observed to receive refeeding-activated inputs from limbic structures, including the CEA and the BST. Activation of neurons in these brain areas is known to reduce appetite (Carter et al., 2013; Jennings et al., 2013), but also to be involved in the integration of motivation, stress, and learning (Petrovich et al., 2007; Roman et al., 2012).

To understand where the PBN may transmit the refeeding related information, the connections of the PBN with refeeding-activated neuronal groups were traced. The mapping of the input source areas of PBN followed by the tracing of PBN projection fields. Conspicuous anterograde connection was observed between the neurons of PBN

and activated cells of CEA. In addition to the PBNel-CEAlc pathway described by Carter et al. (Carter et al., 2013) our anterograde tract tracing, however, also identified massive projections from the PBN to the CEAm primarily originating from the PBm, indicative of a second major projection from the PBN to this nucleus and the existence of a PBm to CEAm anorexigenic pathway.

A major projection from the PBN was also observed to refeeding-activated neurons of BST. Although recent studies were unable to demonstrate that activation of the CGRP expressing PBN-BST pathway has an effect on food intake when stimulated optogenetically (Carter et al., 2013), these data do not exclude the possibility that projection of refeeding-activated PBN neurons to the BST is involved in the regulation of food intake. CGRP input from the PBN may represent only a fraction of the total PBN-BST input. Therefore, further, studies are needed to determine the role of the medial PBN-BST projection, observed in this study, on appetite regulation.

Intense axonal projection was detected from PBN to PSTN activated neurons. Currently, no information is available about the physiological function of PBN-PSTN pathway. Since, it is known that both of PBN and PSTN have role in the development of conditioned taste aversion. (Roman et al., 2016; Yasoshima et al., 2006) It is possible that the PSTN is also involved the taste perception. We hypothesize on the basis of the anatomical data presented in the study, furthermore, that the PSTN is another, major, integrating anorexigenic center in the regulation of food intake, as it receives inputs from multiple feeding-related centers such as the PBN, CEA and POMC neurons of the ARC. Further studies using optogenetic activation of this center are necessary to prove this hypothesis.

Since the PBN is known to receive inhibitory inputs from AgRP neurons of the ARC (Wu et al., 2009), inhibitory pathways may also contribute to the refeeding-induced activation of the PBN neurons. It is likely, therefore, that PBN neurons have wider refeeding-related inputs than recognized in the current study. Unfortunately, markers to allow immunocytochemical detection of inhibited neurons are not currently unavailable.

We demonstrated that, the PBN is highly interconnected with a large number of refeeding-activated neuronal groups in the brain through bidirectional connections, suggesting that the network of refeeding-activated neurons regulated by the PBN is not

unidirectionally connected, but rather is composed of a series of feedback loops that simultaneously facilitate or restrain information in multiple regions of the brain.

7.4. Connections of the CEA with other refeeding-activated neuronal groups

To further elucidate the connectivity of the satiety-related neuronal network, connections of the CEA with the other refeeding-activated neuronal populations were mapped using retrograde and anterograde tract-tracing methods.

However, data from the literature describe the innervation of CEA by NTS neurons (van der Kooy et al., 1984), the NTS-CEA pathway does not appear to be a major refeeding-related input of CEA, as only few refeeding-activated neurons of the NTS were observed to project to the CEA in our study. In contrast, a major refeeding-related input to the CEA was found to originate from the PBN in agreement with our studies focusing on the connectivity of the PBN.

Similarly to the NTS, we have observed only few refeeding-activated ARC POMC neurons projecting to the CEA. These data indicate that the CEA does not receive the feeding-related sensory inputs directly from the sensory areas of the brain, but rather through relay nuclei suggesting that the CEA receives already integrated, processed information about the energy homeostasis-related conditions of the peripheral organs. A major refeeding-activated input to the CEA was observed to originate from the PSTN. In agreement with previous studies (Chometton et al., 2016; Goto and Swanson, 2004) describing projection from the PSTN to the CEA, large number of retrogradely labeled neurons were observed in the PSTN after CTB deposition to the CEA. A major portion of these cells were refeeding-activated suggesting that the PSTN may mediate refeeding-related information to the CEA, likewise as shown in case of PBN. Currently, little is known about the role of this nucleus in the regulation of energy homeostasis. These authors (Chometton et al., 2016) also suggest that the PSTN may be involved in the processing of the hedonic value of food. Therefore, the PSTN may integrate the POMC derived inputs with hedonic information and may modulate the activity of the NTS-PBN-CEA satiety pathway.

The PVT is also a component of the neural circuitry controlling feeding behavior and was found to be a major source of the refeeding-activated inputs of the CEA. The PVT projects to and receives inputs from a number of other feeding-related sites such as

the PBN, NTS, ARC and LH (Chen and Su, 1990; Cornwall and Phillipson, 1988; Moga et al., 1995). Many of these connections contain feeding-related peptides, such as glucagon-like peptide 1 (Llewellyn-Smith et al., 2011), CART (Kirouac et al., 2006), CCK (Otake, 2005) and orexin (Kirouac et al., 2005), all which have been shown to influence food intake. Lesions or inhibition of PVT neurons have been reported to increase food intake and weight gain in rats (Bhatnagar and Dallman, 1999; Stratford and Wirtshafter, 2013), supporting its role in the termination of food intake.

A less dense refeeding-related input to the CEA was found to originate from parts of the prefrontal cortex. This observation is of interest as the prefrontal cortex has been implicated in goal-directed actions, including food reward and memories required for obtaining food. Specifically, the Prl is heavily involved in instrumental learning and performance (Baldwin et al., 2000; Baldwin et al., 2002; Balleine and Dickinson, 1998), and the agranular insular cortical area in working memory for food reward value (DeCoteau et al., 1997), as anticipatory discriminability is impaired in rats with AIA lesions (Kesner and Gilbert, 2007).

To elucidate the neuronal pathways mediating the effects of refeeding-activated CEA neurons on food intake, the efferent connections of the CEA with refeeding-activated neuronal groups were also studied. These experiments demonstrated that refeeding-activated CEA neurons have bidirectional connections with the PSTN, PBN, BST and the PVT. Since these areas appear to mediate the effects of peripheral refeeding-related signals to the CEA, projections from the CEA to these cell populations may serve as a short feedback loop that facilitates or restrains refeeding-activated neuronal inputs to the CEA. Although the CEA projects to the NTS, it does not receive major, refeeding-related, direct inputs from the NTS. Nevertheless, the NTS may still be capable of relaying satiety information to the CEA indirectly via the NTS-PBN-CEA pathway. Since the CEA-NTS pathway is primarily GABAergic (Serrats and Sawchenko, 2006), it is likely that the CEA projection to the NTS decreases the sensitivity of the NTS neurons to the peripheral signals rather than facilitate the satiety response.

Another refeeding-related region of the brain demonstrating reciprocal connections with the CEA is the midbrain PAG. Reciprocal connections between these two regions were previously recognized by Rizvi et al (Rizvi et al., 1991). This region is of interest because similar to the CEA, the periaqueductal gray is also involved in emotional and

limbic behaviors and cardiovascular responses, hence, it is suggested to be an important structure mediating functions elicited from CEA (Rizvi et al., 1991). Support for this region in feeding responses was recently reported by Stachiak et al. showing increased food intake after optogenetic inhibition of the descending glutamatergic input to the PAGvl (Stachniak et al., 2014). Refeeding, however, appears to differentially regulate two, separate populations of cells in the PAGvl including a cell group in the lateral part of this region that is inhibited by refeeding, and a medial group that is activated by refeeding. Thus, the PAGvl may contain both orexigenic and anorexigenic neurons. Further studies are needed to characterize these cells, support the existence of orexigenic cells in this brain region and determine whether the refeeding-inhibited cells also receive input from the CEA. Given that the CEA has major, GABAergic, efferent projections (Serrats and Sawchenko, 2006), the possibility that some PAGvl neurons may be inhibited is quite possible. In fact, there may be other refeeding-related targets of CEA that show inhibition during refeeding and would not be detected by c-Fos immunocytochemistry. Thus, it is likely that CEA may have an even wider refeeding-related output than recognized by these studies.

The CEA also has a major unilateral projection to the LH. This hypothalamic region is an integrative site for signals underlying the motivation to eat that includes physiological signals from the body and external signals from the environment contributing to feeding, reward, and motivation (Elmquist et al., 1999; Kelley et al., 2005; Morton et al., 2006; Swanson, 2000; Wise, 1974). Results to date suggest that glutamate in the LH may have a major role in the generation of feeding, whereas GABA induces satiety (Delgado and Anand, 1953; Stanley et al., 2011; Turenius et al., 2009). Since the CEA contains both glutamatergic and GABAergic neurons (Archer et al., 1999), further experiments are needed to reveal the classical neurotransmitter content of the CEA-LH pathway and understand its role in the development of refeeding-induced satiety. Since neurons in the LH have an important role in food reward, the CEA-LH pathway may also modulate the reward value of food that facilitates termination of food intake.

In summary, the present tract-tracing experiments reveal that the CEA similarly to the PBN is highly interconnected with refeeding-activated brain areas. The interconnection particularly robust with the PBN, PSTN, PVT and the BST. Information

from the NTS, however, would appear to be primarily transmitted to the CEA through the PBN and from the ARC POMC neurons through the PSTN.

7.5. Role of CEA subnuclei in the development of satiety during refeeding

The functional role of the CEA in the regulation of food intake has been demonstrated using optogenetic tools (Carter et al., 2013). However, in these studies, only the role of the PBN CGRP neurons-PBNel pathway was investigated (Carter et al., 2013). However, our studies suggested that a PBm-CEAm pathway is involved in the regulation of food intake during refeeding. To test this possibility, we studied whether optogenetic activation of CEA subnuclei can alter the food intake during refeeding.

Chemogenetic activation caused neuronal activation only in the virus infected cells within the CEA. This specific activation pattern allowed the examination of the effects of CEAm and CEAlc activations separately. During refeeding, the activation of CEAlc neurons had no significant effect on the food intake. In contrast, activation of CEAm resulted in a marked decrease of food intake in the first hour of refeeding. However, the second hour food intake of the CEAm activated rats was higher than that of the saline treated animals. Therefore, the food intake during the first two hours was not different between the groups. These data suggest that the activation of CEAm did not influence the amount of food required for satiety, but the animals consumed this amount of food during a longer period of time. Therefore, we hypothesize that CEAm activation decreased the motivation to eat.

To determine which refeeding-activated neuron groups are directly activated by neurons of CEA subnuclei, we studied the effect of CEA activation on the c-Fos expression in refeeding-activated brain areas and determined whether these cell groups are innervated by CEA neurons. The chemogenetic activation of CEAm resulted in significant increase in the number of c-Fos-IR neurons in the BST, PSTN, and PBN indicating that the CEA activates these brain regions. As CEAm neurons establish contact with a large number of c-Fos-IR cells in these areas on the ipsilateral site, our data indicate that the CEAm is involved in the refeeding-induced activation of the BST, PSTN and PBN. In contrast, the activation of CEAlc caused neuronal activation only in the PBN and the CEAlc induced increase in the number of activated neurons was significantly lower than that after CEAm activation.

DOI:10.14753/SE.2017.2041

Further studies will be necessary to determine the role of the CEAm-BST, CEAm-PSTN and CEAm-PBN pathways in the regulation of food intake.

Our results indicate that the CEAm does not regulate the meal size, but rather influence the motivation for eating. In addition, our data demonstrate that in addition to the PBN-CGRP-CEAlc pathway, a parallel PBm-CEAm pathway is also involved in the regulation of food intake.

DOI:10.14753/SE.2017.2041

8. CONCLUSIONS

Our studies provide detailed map of the pattern of refeeding-induced neuronal activation. This information contributes to the better understanding of the neural network involved in the development of satiety. These data verify the involvement of the well-known feeding-related nuclei such as the NTS, PBN and CEA in the regulation of refeeding-induced satiety. In addition, our data also suggest the role of other brain areas, like the PSTN and ARCdmp, in the regulation of satiety. Further examination of the role of these brain regions in the development of satiety may contribute to the better understanding of the neuronal regulation of energy homeostasis.

We also demonstrated that the ARC POMC neurons are activated independently from the vagus nerve and from the ascending brainstem pathways. These data suggest that the POMC neurons are activated solely by direct effects of circulating hormones or metabolites during refeeding. We presume that the information reaching the brain via the ARC and the NTS is integrated at the level of the NTS by the influence of the ARC POMC neuron-PVNv-NTS pathway on the sensitivity of the NTS neurons for the vagus nerve derived inputs.

The mapping of the connectivity of PBN and CEA with refeeding-activated neuronal groups revealed that these areas have bidirectional connections with each other and with other refeeding-activated cell groups suggesting that the information flow is not unidirectional in the satiety network, but this network rather utilizes short feedback mechanisms to support the precise tuning of neuronal activity. The rich connectivity of the PSTN with the other refeeding-activated groups suggests that PSTN is an important node of this network that may have critical role in the integration of neuronal activity in the satiety network.

In addition, our tract tracing data together with the chemogenetic examination of the role of CEA subnuclei in the regulation of feeding indicate that a PBm-CEAm pathway plays important role in the regulation of food intake during refeeding. This pathway is different than the PBNel-CEAlc pathway described by Palmiter's research laboratory which pathway is involved in the development of conditional taste aversion. Thus, we presume that parallel PBN-CEA pathways regulate different aspect of food intake.

DOI:10.14753/SE.2017.2041

9. SUMMARY

In rodents, satiety is observed within 2 hours after the onset of food intake when animals are refed after fasting. At this time point, the expression of the neuronal activation marker c-Fos is increased in some brain areas involved in the regulation of energy homeostasis. Despite the early termination of food intake, the energy expenditure is only increased 24h after eating. Hence, we used the refeeding as a model to examine the satiety regulating neuronal network. As a first step, we mapped the refeeding-activated neuronal groups. Increased number of c-Fos-containing neurons was observed in several brain regions, known to have role in the regulation of feeding such as PVN, ARC, NTS, CEA, and PBN. In addition, neuronal activation was also observed in brain areas with less evident role in the regulation of energy homeostasis, like the ARCdmp and PSTN.

The NTS and the refeeding-activated POMC neurons of ARC are important sensors of metabolic signals. Since, the NTS plays critical role in the termination of food intake, we presumed that signals carried by the vagus nerve and the ascending brainstem pathways are involved in the activation of POMC neurons during refeeding. However, neither the vagotomy, nor the unilateral transection of ascending brainstem pathways prevented the activation of ARC POMC neurons indicating that the activation of these cells is caused by direct effects of circulating factors. To examine the satiety network of the brain, we used anterograde and retrograde tract tracing and mapped the connections of PBN and CEA with other refeeding-related areas. These two areas establish bidirectional connections with other refeeding-activated areas in the forebrain, midbrain and brainstem. Based on the anatomical connections and the locations of c-Fos-containing neurons in refed animals, we presume that the medial subnuclei of these two brain regions have major role in the development of satiety during refeeding. To test this, we investigated the effect of chemogenetic activation of CEAm and CEAlc on the food intake and neuronal activation during refeeding. The activation of CEAm increased the number of c-Fos-IR nuclei in the BST, PSTN and PBN, which areas are also activated during refeeding. The activation of CEAlc resulted less activation only in the PBN. The activation of CEAm decreased of food intake in the first hour of refeeding, however, this was compensated by the food intake in the second hour. These data indicate that the activation of CEAm decreases the motivation for eating, but does not affect the amount of food necessary for satiety. Thus, the CEAm activation causes less intense but longer food intake. The activation of CEAlc had no effect on the food intake during refeeding.

DOI:10.14753/SE.2017.2041

10. ÖSSZEFOGLALÁS

Rágcsálókban éhezést követő újraetetés során 2 órán belül jóllakottság alakul ki, az állatok befejezik az evést. Ekkor egyes energiaháztartás szabályozásában részt vevő agyterületen neuronális aktivációra utaló, fokozott c-Fos expresszió történik. Mivel az állatok energialeadása az újraetetés után csak 24 óra elteltével változik, az újraetetést használtuk, mint modellt, a jóllakottságot szabályozó neuronális hálózat vizsgálatára. Első lépésként feltérképeztük az újraetetés során aktiválódó agyterületeket. A c-Fos tartalmú idegsejtek számának növekedését figyeltük meg számos, a táplálékfelvétel szabályozásában kulcsszerepet játszó agyterületen, mint a PVN, ARC, NTS, CEA és PBN területén, emellett olyan agyterületeken is, amelyek szerepe a táplálkozás szabályozásában még nem tisztázott, mint amilyen az ARCdmp és a PSTN.

Az ARC újraetetés során aktiválódó anorexigén POMC idegsejtjei és az NTS is a perifériás metabolikus jelek érzékelői. Mivel az NTS-nek fontos szerepe van a táplálékfelvétel befejezésének szabályozásában, feltételeztük, hogy a nervus vaguson és az NTS-en keresztül érkező jelek idézik elő a POMC sejtek aktivációját újraetetés során. Azonban sem a nervus vagus átvágása, sem a felszálló agytörzsi pályák féloldali átvágása nem védte ki az ARC POMC sejtjeinek aktiválódását, ami arra utal, hogy ezt közvetlenül a vérben keringő faktorok eredményezik. A jóllakottságot szabályozó agyi hálózat feltárása érdekében a retrográd és anterográd pályajelöléssel feltérképeztük a PBN és a CEA kapcsolatait az újraetetés során aktiválódó területekkel. E két agyterület kétirányú kapcsolattal bír számos előagyi, köztiagyi és agytörzsi újraetetés hatására aktiválódó sejtcsoporttal. A c-Fos tartalmú neuronok elhelyezkedése és az anatómiai kapcsolatok alapján feltételezzük, hogy az újraetetés után kialakuló anorexiában a PBN és a CEA almagjai közül mindkét mag mediális almagja játszik nagyobb szerepet. Ennek tisztázása érdekében a CEA almagjainak, a CEAm és a CEAlc, kemogenetikai aktiválásának neuronális aktivációra és táplálékfelvételre kifejtett hatását vizsgáltuk. A CEAm aktivációja az újraetetés során is aktiválódó BST, PSTN, PBN területén fokozta a c-Fos tartalmú sejtek számát. A CEAlc a PBN-ben okozott csak kisebb aktivációt. A CEAm aktivációja éheztetést követő újraetetés első órájában csökkentette a felvett táplálék mennyiségét, amit az állatok 2. órai táplálékfelvétele kiegyenlített. Ez arra utal, hogy a CEAm aktivációja csökkenti az étvágyat (motivációt), de a jóllakottsághoz szükséges tápanyagmennyiséget nem befolyásolja, így kevésbé intenzív, de időben elnyújtottabb táplálékfelvételt eredményez. A CEAlc aktivációja nem volt hatással a táplálékfelvételre.

11. REFERENCES

Adan RA, Tiesjema B, Hillebrand JJ, la Fleur SE, Kas MJ, de Krom M. 2006. The MC4 receptor and control of appetite. Br J Pharmacol 149(7):815-827.

Alexander GM, Rogan SC, Abbas AI, Armbruster BN, Pei Y, Allen JA, Nonneman RJ, Hartmann J, Moy SS, Nicolelis MA, McNamara JO, Roth BL. 2009. Remote control of neuronal activity in transgenic mice expressing evolved G protein-coupled receptors. Neuron 63(1):27-39.

Andre V, Dube C, Francois J, Leroy C, Rigoulot MA, Roch C, Namer IJ, Nehlig A. 2007. Pathogenesis and pharmacology of epilepsy in the lithium-pilocarpine model. Epilepsia 48:41-47.

Archer S, Li TT, Evans AT, Britland ST, Morgan H. 1999. Cell reactions to dielectrophoretic manipulation. Biochem Biophys Res Commun 257(3):687-698.

Baldwin AE, Holahan MR, Sadeghian K, Kelley AE. 2000. N-methyl-D-aspartate receptor-dependent plasticity within a distributed corticostriatal network mediates appetitive instrumental learning. Behav Neurosci 114(1):84-98.

Baldwin AE, Sadeghian K, Kelley AE. 2002. Appetitive instrumental learning requires coincident activation of NMDA and dopamine D1 receptors within the medial prefrontal cortex. J Neurosci 22(3):1063-1071.

Balleine BW, Dickinson A. 1998. Goal-directed instrumental action: contingency and incentive learning and their cortical substrates. Neuropharmacology 37(4-5):407-419.

Balthasar N, Dalgaard LT, Lee CE, Yu J, Funahashi H, Williams T, Ferreira M, Tang V, McGovern RA, Kenny CD, Christiansen LM, Edelstein E, Choi B, Boss O, Aschkenasi C, Zhang CY, Mountjoy K, Kishi T, Elmquist JK, Lowell BB. 2005. Divergence of melanocortin pathways in the control of food intake and energy expenditure. Cell 123(3):493-505.

Baxter MG, Murray EA. 2002. The amygdala and reward. Nat Rev Neurosci 3(7):563-573.

Begg DP, Woods SC. 2012. The Central Insulin System and Energy Balance. In: Joost HG, ed. Appetite Control. Handbook of Experimental Pharmacology, Hofman FB ed. New York: Springer. p 111-130.

Berthoud HR. 2008. The vagus nerve, food intake and obesity. Regul Pept 149(1-3):15-25.

Bhatnagar S, Dallman MF. 1999. The paraventricular nucleus of the thalamus alters rhythms in core temperature and energy balance in a state-dependent manner. Brain Res 851(1-2):66-75.

Blevins JE, Morton GJ, Williams DL, Caldwell DW, Bastian LS, Wisse BE, Schwartz MW, Baskin DG. 2009. Forebrain melanocortin signaling enhances the hindbrain satiety response to CCK-8. Am J Physiol Regul Integr Comp Physiol 296(3):R476-484.

Blouet C, Jo YH, Li X, Schwartz GJ. 2009. Mediobasal hypothalamic leucine sensing regulates food intake through activation of a hypothalamus-brainstem circuit. J Neurosci 29(26):8302-8311.

Callahan LB, Tschetter KE, Ronan PJ. 2013. Inhibition of corticotropin releasing factor expression in the central nucleus of the amygdala attenuates stress-induced behavioral and endocrine responses. Front Neurosci 7:195.

Campos CA, Bowen AJ, Schwartz MW, Palmiter RD. 2016. Parabrachial CGRP Neurons Control Meal Termination. Cell Metab 23(5):811-820.

Carter ME, Han S, Palmiter RD. 2015. Parabrachial calcitonin gene-related peptide neurons mediate conditioned taste aversion. J Neurosci 35(11):4582-4586.

Carter ME, Soden ME, Zweifel LS, Palmiter RD. 2013. Genetic identification of a neural circuit that suppresses appetite. Nature 503(7474):111-114.

Cervero F, Foreman RD. 1990. Sensory Innervation of Viscera. In: Loewy AD, Spyer KM, eds. Central Regulation of Autonomic Functions. Oxford: Oxford publisher. p 104-125.

Chen S, Su HS. 1990. Afferent connections of the thalamic paraventricular and parataenial nuclei in the rat--a retrograde tracing study with iontophoretic application of Fluoro-Gold. Brain Res 522(1):1-6.

Cho YK, Li CS, Smith DV. 2002. Gustatory projections from the nucleus of the solitary tract to the parabrachial nuclei in the hamster. Chem Senses 27(1):81-90.

Chometton S, Pedron S, Peterschmitt Y, Van Waes V, Fellmann D, Risold PY. 2016. A premammillary lateral hypothalamic nuclear complex responds to hedonic but not aversive tastes in the male rat. Brain Struct Funct 221(4):2183-2208.

Ciriello J. 2007. Cardiovascular depressor responses to stimulation of the parasubthalamic nucleus. Faseb Journal 21(5):A474-A474.

Ciriello J, Solano-Flores LP, Rosas-Arellano MP, Kirouac GJ, Babic T. 2008. Medullary pathways mediating the parasubthalamic nucleus depressor response. Am J Physiol Regul Integr Comp Physiol 294(4):R1276-1284.

Corander MP, Coll AP. 2011. Melanocortins and body weight regulation: glucocorticoids, Agouti-related protein and beyond. Eur J Pharmacol 660(1):111-118.

Cornwall J, Phillipson OT. 1988. Afferent projections to the dorsal thalamus of the rat as shown by retrograde lectin transport. II. The midline nuclei. Brain Res Bull 21(2):147-161.

Cui RJ, Li X, Appleyard SM. 2011. Ghrelin inhibits visceral afferent activation of catecholamine neurons in the solitary tract nucleus. J Neurosci 31(9):3484-3492.

Date Y, Kojima M, Hosoda H, Sawaguchi A, Mondal MS, Suganuma T, Matsukura S, Kangawa K, Nakazato M. 2000. Ghrelin, a novel growth hormone-releasing acylated peptide, is synthesized in a distinct endocrine cell type in the gastrointestinal tracts of rats and humans. Endocrinology 141(11):4255-4261.

Davis JD, Gallagher RL, Ladove R. 1967. Food intake controlled by a blood factor. Science 156(3779):1247-1248.

Dawson R, Pelleymounter MA, Millard WJ, Liu S, Eppler B. 1997. Attenuation of leptin-mediated effects by monosodium glutamate-induced arcuate nucleus damage. Am J Physiol 273(1 Pt 1):E202-206.

de Lartigue G, Diepenbroek C. 2016. Novel developments in vagal afferent nutrient sensing and its role in energy homeostasis. Curr Opin Pharmacol 31:38-43.

de Lartigue G, Ronveaux CC, Raybould HE. 2014. Deletion of leptin signaling in vagal afferent neurons results in hyperphagia and obesity. Mol Metab 3(6):595-607.

Debons AF, Krimsky I, Maayan ML, Fani K, Jemenez FA. 1977. Gold thioglucose obesity syndrome. Fed Proc 36(2):143-147.

DeCoteau WE, Kesner RP, Williams JM. 1997. Short-term memory for food reward magnitude: the role of the prefrontal cortex. Behav Brain Res 88(2):239-249.

Delgado JM, Anand BK. 1953. Increase of food intake induced by electrical stimulation of the lateral hypothalamus. Am J Physiol 172(1):162-168.

Dinulescu DM, Cone RD. 2000. Agouti and agouti-related protein: analogies and contrasts. J Biol Chem 275(10):6695-6698.

Elias CF, Aschkenasi C, Lee C, Kelly J, Ahima RS, Bjorbaek C, Flier JS, Saper CB, Elmquist JK. 1999. Leptin differentially regulates NPY and POMC neurons projecting to the lateral hypothalamic area. Neuron 23(4):775-786.

Elmquist JK, Elias CF, Saper CB. 1999. From lesions to leptin: hypothalamic control of food intake and body weight. Neuron 22(2):221-232.

Elmquist JK, Saper CB. 1996. Activation of neurons projecting to the paraventricular hypothalamic nucleus by intravenous lipopolysaccharide. J Comp Neurol 374(3):315-331.

Farooqi IS, O'Rahilly S. 2008. Mutations in ligands and receptors of the leptin-melanocortin pathway that lead to obesity. Nat Clin Pract Endocrinol Metab 4(10):569-577.

Farooqi S, Rau H, Whitehead J, O'Rahilly S. 1998. ob gene mutations and human obesity. Proc Nutr Soc 57(3):471-475.

Fekete C, Legradi G, Mihaly E, Huang QH, Tatro JB, Rand WM, Emerson CH, Lechan RM. 2000. alpha-Melanocyte-stimulating hormone is contained in nerve terminals innervating thyrotropin-releasing hormone-synthesizing neurons in the hypothalamic paraventricular nucleus and prevents fasting-induced suppression of prothyrotropin-releasing hormone gene expression. J Neurosci 20(4):1550-1558.

Fekete C, Singru PS, Sanchez E, Sarkar S, Christoffolete MA, Riberio RS, Rand WM, Emerson CH, Bianco AC, Lechan RM. 2006. Differential effects of central leptin, insulin, or glucose administration during fasting on the hypothalamic-pituitary-thyroid axis and feeding-related neurons in the arcuate nucleus. Endocrinology 147(1):520-529.

Fekete C, Singru PS, Sarkar S, Rand WM, Lechan RM. 2005. Ascending brainstem pathways are not involved in lipopolysaccharide-induced suppression of thyrotropin-releasing hormone gene expression in the hypothalamic paraventricular nucleus. Endocrinology 146(3):1357-1363.

Fekete C, Zseli G, Singru PS, Kadar A, Wittmann G, Fuzesi T, El-Bermani W, Lechan RM. 2012. Activation of anorexigenic pro-opiomelanocortin neurones during refeeding is independent of vagal and brainstem inputs. J Neuroendocrinol 24(11):1423-1431.

Frederich RC, Lollmann B, Hamann A, Napolitano-Rosen A, Kahn BB, Lowell BB, Flier JS. 1995. Expression of ob mRNA and its encoded protein in rodents. Impact of nutrition and obesity. J Clin Invest 96(3):1658-1663.

Fuzesi T, Sanchez E, Wittmann G, Singru PS, Fekete C, Lechan RM. 2008. Regulation of cocaine- and amphetamine-regulated transcript-synthesising neurons of the hypothalamic paraventricular nucleus by endotoxin; implications for lipopolysaccharide-induced regulation of energy homeostasis. J Neuroendocrinol 20(9):1058-1066.

Garfield AS, Li C, Madara JC, Shah BP, Webber E, Steger JS, Campbell JN, Gavrilova O, Lee CE, Olson DP, Elmquist JK, Tannous BA, Krashes MJ, Lowell BB. 2015. A neural basis for melanocortin-4 receptor-regulated appetite. Nat Neurosci 18(6):863-871.

Ghamari-Langroudi M, Digby GJ, Sebag JA, Millhauser GL, Palomino R, Matthews R, Gillyard T, Panaro BL, Tough IR, Cox HM, Denton JS, Cone RD. 2015. G-protein-

independent coupling of MC4R to Kir7.1 in hypothalamic neurons. Nature 520(7545):94-98.

Gibbs J, Young RC, Smith GP. 1973. Cholecystokinin elicits satiety in rats with open gastric fistulas. Nature 245(5424):323-325.

Goto M, Swanson LW. 2004. Axonal projections from the parasubthalamic nucleus. J Comp Neurol 469(4):581-607.

Grill HJ, Hayes MR. 2009. The nucleus tractus solitarius: a portal for visceral afferent signal processing, energy status assessment and integration of their combined effects on food intake. Int J Obes (Lond) 33 Suppl 1:S11-15.

Grill HJ, Hayes MR. 2012. Hindbrain neurons as an essential hub in the neuroanatomically distributed control of energy balance. Cell Metab 16(3):296-309.

Grill HJ, Norgren R. 1978. Chronically Decerebrate Rats Demonstrate Satiation but Not Bait Shyness. Science 201(4352):267-269.

Gropp E, Shanabrough M, Borok E, Xu AW, Janoschek R, Buch T, Plum L, Balthasar N, Hampel B, Waisman A, Barsh GS, Horvath TL, Bruning JC. 2005. Agouti-related peptide-expressing neurons are mandatory for feeding. Nat Neurosci 8(10):1289-1291.

Hajnal A, Takenouchi K, Norgren R. 1999. Effect of intraduodenal lipid on parabrachial gustatory coding in awake rats. J Neurosci 19(16):7182-7190.

Halaas JL, Gajiwala KS, Maffei M, Cohen SL, Chait BT, Rabinowitz D, Lallone RL, Burley SK, Friedman JM. 1995. Weight-reducing effects of the plasma protein encoded by the obese gene. Science 269(5223):543-546.

Hayes MR, Covasa M. 2006. Gastric distension enhances CCK-induced Fos-like immunoreactivity in the dorsal hindbrain by activating 5-HT3 receptors. Brain Res 1088(1):120-130.

Hayes MR, Skibicka KP, Leichner TM, Guarnieri DJ, DiLeone RJ, Bence KK, Grill HJ. 2010. Endogenous leptin signaling in the caudal nucleus tractus solitarius and area postrema is required for energy balance regulation. Cell Metab 11(1):77-83.

Hill JW, Williams KW, Ye C, Luo J, Balthasar N, Coppari R, Cowley MA, Cantley LC, Lowell BB, Elmquist JK. 2008. Acute effects of leptin require PI3K signaling in hypothalamic proopiomelanocortin neurons in mice. J Clin Invest 118(5):1796-1805.

Hokama A, Nakamoto M, Kinjo F, Fujita J. 2006. 'The sandwich sign' of mesenteric lymphoma. Eur J Haematol 77(4):363-364.

Iritani N, Sugimoto T, Fukuda H. 2000. Gene expressions of leptin, insulin receptors and lipogenic enzymes are coordinately regulated by insulin and dietary fat in rats. J Nutr 130(5):1183-1188.

Iwakura H, Kangawa K, Nakao K. 2015. The regulation of circulating ghrelin - with recent updates from cell-based assays. Endocr J 62(2):107-122.

Jennings JH, Rizzi G, Stamatakis AM, Ung RL, Stuber GD. 2013. The inhibitory circuit architecture of the lateral hypothalamus orchestrates feeding. Science 341(6153):1517-1521.

Ji H, Friedman MI. 1999. Compensatory hyperphagia after fasting tracks recovery of liver energy status. Physiol Behav 68(1-2):181-186.

Kanoski SE, Zhao S, Guarnieri DJ, DiLeone RJ, Yan J, De Jonghe BC, Bence KK, Hayes MR, Grill HJ. 2012. Endogenous leptin receptor signaling in the medial nucleus tractus solitarius affects meal size and potentiates intestinal satiation signals. Am J Physiol Endocrinol Metab 303(4):E496-503.

Kelley AE, Baldo BA, Pratt WE, Will MJ. 2005. Corticostriatal-hypothalamic circuitry and food motivation: integration of energy, action and reward. Physiol Behav 86(5):773-795.

Kesner RP, Gilbert PE. 2007. The role of the agranular insular cortex in anticipation of reward contrast. Neurobiol Learn Mem 88(1):82-86.

Kirouac GJ, Parsons MP, Li S. 2005. Orexin (hypocretin) innervation of the paraventricular nucleus of the thalamus. Brain Res 1059(2):179-188.

Kirouac GJ, Parsons MP, Li S. 2006. Innervation of the paraventricular nucleus of the thalamus from cocaine- and amphetamine-regulated transcript (CART) containing neurons of the hypothalamus. J Comp Neurol 497(2):155-165.

Kojima M, Hosoda H, Date Y, Nakazato M, Matsuo H, Kangawa K. 1999. Ghrelin is a growth-hormone-releasing acylated peptide from stomach. Nature 402(6762):656-660.

Lamprecht R, Dudai Y. 1995. Differential modulation of brain immediate early genes by intraperitoneal LiCl. Neuroreport 7(1):289-293.

Lechan RM, Fekete C. 2006. The TRH neuron: a hypothalamic integrator of energy metabolism. Prog Brain Res 153:209-235.

Li Y. 2007. Sensory signal transduction in the vagal primary afferent neurons. Curr Med Chem 14(24):2554-2563.

Liposits Z, Setalo G, Flerko B. 1984. Application of the silver-gold intensified 3,3'-diaminobenzidine chromogen to the light and electron microscopic detection of the

luteinizing hormone-releasing hormone system of the rat brain. Neuroscience 13(2):513-525.

Llewellyn-Smith IJ, Reimann F, Gribble FM, Trapp S. 2011. Preproglucagon neurons project widely to autonomic control areas in the mouse brain. Neuroscience 180:111-121.

Loewy AD. 1990. Central Autonomic Pathways. In: Loewy AD, Spyer KM, eds. Central Regulation of Autonomic Functions. Oxford: Oxford publisher. p 88-103.

Luquet S, Perez FA, Hnasko TS, Palmiter RD. 2005. NPY/AgRP neurons are essential for feeding in adult mice but can be ablated in neonates. Science 310(5748):683-685.

Magableh A, Lundy R. 2014. Somatostatin and corticotrophin releasing hormone cell types are a major source of descending input from the forebrain to the parabrachial nucleus in mice. Chem Senses 39(8):673-682.

Mayer J, Thomas DW. 1967. Regulation of food intake and obesity. Science 156(3773):328-337.

Menyhert J, Wittmann G, Lechan RM, Keller E, Liposits Z, Fekete C. 2007. Cocaine- and amphetamine-regulated transcript (CART) is colocalized with the orexigenic neuropeptide Y and agouti-related protein and absent from the anorexigenic alpha-melanocyte-stimulating hormone neurons in the infundibular nucleus of the human hypothalamus. Endocrinology 148(9):4276-4281.

Moga MM, Weis RP, Moore RY. 1995. Efferent projections of the paraventricular thalamic nucleus in the rat. J Comp Neurol 359(2):221-238.

Morton GJ, Cummings DE, Baskin DG, Barsh GS, Schwartz MW. 2006. Central nervous system control of food intake and body weight. Nature 443(7109):289-295.

Nakazato M, Murakami N, Date Y, Kojima M, Matsuo H, Kangawa K, Matsukura S. 2001. A role for ghrelin in the central regulation of feeding. Nature 409(6817):194-198.

Nilaweera KN, Archer ZA, Campbell G, Mayer CD, Balik A, Ross AW, Mercer JG, Ebling FJP, Morgan PJ, Barrett P. 2009. Photoperiod Regulates Genes Encoding Melanocortin 3 and Serotonin Receptors and Secretogranins in the Dorsomedial Posterior Arcuate of the Siberian Hamster. Journal of Neuroendocrinology 21(2):123-131.

Norsted E, Gomuc B, Meister B. 2008. Protein components of the blood-brain barrier (BBB) in the mediobasal hypothalamus. J Chem Neuroanat 36(2):107-121.

Otake K. 2005. Cholecystokinin and substance P immunoreactive projections to the paraventricular thalamic nucleus in the rat. Neurosci Res 51(4):383-394.

Paues J, Mackerlova L, Blomqvist A. 2006. Expression of melanocortin-4 receptor by rat parabrachial neurons responsive to immune and aversive stimuli. Neuroscience 141(1):287-297.

Paxinos G, Watson C. 1998. The Rat Brain in Stereotaxic Coordinates: Academic Press.

Pedragosa-Badia X, Stichel J, Beck-Sickinger AG. 2013. Neuropeptide Y receptors: how to get subtype selectivity. Front Endocrinol (Lausanne) 4:5.

Petrovich GD, Ross CA, Gallagher M, Holland PC. 2007. Learned contextual cue potentiates eating in rats. Physiol Behav 90(2-3):362-367.

Phillips RJ, Powley TL. 2000. Tension and stretch receptors in gastrointestinal smooth muscle: re-evaluating vagal mechanoreceptor electrophysiology. Brain Res Brain Res Rev 34(1-2):1-26.

Reilly S, Trifunovic R. 2000. Lateral parabrachial nucleus lesions in the rat: aversive and appetitive gustatory conditioning. Brain Res Bull 52(4):269-278.

Rinaman L, Dzmura V. 2007. Experimental dissociation of neural circuits underlying conditioned avoidance and hypophagic responses to lithium chloride. Am J Physiol Regul Integr Comp Physiol 293(4):R1495-1503.

Rizvi TA, Ennis M, Behbehani MM, Shipley MT. 1991. Connections between the central nucleus of the amygdala and the midbrain periaqueductal gray: topography and reciprocity. J Comp Neurol 303(1):121-131.

Rollins BL, King BM. 2000. Amygdala-lesion obesity: what is the role of the various amygdaloid nuclei? Am J Physiol Regul Integr Comp Physiol 279(4):R1348-1356.

Roman CW, Derkach VA, Palmiter RD. 2016. Genetically and functionally defined NTS to PBN brain circuits mediating anorexia. Nat Commun 7:11905.

Roman CW, Lezak KR, Kocho-Schellenberg M, Garret MA, Braas K, May V, Hammack SE. 2012. Excitotoxic lesions of the bed nucleus of the stria terminalis (BNST) attenuate the effects of repeated stress on weight gain: evidence for the recruitment of BNST activity by repeated, but not acute, stress. Behav Brain Res 227(1):300-304.

Rothwell NJ, Saville ME, Stock MJ. 1983. Metabolic responses to fasting and refeeding in lean and genetically obese rats. Am J Physiol 244(5):R615-620.

Sabbatini M, Molinari C, Grossini E, Mary DA, Vacca G, Cannas M. 2004. The pattern of c-Fos immunoreactivity in the hindbrain of the rat following stomach distension. Exp Brain Res 157(3):315-323.

Sarkar S, Lechan RM. 2003. Central administration of neuropeptide Y reduces alpha-melanocyte-stimulating hormone-induced cyclic adenosine 5'-monophosphate response

element binding protein (CREB) phosphorylation in pro-thyrotropin-releasing hormone neurons and increases CREB phosphorylation in corticotropin-releasing hormone neurons in the hypothalamic paraventricular nucleus. Endocrinology 144(1):281-291.

Schwartz MW, Woods SC, Porte D, Jr., Seeley RJ, Baskin DG. 2000. Central nervous system control of food intake. Nature 404(6778):661-671.

Schwinkendorf DR, Tsatsos NG, Gosnell BA, Mashek DG. 2011. Effects of central administration of distinct fatty acids on hypothalamic neuropeptide expression and energy metabolism. Int J Obes (Lond) 35(3):336-344.

Scott MM, Lachey JL, Sternson SM, Lee CE, Elias CF, Friedman JM, Elmquist JK. 2009. Leptin targets in the mouse brain. J Comp Neurol 514(5):518-532.

Scott TR, Small DM. 2009. The role of the parabrachial nucleus in taste processing and feeding. Ann N Y Acad Sci 1170:372-377.

Serrats J, Sawchenko PE. 2006. CNS activational responses to staphylococcal enterotoxin B: T-lymphocyte-dependent immune challenge effects on stress-related circuitry. J Comp Neurol 495(2):236-254.

Singru PS, Sanchez E, Fekete C, Lechan RM. 2007. Importance of melanocortin signaling in refeeding-induced neuronal activation and satiety. Endocrinology 148(2):638-646.

Singru PS, Wittmann G, Farkas E, Zseli G, Fekete C, Lechan RM. 2012. Refeeding-activated glutamatergic neurons in the hypothalamic paraventricular nucleus (PVN) mediate effects of melanocortin signaling in the nucleus tractus solitarius (NTS). Endocrinology 153(8):3804-3814.

Stachniak TJ, Ghosh A, Sternson SM. 2014. Chemogenetic synaptic silencing of neural circuits localizes a hypothalamus-->midbrain pathway for feeding behavior. Neuron 82(4):797-808.

Stanley BG, Urstadt KR, Charles JR, Kee T. 2011. Glutamate and GABA in lateral hypothalamic mechanisms controlling food intake. Physiol Behav 104(1):40-46.

Stengel A, Tache Y. 2011. Interaction between gastric and upper small intestinal hormones in the regulation of hunger and satiety: ghrelin and cholecystokinin take the central stage. Curr Protein Pept Sci 12(4):293-304.

Stratford TR, Wirtshafter D. 2013. Injections of muscimol into the paraventricular thalamic nucleus, but not mediodorsal thalamic nuclei, induce feeding in rats. Brain Res 1490:128-133.

Swank MW, Bernstein IL. 1994. c-Fos induction in response to a conditioned stimulus after single trial taste aversion learning. Brain Res 636(2):202-208.

Swanson LW. 2000. Cerebral hemisphere regulation of motivated behavior. Brain Res 886(1-2):113-164.

Swanson LW. 2004. Brain Maps III: Structure of the Rat Brain: Academic.

Takahashi KA, Cone RD. 2005. Fasting induces a large, leptin-dependent increase in the intrinsic action potential frequency of orexigenic arcuate nucleus neuropeptide Y/Agouti-related protein neurons. Endocrinology 146(3):1043-1047.

Timofeeva E, Baraboi ED, Richard D. 2005. Contribution of the vagus nerve and lamina terminalis to brain activation induced by refeeding. Eur J Neurosci 22(6):1489-1501.

Timofeeva E, Picard F, Duclos M, Deshaies Y, Richard D. 2002. Neuronal activation and corticotropin-releasing hormone expression in the brain of obese (fa/fa) and lean (fa/?) Zucker rats in response to refeeding. Eur J Neurosci 15(6):1013-1029.

Tokita K, Boughter JD, Jr. 2016. Topographic organizations of taste-responsive neurons in the parabrachial nucleus of C57BL/6J mice: An electrophysiological mapping study. Neuroscience 316:151-166.

Trifunovic R, Reilly S. 2002. Medial versus lateral parabrachial nucleus lesions in the rat: effects on mercaptoacetate-induced feeding and conditioned taste aversion. Brain Res Bull 58(1):107-113.

Turenius CI, Htut MM, Prodon DA, Ebersole PL, Ngo PT, Lara RN, Wilczynski JL, Stanley BG. 2009. GABA(A) receptors in the lateral hypothalamus as mediators of satiety and body weight regulation. Brain Res 1262:16-24.

van der Kooy D, Koda LY, McGinty JF, Gerfen CR, Bloom FE. 1984. The organization of projections from the cortex, amygdala, and hypothalamus to the nucleus of the solitary tract in rat. J Comp Neurol 224(1):1-24.

Vong L, Ye C, Yang Z, Choi B, Chua S, Jr., Lowell BB. 2011. Leptin action on GABAergic neurons prevents obesity and reduces inhibitory tone to POMC neurons. Neuron 71(1):142-154.

Wang L, Martinez V, Barrachina MD, Tache Y. 1998. Fos expression in the brain induced by peripheral injection of CCK or leptin plus CCK in fasted lean mice. Brain Res 791(1-2):157-166.

Warne JP, Foster MT, Horneman HF, Pecoraro NC, Ginsberg AB, Akana SF, Dallman MF. 2007. Afferent signalling through the common hepatic branch of the vagus inhibits voluntary lard intake and modifies plasma metabolite levels in rats. J Physiol 583(Pt 2):455-467.

Watts AG, Sanchez-Watts G, Kelly AB. 1999. Distinct patterns of neuropeptide gene expression in the lateral hypothalamic area and arcuate nucleus are associated with dehydration-induced anorexia. J Neurosci 19(14):6111-6121.

Wierup N, Richards WG, Bannon AW, Kuhar MJ, Ahren B, Sundler F. 2005. CART knock out mice have impaired insulin secretion and glucose intolerance, altered beta cell morphology and increased body weight. Regul Pept 129(1-3):203-211.

Wise RA. 1974. Lateral hypothalamic electrical stimulation: does it make animals 'hungry'? Brain Res 67(2):187-209.

Woods SC. 2013. Metabolic signals and food intake. Forty years of progress. Appetite 71:440-444.

Woods SC, Lotter EC, McKay LD, Porte D, Jr. 1979. Chronic intracerebroventricular infusion of insulin reduces food intake and body weight of baboons. Nature 282(5738):503-505.

Wu Q, Boyle MP, Palmiter RD. 2009. Loss of GABAergic signaling by AgRP neurons to the parabrachial nucleus leads to starvation. Cell 137(7):1225-1234.

Wu Q, Clark MS, Palmiter RD. 2012. Deciphering a neuronal circuit that mediates appetite. Nature 483(7391):594-597.

Wu Q, Palmiter RD. 2011. GABAergic signaling by AgRP neurons prevents anorexia via a melanocortin-independent mechanism. Eur J Pharmacol 660(1):21-27.

Yamamoto T, Shimura T, Sakai N, Ozaki N. 1994. Representation of hedonics and quality of taste stimuli in the parabrachial nucleus of the rat. Physiol Behav 56(6):1197-1202.

Yamamoto T, Shimura T, Sako N, Azuma S, Bai WZ, Wakisaka S. 1992. C-fos expression in the rat brain after intraperitoneal injection of lithium chloride. Neuroreport 3(12):1049-1052.

Yamamoto T, Takemura M, Inui T, Torii K, Maeda N, Ohmoto M, Matsumoto I, Abe K. 2009. Functional organization of the rodent parabrachial nucleus. Ann N Y Acad Sci 1170:378-382.

Yasoshima Y, Scott TR, Yamamoto T. 2006. Memory-dependent c-Fos expression in the nucleus accumbens and extended amygdala following the expression of a conditioned taste aversive in the rat. Neuroscience 141(1):35-45.

Yaswen L, Diehl N, Brennan MB, Hochgeschwender U. 1999. Obesity in the mouse model of pro-opiomelanocortin deficiency responds to peripheral melanocortin. Nat Med 5(9):1066-1070.

Zheng H, Patterson LM, Rhodes CJ, Louis GW, Skibicka KP, Grill HJ, Myers MG, Jr., Berthoud HR. 2010. A potential role for hypothalamomedullary POMC projections in leptin-induced suppression of food intake. Am J Physiol Regul Integr Comp Physiol 298(3):R720-728.

Zhu X, Krasnow SM, Roth-Carter QR, Levasseur PR, Braun TP, Grossberg AJ, Marks DL. 2012. Hypothalamic signaling in anorexia induced by indispensable amino acid deficiency. Am J Physiol Endocrinol Metab 303(12):E1446-1458.

DOI:10.14753/SE.2017.2041

12. PUBLICATION LIST

12.1. List of publications the thesis is based on

Zséli G, Vida B, Martinez A, Lechan R M, Khan A M, Fekete C (2016) Elucidation of the Anatomy of a Satiety Network: Focus on Connectivity of the Parabrachial Nucleus in the Adult Rat. *J Comp Neurol* 524 (14), pp. 2803-27

Fekete C*, **Zséli G***, Singru PS, Kádár A, Wittmann G, Füzesi T, El-Bermani W, Lechan RM (2012) Activation of Anorexigenic Pro-Opiomelanocortin Neurones during Refeeding is Independent of Vagal and Brainstem Inputs. *J Neuroendocrinol* 24 (11), pp. 1423-1431
*equally contributed

Singru PS, Wittmann G, Farkas E, **Zséli G**, Fekete C, Lechan RM (2012) Refeeding-activated glutamatergic neurons in the hypothalamic paraventricular nucleus (PVN) mediate effects of melanocortin signaling in the nucleus tractus solitarius (NTS). *Endocrinology* 153 (8), pp. 3804-3814

12.2. Other publications

Sárvári A, Farkas E, Kádár A, **Zséli G**, Füzesi T, Lechan RM, Fekete C (2012) Thyrotropin-releasing hormone-containing axons innervate histaminergic neurons in the tuberomammillary nucleus. *Brain Res* 1488, pp. 72-80

Kiss L, Pintye A, **Zséli G**, Jankovics T, Szentiványi O, Hafez YM, Cook RTA (2010) Microcyclic conidiogenesis in powdery mildews and its association with intracellular parasitism by Ampelomyces. *Eur J Plant Pathol* 126 (4), pp. 445-451

DOI:10.14753/SE.2017.2041

13. ACKNOWLEDGMENTS

I would like to thank my supervisor, Dr. Csaba Fekete for his support and the opportunity to perform my doctoral work in his laboratory.

I am very grateful to Professor Zsolt Liposits, Head of the Laboratory of Endocrine Neurobiology.

I am very thankful to my closest colleague Barbara Vida for her professional help.

I wish to thank to Stiftné Szilvásy-Szabó Anett, and the assistants of the laboratory, Veronika Maruzs and Ágnes Simon for their excellent technical help.